

Dear Reviewer,

We thank you for doing this review and for your suggestions. Below, please find your original comments in blue and our responses in black. When referencing page and line numbers, we are always referring to the new versions of manuscript and SI, which are attached at the end. Concerning the literature cited in this answer to your review, we ask you to refer to the attached new version of the manuscript with tracked changes.

The manuscript presents an analysis of filter and water samples for their content of ice nucleating particles (INPs). Samples were collected at the Cabo Verde Island as part of the MarParCloud project.

What makes this study unique is that samples were simultaneously taken at sea and cloud level, and include filter samples of ambient air as well as cloud water and sea water samples. By comparing the INP content in these different compartments of the environment the authors infer the contribution of particles of certain origin and characteristics to the atmospheric INP population. There are several points that need to be improved -- these are listed in detail below. Once these are addressed, the paper should be published in ACP.

#### Specific comments

1) P.1 ln.14f Attributing the difference in NINP from PM10 and PM1 samples to biological particles only based on the temperature of activation is speculative and over-reaching, eg. super-micron mineral dust particles can also cause ice formation at -10°C (see Hoose and Möhler, 2012). Are there indications against mineral dust particles being responsible for the higher activity? Were elevated NINP observed during dust events?

Thanks for your comments. We did additional measurements, as still filter material was left, and heated filter pieces from the three samples CVAO 1596, CVAO 1641 and CVAO 1643, i.e., those with high ice activity at high temperatures, at 95 °C for 1 hour. The elevated  $N_{INP}$  at warm temperatures disappeared, as shown in the new Fig. 3. The respective values of  $N_{INP}$  and  $f_{ice}$  (only

for CVAO 1596, CVAO 1641 and CVAO 1643 before and after heating) are shown in the supplement, Fig. S6 and Fig. S7.

Page 1, lines 13-14 was changed to:

“After heating samples at 95 °C for 1 hour, the elevated  $N_{INP}$  at the warm temperatures disappeared, indicating that these highly ice active INPs were most likely biological particles.”

This supports the statement in the last sentence in this paragraph, which we hence did not change.

2) P.1 ln.18 Same as above. Most particles  $>1\mu m$  are probably activated as CCN. There is no evidence for a biological origin of these INPs.

Based on the additional measurements mentioned at your comment above, we left this statement here as it was.

3) P.2 ln.7 In addition to homogeneous ice nucleation, heterogeneous ice nucleation by deposition nucleation is active also below -38°C. As the sentence is written it indicates that only homogeneous nucleation would be active below -38°C, which is incorrect.

Thanks for your comment. We changed it to:

“Ice crystals in the atmosphere can be formed either via homogeneous nucleation below -38 °C or via heterogeneous nucleation aided by aerosol particles known as ice nucleating particles (INPs) at any temperature below 0 °C.”

4) P.2 ln.9 Are all droplets aqueous solutions?

Concerning droplets in the atmosphere, it can be assumed that all droplets are aqueous solutions.

5) P.2 ln.12 If there is a special aspect to the -20°C reported in Augustin-Bauditz et al., 2014 it should be mentioned. If not, the “below -15°C” from Hoose and Möhler, 2012 already includes -20°C and the Augustin-Bauditz et al., 2014 reference can be omitted. According to Fig. 3d in

Hoose and Möhler, 2012, super-micron mineral dust particles can be active INP already below -10°C and not -15°C.

Thanks for your comment. It was changed to:

“Submicron dust particles are recognized as effective INPs below -20 °C (Augustin-Bauditz et al., 2014) and super-micron dust particles were reported to be ice active even up to -10 °C (Hoose and Möhler, 2012; Murray et al., 2012).”

6) P.2 ln.17 The results in Boose et al., 2016 suggest desert dust to nucleate ice mostly below -25°C, especially airborne samples and the study shows differences among samples from different regions. This seems to contradict what is stated in ln.12-16. This section of the introduction should be revised, distinguishing mineral dust from desert dust studies and motivating the relevance of desert dust for the results presented here.

You are right, and we changed this part as follows:

“Boose et al. (2016) found that ice activity of desert dust particles at temperatures between -35 and -28 °C can be attributed to the sum of the feldspar and quartz content. A high clay content, in contrast, was associated with lower ice nucleation activity. In contrast to field measurements, in laboratory studies often separate types of mineral dusts are examined.”

7) P.2 ln.26 Specify what is meant by “differences in desert sources”.

Desert dust particles from different regions in a desert can have different mineral compositions. In order to specify, we changed this part as follows:

“Price et al. (2018) observed two orders of magnitude variability in  $N_{INP}$  at any particular temperature from ~ -13 to ~ -25 °C, which was related to the variability in atmospheric dust loading. This desert dust’s ice nucleating activity was only weakly dependent on differences in desert sources, i.e., on the differences in mineral composition that particles emitted from different locations in the desert may have.”

8) P.2 ln.28 Is  $N_{INP}$  at ground level lower because the dust loading was lower at ground level?

Yes, it is. We added to the end of this sentence: "... level, where the dust loading was lower."

9) P.2 ln.32f This is incorrect. Bigg, 1973 suggested that INPs "are transported from a distant land source, or from a stratospheric source, and brought to sea level by convective mixing." Schnell and Vali, 1976 suggested a marine source could explain the observations of Bigg 1973.

Thanks for clarifying this. It was changed to:

"Based on a long-term measurement of INPs in the marine boundary layer in the south of and around Australia, Bigg (1973) suggested that INPs in ambient air were from a distant land source, or from a stratospheric source, and brought to sea level by convective mixing. Schnell and Vali. (1976) suggested a marine source could explain the observations of Bigg (1973)."

10) P.3 ln.2 What further evidence? This sentence seems to refer in a more general tone to the same study as the sentence before. Please clarify.

"Further evidence" was changed to "Furthermore".

11) P.3 ln.10f DeMott et al. 2010, 2015 suggest a correlation of NINP and the concentration of particles above a certain size. However they do not specify that only a fraction of large particles would act as INPs. Double check.

It is correct that these two publications rather describe parameterizations. However, as not all large particles act as INP (otherwise number concentrations of INP and all large particles would be the same), it is correct to say that only a fraction of these large particles is an INP. We reworded this sentence as follows:

"Simultaneous measurements of  $N_{INP}$  and particle number size distributions were used to develop parameterizations in which  $N_{INP}$  depends on a temperature dependent fraction of all particles with sizes above 500 nm (DeMott et al., 2010, 2015)."

12) P.3 ln.20 The deduction that most biological INPs occur together with their original carrier appears incomplete. Clarify.

The explanation was meant to be given earlier in the sentence, which we now clarified as follows:

“, but based on the fact that most atmospheric INPs seem to be super-micron in size, as observed in the above cited literature, it seems that most of the biological ice active macromolecules still occur together with their original carrier in the atmosphere.”

13) P.4 first paragraph of Sec. 2.1.1. If the CVAO station is located on the northwest shore (ln. 11) of the island and wind direction is from the northeast (ln. 17), does this mean air first crossed the island before reaching the station? I think the CVAO is located on the northeast shore.

Thanks for catching this. CVAO is located at the northeastern shore of the São Vicente island. We changed this in the manuscript accordingly.

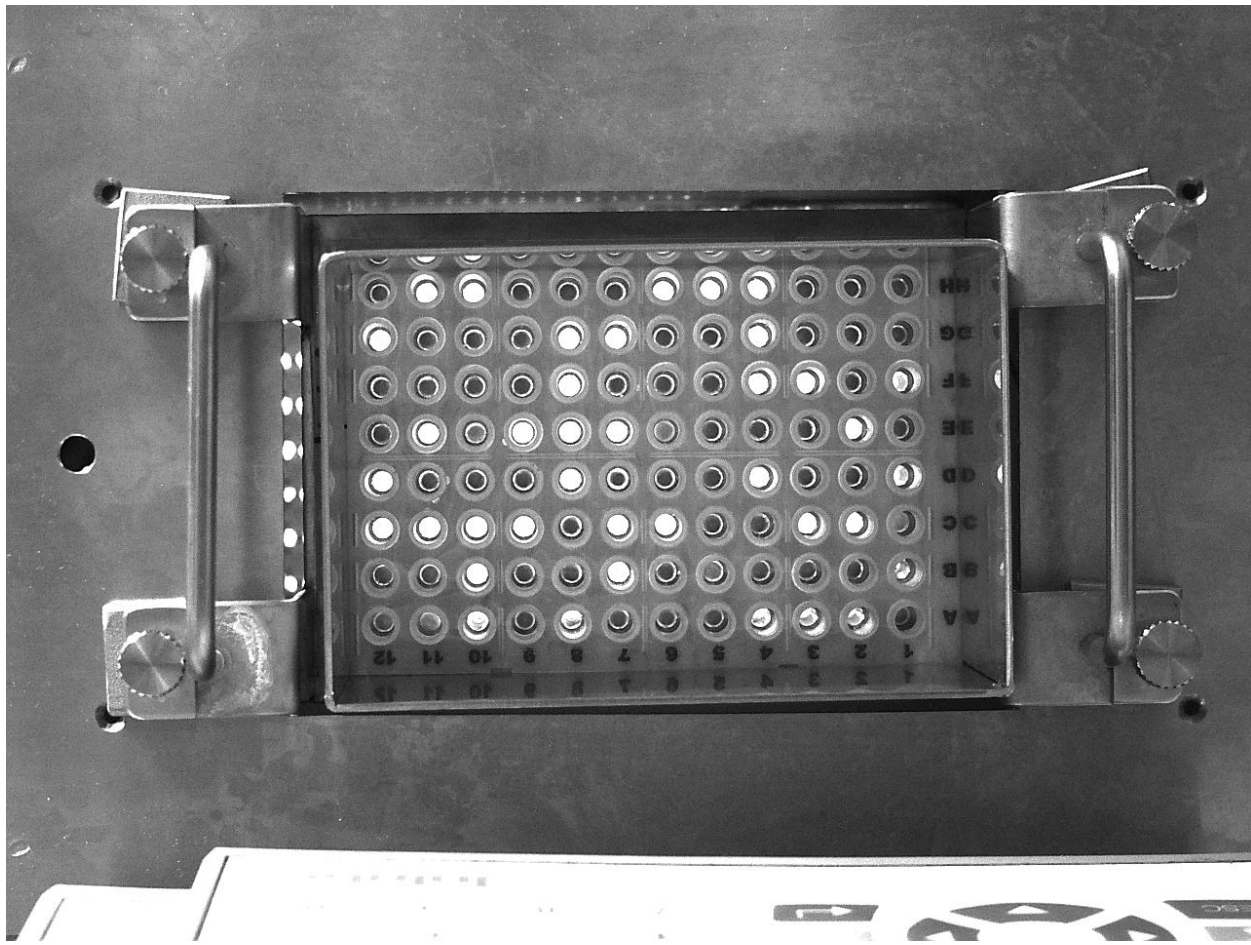
14) P.5 ln.16 It is mentioned in Sec. 2.1.1. that measurements took place during 31 days. Why where only 17 or 19 filters collected? How long was the sampling period per filter?

In the companion paper, the on-line measurement, including particle number size distribution, particle number concentration, CCN number concentration, started on 13 September and ended on 13 October. In order to keep consistency, we still used the same period in this paper. However, the filter samples were only collected from 19 September to 8 October. The sampling period was about 24 hours for each filter, with sampling times given in Table S1 in the supplement. We changed the beginning of Section 2.1.1. to:

“The measurement campaign was carried out”

15) P.6 ln.29 By “brightness change” do you mean a change in transmitted light due to a change in opacity when droplets freeze?

You are right. The transmission light will decrease when the droplet freeze. As you can see in the image below, the dark circles mean the droplets were already frozen.



16) P.7 ln.8f Can you explain how the assumption of a Poisson distribution influences the result of Eq.1?

We are sorry but it is not totally clear to us what you mean, as Eq. 1 is derived based on the Poisson distribution as follows:

The Poisson distribution is a discrete probability distribution that expresses the probability of a given number of events occurring in a fixed interval of time or space if these events occur with a known constant rate and independently of the time since the last event (Haight, 1967). The probability of observing  $k$  events in an interval is given by the equation:

$$P_{(k)} = \frac{\lambda^k \cdot e^{-\lambda}}{k!}$$

Where

$\lambda$  is the average number of events per interval.

$e$  is the number 2.71828... (Euler's number) the base of the natural logarithms.

$k$  takes values 0, 1, 2, ....

$k! = k \times (k - 1) \times (k - 2) \times \dots \times 2 \times 1$  is the factorial of  $k$ .

In the freezing array experiment, the probability of observing a certain number of INP in each droplet can be assumed to follow the Poisson distribution. And  $\lambda = N_{INP}(\theta) \cdot V$ . Once there is at least one INP that is active at a certain temperature in a droplet, this droplet will freeze upon being cooled to this temperature, and then  $P_{(0)} = 1 - f_{ice}(\theta)$ .

In the Poisson distribution:

$$P_{(0)} = e^{-\lambda}$$

Then we can get:

$$1 - f_{ice}(\theta) = e^{-N_{INP}(\theta) \cdot V}$$

$$N_{INP}(\theta) = \frac{-\ln(1 - f_{ice}(\theta))}{V}$$

17) P.7 sec.2.3.1. The principle of determining the cumulative INP concentration as well as the difference between INDA and LINA experiments are not very well explained. The explanation should mention that all wells contain multiple INPs but only the most active one (active at the highest temperature) causes freezing. The probability to find an active INP at a certain temperature increases with sample volume.

We added the following to page 7, line 25:

“This way, the cumulative number of INP active at any temperature will be obtained although only the most ice active INP (nucleating ice at the highest temperature) present in each droplet / well will be observed.”

Other than this, we already had said before that “The larger volume of water corresponds to a higher probability of the presence of INPs in each well, therefore INDA can detect INPs at warmer temperatures, . . . .” So nothing was changed in this regard.

18) P.7 Sec.2.3.2 Provide the equations you used for this calculation and some values to inform the reader how large statistical error and background are.

We included the equation and background results in the supplement page 6, lines 1-5.

19) P.7 ln.18 It is not explained previously that washing water was used or how it was prepared.

The “washing” is misleading here. We removed “washing”.

20) P.7 ln.18 How was the information about the number of INPs per well obtained?

This is what is at the base of using the Poisson distribution, i.e., Eq. 1 will yield  $N_{INP}$  based on the observed number of frozen droplets at each temperature where a measurement was made.

21) P.7 ln.20 A short explanation of the method from Agresti and Coull, 1998 would be helpful here.

We add the following in page 8, line 7:

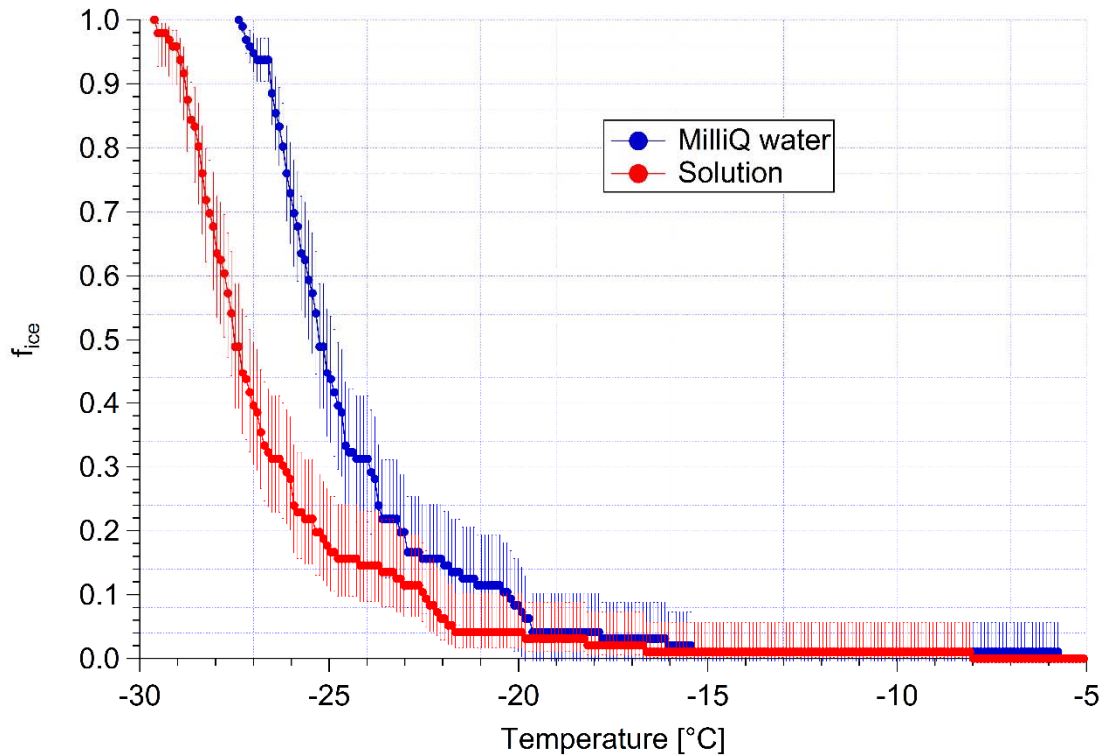
“These confidence intervals were estimated according to the improved Wald interval which implicitly assumes a normal approximation for binomially distributed measurement errors.”

22) P.8 ln.3f Can you provide a range of the derived freezing point depression for the samples. Was the freezing point depression experimentally confirmed, eg. by measuring the melting point depression?

The seawater salinity varied from 34.1 to 36.7 g L<sup>-1</sup>. Based on this, according to theory, the freezing point depression varied from 2.1 to 2.3 °C.

We did not test the freezing point depression with seawater samples. Since the seawater samples are no longer available, we tested the freezing point depression of pure sodium chloride solution.

We dissolved 0.72 g sodium chloride in 20 mL MilliQ water to get a solution with a salinity similar to that of the SML and ULW samples. The frozen fraction ( $f_{ice}$ ) of MilliQ water and of this sodium chloride solution are shown in the figure below. The error bars show 95% confidence intervals of  $f_{ice}$ . Due to large measurement uncertainties for the first frozen droplets, the freezing point depression should rather be determined from temperatures below approx.  $-25^{\circ}\text{C}$ , where, indeed, a freezing point depression temperature about  $\sim 2.2^{\circ}\text{C}$  was observed. It is therefore acceptable to use a freezing point depression of  $2.2^{\circ}\text{C}$  in this study.



23) P.8 ln.9 The description of  $ns$  is imprecise.  $ns$  gives the number of ice active sites per surface area, here the surface of all aerosol, ice active or not. Revise.

Following one of the first reviewer's (Paul DeMott) remarks, we extended this part to explain the  $n_s$  for field measurement.

"For cases where a single type of aerosol, such as one type of mineral dust, is examined in laboratory studies,  $A_{total}$  can be the total particle surface area. However, when field experiments are done, using the total particle surface area of the atmospheric aerosol assumes that all particles contribute to INP and have the same  $n_s$ , while the vast majority of these particles will not even be an INP. On the other hand, singling out the contribution of separate INP types in the atmospheric aerosol and relying  $n_s$  only to them by using their contribution to the total surface area is at least demanding if not often impossible. This has to be kept in mind when interpreting heterogeneous ice nucleation in terms of  $n_s$ "

24) P.8 ln.20-26 This section is speculative and it is not clear why this comparison is relevant for the present study. Clarify.

So far, there are only a few publications in literature which discuss  $N_{INP}$  in seawater. And while values for  $N_{INP}$  in bulk water in these publications are similar to ours, those for SML are above ours, which, in itself, is an interesting observation. So we would want to keep this comparison here to show the  $N_{INP}$  similarities and variations that can be there in seawater from different location of the world.

25) P.8 ln.27 Add an introducing sentence mentioning that the following analysis is done to compare  $N_{INP}$  found in SML and ULW at Cabo Verde and explain why enrichment/depletion could be expected. Could INP in the SML originate from settling aerosol?

In page 9, lines 24-25 we already explained "To better quantify the enrichment or depletion of  $N_{INP}$  in SML to ULW, we derived an enrichment factor (EF). The EF in SML was calculated by dividing  $N_{INP}$  in SML ( $N_{INP, SML}$ ) by the respective  $N_{INP}$  measured in ULW ( $N_{INP, ULW}$ ).". So it is not clear to us what more we could add here that has not already been said.

As organic material attaches to air bubbles rising to the surface (an effect well known in some industries and for aquaria, where it is used to clean liquids from organic contaminants), it may be expected that INP might also be enriched at the surface. And while settling of airborne aerosol

particles may contribute to INP in the SML, this contribution would only be very small, so that in general it will not play a big role. We added:

“An enrichment might be expected as organic material is known to attach to air bubbles rising to the ocean surface.”

26) P.9 Fig.1 Why were samples 6, 7, 8, 10 and 11 not used? Instead of comparing to Wilson’s data from a different environment, a direct comparison of SML to ULW by plotting both data on top of each other might show more clearly that NINP are the same between the two.

Samples 6, 7, 8, 10, 11 were collected for chemical measurements first. The remaining samples are not enough for INP measurement.

It is too crowded if we plot  $N_{INP}$  of SML and ULW in the same figure.

27) P.9 ln.2 Clarify that you refer to the temperature at which NINP was determined in the drop freezing experiment. As is, it could be misunderstood as water temperature during sampling.

We changed this part as:

“Fig. 2 shows the EF as a function of the temperature at which  $N_{INP}$  was determined in the freezing devices.”

28) P.9 ln.3 Can you provide an explanation for the variation in EF with temperature? Does the interpretation change when considering the confidence interval of NINP? Do an error propagation of Eq. (5) and estimate the error in EF (should be included in Fig.2).

So far, it is still not clear which kind of particles in the seawater contribute INP. However, it can be assumed that there are several different ice active entities in seawater, which all can have different ice nucleation temperatures. So the variations in EF with temperature likely indicate that there are different amounts of these different types of ice active entities present in the different samples. Moreover, the many small wiggles in the curves displayed in this Figure are likely due to measurement uncertainties. To show this, and to follow your suggestion, we did the error

propagation for EF. This leads to a very busy plot, so we put this plot, i.e., the EF with error bars in the supplement, Fig. S3.

We added the following in page 9, lines 31-32:

“Most of the variation seen here is likely caused by measurement uncertainties, which are indicated in Fig. S3 in the supplement.”

**29) P.9 ln.8 Shouldn't SML thickness be related to concentration of dissolved organic matter? Explain why SML at Cabo Verde is larger than the SML in the Wilson et al., 2015 study even though conditions are oligotrophic.**

The thickness of SML mainly depends on the collection techniques (Agogué et al., 2004; Aller et al., 2017). In Wilson et al. (2015), two techniques were deployed to collect SML samples. First, SML samples were collected into borosilicate glass bottles from a hydrophilic Teflon film on a rotating drum fitted to the ‘Interface II’ remote-controlled sampling catamaran, featured thickness around 20  $\mu\text{m}$ . Secondly, SML samples were collected by glass plate, featured thickness around 80  $\mu\text{m}$ . In this study, we collected the SML by using glass plate, with a thickness around 91  $\mu\text{m}$ . Previous studies pointed out that rotating drum sampler and the glass dipping method probe different thicknesses of the SML, thus making a direct comparison of both SML thickness as well as enrichment factors generally difficult (Agogué et al., 2004; Aller et al., 2017). We added this information in page 10, lines 7-10.

**30) P.10 Fig.2 add error estimation of EF.**

See response to comment 28.

**31) P.10 ln.9-11 What could be the reason for the variation between samples and why is the range of variation consistent to measurements at other locations?**

$N_{\text{INP}}$  at one specific temperature is controlled by the number concentration of a mixture of different kinds of INP, which is explained in Welti et al. (2018). The fact that  $N_{\text{INP}}$  at warm temperatures span 2 orders of magnitude is generally assumed to be due to a variation of the presence of

biological particles, which can serve as INPs. The commonality of this study and two cited experiments (Gong et al., 2019; O’Sullivan et al., 2018) is striking, and it may be assumed that land sources contribute to the INPs from long-range transport over broad regions, so that similar mixtures of INP can be present in different areas.

#### Could the number of samples or sampling duration determine the range of variation?

High variations in  $N_{INP}$  have been observed from highly time resolved in-situ measurements (see e.g., Welti et al. (2018)), so that it can be assumed that longer sampling will somewhat smooth the detected concentrations. However, when comparing the ranges of values that are found with a number of different methods with different sampling times, high variations are found for all of the different methods (besides for Welti et al. (2018), also in DeMott et al. (2016) or in McCluskey et al. (2018b), which all include in-situ as well as filter based INP analysis). It can be assumed that there are times with either comparably persistently high or persistently low  $N_{INP}$  on continental sites, in general. Even for samples that were collected for one or two weeks in the Arctic, a high variability in  $N_{INP}$  was still observed, notwithstanding these long sampling times (Wex et al., 2019).

#### 32) P.10 ln.12f Testing the heat sensitivity of the 3 samples could substantiate the interpretation that biological particles are responsible for the enhanced NINP.

Thank you for the suggestion. Samples CVAO 1596, CVAO 1641 and CVAO 1643 were heated to 95 °C for 1 hour and a large reduction of in  $N_{INP}$  was observed. Based on this, we added one paragraph in page 12, line 3:

“Biological INPs contain specific ice-nucleating proteins. These proteins are disrupted and denatured by heating which causes them to lose their ice-nucleating ability. However, the inorganic ice-nucleating material, such as dust particles, is insensitive to heat (Wilson et al., 2015; O’Sullivan et al., 2018). Therefore, a commonly used heat treatment was deployed to assess the contribution of biological INPs to the total INPs in this study. Samples CVAO 1596, CVAO 1641 and CVAO 1643 were heated to 95 °C for 1 hour and the resulting NP are shown in Fig. S6. A clear comparison of before and after heating  $f_{ice}$  is shown in Fig. S7. A large reduction of more than one order of magnitude in  $N_{INP}$  at  $T > -15$  °C was observed in the samples after heating. The reductions in  $N_{INP}$  became smaller at colder temperature and were, for example, less than one order of magnitude at

$T = -20^\circ\text{C}$ . This shows that biological aerosol contributed a large fraction of total INPs in  $\text{PM}_{10}$  at  $T > -20^\circ\text{C}$ .”

33) P.10 ln.14ff. This paragraph is difficult to follow. Do you mean above  $-16.8^\circ\text{C}$  concentrations within  $2^\circ\text{C}$  of each other are correlated? Looking at the data in Fig.3, NINP seem to change very little in  $0.1^\circ\text{C}$  steps, but are different between individual measurements.

In this paragraph, we describe the analysis of separate curves, i.e., we tested how well measurements from one sample were correlated with measurements of that same sample at different temperatures. We had already mentioned before:

““As long as the examined temperature difference was less than  $2^\circ\text{C}$ ,  $N_{\text{INP}}$  were correlated.”

To make this clearer, the first sentence in this paragraph was changed to:

“The correlation of  $N_{\text{INP}}$  at different temperatures within one sample was calculated, by comparing each INP at each temperature to that at each other temperature at which a measurement had been made. That was done separately for each of the samples.”

We added the tables that give all the values for  $R^2$  and  $p$  for all temperatures for all different samples at the end of this response.

**What is the actual regression model for which you report  $R^2$  and  $p$  value?**

We used Pearson Correlation Coefficient.

**What data was used for the regression?**

The correlation of  $N_{\text{INP}}$  at different temperatures was calculated.

**Check the statistical power of correlating only few data points. Looking at the data in a differential spectrum (see Vali, 1971) might be a better method to identify temperatures where INPs of different origin become active.**

The differential spectrum is good if only few different INP sources contribute (corresponding to clear bumps, i.e., a region of an increase in INP followed by a plateau), which is clearly explained in Welti et al. (2018). We have also used it for the analysis of INP from pollen in a laboratory study in the past (Augustin et al., 2013). In the present study, we only observed very few samples

(roughly 4 samples) with clear bumps at warm temperatures. Therefore, a differential spectrum is not a good way to generally characterize atmospheric INP sources, while it might work well close to strong INP sources or for laboratory studies.

34) P.11 ln.5 The dataset is by far not large enough to construct a robust pdf. The result in Fig.4 is vastly dependent on the choice of intervals to bin the data. The given pdf is therefore not suitable to perform any data analysis as the result could depend on the binning of data.

We deleted Fig. 4.

35) P.12 Fig.4 I suggest to remove Fig.4. It is not illustrating new information that is not already contained in Fig.3 and Fig.5. If you chose to keep Fig.4 check y-axis, the area under the pdf should be 1 or 100%.

We deleted Fig. 4.

PDF=N<sub>i</sub>/N<sub>total</sub>/ΔX.

However, the total area was 1 for sure, but this could not easily be seen as the bin width (ΔX) was far smaller than 1.

36) P.12 ln.6ff Explain how the values in this paragraph were derived. I assume you compare the NINP,PM10 to NINP,PM1 from filters collected during the same time period and take the ratio?

Yes, that is what it is.

Page 12, line 31 was changed to:

“As for the first feature, we calculated the ratio of N<sub>INP</sub> in super-micron size range to N<sub>INP</sub> in PM<sub>10</sub> during the same time period and found that 83±22%, 67±18% and 77±14% (median±standard deviation) of INPs had a diameter of >1 μm at ice activation temperatures of -12, -15, and -18 °C, respectively.”

37) P.13 ln.3ff Last sentence of this paragraph is speculative and repeating for the 6th time in this manuscript that high temperature activity of PM10 filter samples could be due to biological particles. As this seems to be a central point in your interpretation of the data I strongly recommend to experimentally test the heat sensitivity of NINP (eg. following the procedure described in Joly et al., 2014) to support that biological particles are causing the mentioned difference.

Done. See response 32.

38) P.14 ln.1 The difference in NINP (shown in Fig.6 (b)) is clearly visible above -20°C, not only above -17°C.

We said: "INPs that were ice active above  $\sim -17$  °C were activated to cloud droplets to **a large degree**."

The difference in  $N_{INP}$  becomes clearly visible above  $-20$  °C.

Both of the statements are true and we would like to keep it as is.

39) P.14 ln.3f Is there evidence for a substantial fraction of droplets below 10um? Even though no direct observations are available from MV, observations in similar environments could help this discussion. Measurements of orographic cloud droplet distributions e.g. from Hawaii showed a bimodal droplet size spectra with both modes  $>10$ um (Squires, 1958).

We did not measure the cloud droplet size at MV. Indeed, according to laboratory (Chandrakar et al., 2016), model simulation (Igel and Heever, 2017) and field measurements (Miles et al., 2000; Siebert and Shaw, 2017), the cloud droplet size may smaller than 10  $\mu$ m. Even in the Squires (1958), the paper you shared, Fig. 2 and Fig. 3 also indicated that some droplets have size is between 5 to 15  $\mu$ m.

We cited one of the more newly published papers which talked about the droplet size distribution during the early stage of cumulus clouds, which is the closest to our conditions and added the following:

“These observations are consistent with results by Siebert and Shaw (2017) who observed broad cloud droplet size distributions in a size range from  $\sim 5$  to  $25 \mu\text{m}$  in shallow cumulus clouds, with the maximum of the distribution still being below  $10 \mu\text{m}$ .”

40) P.14 ln.5 This speculation is repeated several times throughout the paper but no evidence to support the biological nature of these INPs is presented. Either conduct heat sensitivity experiments and/or provide electron microscope images of large biological particles on the filters to demonstrate that this is a plausible interpretation, or delete the statement.

Done. Please see response 32.

41) P.15 ln.4ff In some cases over 100% difference in  $\text{Na}^+$  and  $\text{Cl}^-$  concentration between the present study and Gioda et al., 2009 seem large and not comparable. In contrast to what other values do the authors think concentrations are comparable?

Thank you for the suggestion. It was changed to:

“Somewhat different values which are still roughly in the same range were reported by Gioda et al. (2009), who found in Puerto Rico the  $\text{Na}^+$  and  $\text{Cl}^-$  concentration in the cloud water varied from 3.79 to 15.53 and 5.90 to 23.20  $\text{mg L}^{-1}$ , with a mean of 10.74 and 15.67  $\text{mg L}^{-1}$ , respectively”

42) P.16 ln.13ff Couldn't  $F_{\text{cloud\_air}}$  be estimated directly from the water collection rate of the CASCC2? This would reduce the uncertainty for the estimation of NINP.

The CASSC2 was sampling all the time while the cloud water sampling was intermittent. Therefore, it is not possible to calculate LWC from CASCC2.

43) P.17 ln.1f Does this range include the error estimation from the INP experiment? The two uncertainties (in  $F_{\text{cloud\_air}}$  and NINP in cloud water) should be combined by error propagation when deriving the range of NINP,air.

This range did not include the error estimation from the INP experiment.

However, the INP experiment uncertainty can safely be assumed to be negligible.

Here is the reason:

Assuming a function contains a multiplication with two variables x and y.

$$f(x, y) = x \cdot y \quad (1)$$

$$\delta f = \sqrt{\left(\frac{\partial f}{\partial x} \delta x\right)^2 + \left(\frac{\partial f}{\partial y} \delta y\right)^2} \quad (2)$$

$$\frac{\partial f}{f} = \sqrt{\left(\frac{\delta x}{x}\right)^2 + \left(\frac{\delta y}{y}\right)^2} \quad (3)$$

Now look at the function,  $N_{INP,air} = F_{cloud\_air} * N_{INP,cloud}$ . The uncertainties of  $F_{cloud\_air}$  is at least 150% if we assume the median droplet diameter is 15  $\mu\text{m}$ , with the variation from 7 to 20  $\mu\text{m}$ . However, the uncertainties of  $N_{INP,cloud}$  have a maximum of 80%, and go down to 40%. In function 3, if

$$\left(\frac{\delta x}{x}\right)^2 \gg \left(\frac{\delta y}{y}\right)^2$$

$$\frac{\partial f}{f} \approx \left(\frac{\delta x}{x}\right)$$

Which means the  $N_{INP,cloud}$  uncertainties are negligible.

44) P.17 ln.3 The uncertainty range spreads over 2 orders of magnitude while the NINP cover 4 orders of magnitude. “general agreement” seems to have limited meaning here. The sensitivity on ddrop when calculating NINP,air from water samples determines the result.

As already suggested above, could the amount of collected cloud water be used to determine  $F_{cloud\_air}$  or to constrain the ddrop range?

We agreed that the results from the calculations are very sensitive to the droplet diameter. However, the calculation based on the given size range of cloud droplet was chosen such that it covers all that can be expected to occur.

Alternatively LWC can be estimated from the CASCC2 collection rate (Sec. 2.3. in Demoz, 1996) for different drop size distributions (that could come from the literature eg. Squires, 1958).

The collection rate from CASCC2 cannot be used to calculate LWC, as explained in question 42.

Another option to estimate LWC might be to use the NaCl content in cloud water and air as a tracer, similar to the method applied in Sec.3.4.

Thanks for your suggestion. We calculated the LWC by using the ratio of NaCl concentration in air to that in cloud water during the same period. We found this ratio varied from  $1.1 \times 10^{-7}$  to  $4.2 \times 10^{-7}$ . The meaning of this ratio is the same as  $F_{\text{cloud\_air}}$  in the paper, but based on different calculation methods. This ratio and  $F_{\text{cloud\_air}}$  are comparable as they are in the same order of magnitude.

We added the following in page 17, line 23:

“To see how reliable these values are, we also examined the following: assuming all sodium chloride particles were activated to cloud droplets,  $F_{\text{cloud\_air}}$  can be also estimated from the ratio of sodium chloride mass concentration in air to that in cloud water. This ratio varied from  $1.1 \times 10^{-7}$  to  $4.2 \times 10^{-7}$ , which is at the lower end but still comparable to  $F_{\text{cloud\_air}}$  as we derived it above.”

45) P.17 ln.5 Instead of the collection efficiency at 3.5  $\mu\text{m}$ , it would be more useful to know the collection efficiency above the cut-off of the PM10 inlet of the filter sampler, where the droplet fraction not collected by the filter sampler but the cloud water collector should be found. According to Demoz, 1996 collection efficiency above 10  $\mu\text{m}$  should be >80%. The high collection efficiency above 10  $\mu\text{m}$  does not support the given explanation for a difference in NINP from filter and cloud water samples which is provided at the beginning of the paragraph (ln.3ff). Revise.

We are under the impression that you think that droplets were collected with through the PM<sub>10</sub> inlet onto filters, which is not the case. So that might already explain why you see an open issue here. The filter sampler providing the data shown in Fig. 7 was run on CVAO, so that potentially all INP were collected. On the other hand, the cloud water sampler, which ran at MV, does have a sampling efficiency below 100% through all sizes, starting with the mentioned 50% at 3.5  $\mu\text{m}$  and, as you said, going up to above 80% at 10  $\mu\text{m}$ . As we were at cloud base often, droplet sizes below 10  $\mu\text{m}$  are to be expected, so that it can be assumed that not all droplets with INP were sampled. Particularly, if smaller droplets are collected with a lower collecting efficiency than larger droplets, the derived concentration will be lower compared to if all droplets were collected.

46) P.18 Eq. (7) and Fig.9 An error estimation for NINP from sea spray by error propagation of input variables in Eq. 7. Include error estimate in Fig.9.

Done.

47) P.18 ln.7 Did you use the individually measured NaCl concentration for each sampling period or the median to calculate the INP concentration in air? What is the range of the NaCl ratio on the right hand side of Eq.7?

The  $\text{NaCl}_{\text{mass,seawater}}$  was very stable, with a median value  $\sim 31 \text{ g L}^{-1}$ .  $\text{NaCl}_{\text{mass,air}}$  showed large variability from  $3.40$  to  $17.76 \mu\text{g m}^{-3}$ , with a median of  $13.08 \mu\text{g m}^{-3}$ . We used the individually measured  $\text{NaCl}_{\text{mass,air}}$  for each sampling period to divide the median  $\text{NaCl}_{\text{mass,seawater}}$ .

48) P.18 ln.10f Related to the previous comment. NINP at Cabo Verde and in the Arctic should be the same only if the NaCl ratio in Eq.7 is also the same. Alternatively, this highlights that the result of Eq.7 is largely insensitive to the NaCl ratio. This should be clarified.

Thanks for your comment. The NaCl ratios were both close to  $10^{-10}$  in this study and in the Arctic. Page 20, lines 2-3 was changed to:

“As discussed in section 3.1,  $\text{N}_{\text{INP}}$  from ULW at Cape Verde are comparable to the Arctic, and the NaCl ratios were close to  $10^{-10}$  in both studies, therefore,  $\text{N}_{\text{INP}}^{\text{sea spray,air}}$  (derived from ULW) are also comparable.”

49) P.19 ln.1-12 It is unclear why enrichment of OC in SML is discussed here as no connection to NINP has been established. I recommend to delete this paragraph. All that can be said is that airborne NINP are higher than whatever NINP could have originated from the ocean.

It is correct that it is not clear to what extent INP are enriched in the SML. But it is very important to at least discuss a possible enrichment of  $\text{N}_{\text{INP}}$  in SML to when information about airborne

concentrations are sought for. After all, we assumed the gap between sea spray  $N_{INP}$  derived from SML in this study and McCluskey et al. (2018a) might be due to differences in the enrichment.

Since previous studies found that INPs in the ocean are associated with organic carbon (Wilson et al., 2015), here we used the enrichment of organic carbon in SML to air as reference. It is also clearly said that this is only an approximation in lack of better data: “It is not clear if INPs are included in the organic carbon for which the enrichment was observed.” The discussion given at the location you refer to here gives the background for one of our main results and we would like to keep it as is.

50) P.20 Fig.10 I suggest to include  $n_s$  for all temperatures covered by your experiments and for filter, water, CVOA, MV separately.

We did not have particle information in the water, so there is no way to calculate  $n_s$  for water samples.

We did also not have an aerosol particle sizer (APS) at MV, which means we do not have information on super-micron particle number or surface area. As the main surface area is typically contributed from super-micron particles, we cannot derive  $n_s$  at MV, either.

Also the box plot clearly shows the  $n_s$  range, even although we only show  $n_s$  at three temperatures. Adding  $n_s$  for all temperatures will not change the results, and instead the new plot would look very crowded (we tried), so that we prefer to keep it as it is.

51) P.20 ln.9 Fig.10 should be motivated by stating what the expected  $n_s$  are (SSA or dust) and then argue that the available  $n_s$  parametrizations are not representative for Cabo Verde. It might be not surprising that  $n_s$  parametrizations that are based on measurements in other environments do not capture the situation at Cabo Verde.

Thanks for your suggestion. We added the following in page 21, line 22:

“In the following, we will compare  $n_s$  derived from our data with that from literature.”

We added the following in page 21, line 32:

“These available  $n_s$  parameterizations from previous literature may not be representative for Cape Verde, but we will still compare with them here.”

Additionally, specify which data of “our data” is shown in Fig.10. Is it filter, water, CVAO or MV? As suggested in the previous comment all of these datasets could be of interest.

We changed this sentence:

“In Fig. 9, we show the surface site density derived for  $N_{INP}$  from CVAO PM<sub>10</sub> filters (as shown by black boxes) following...”

52) P.21 ln.5f Here, the authors could suggest future directions, eg. regional, seasonal  $n_s$  parametrizations or parameterizing  $N_{INP}$  directly from field observations without employing surface area specific activity.

We added the following in page 22, lines 10-14:

“These comparisons to literature raise the question if and how  $n_s$  should be used to parameterize atmospheric INP measurements, which, however, is a question far too prominent to be answered in this study. In general, it is still an open issue to which extent  $N_{INP}$  can be parameterized, based on one or a few parameters, to reliably describe  $N_{INP}$  for different locations around the globe. It might prove necessary to develop separate parameterizations for different locations or air masses, as it was already started for parameterizations based on particle number concentrations (see e.g., DeMott et al. (2010), DeMott et al. (2015) and Tobo et al. (2013)).”

53) P.21 ln.19f Repetition of sentence from p.10 ln.12f. What could be the origin of these supermicron biological particles? Doesn’t the evidence in this paper rather point to super-micron mineral dust?

Please see response 32.

54) P.21 ln.24 Provide evidence for biological particles or include dust as a possible source.

Please see response 32.

55) P.21 ln 26-27 Either, add figures showing both NCCN and PNSD at the two locations during cloud events and non-cloud events and provide difference in PNSD where the CCN active INPs are found, or, point the reader to Fig.8 in the companion paper. Was there a trend in NINP related to the particle types indicated in Fig.8 of the companion paper?

Thanks for your comment. We added “(see Fig. 8 in the companion paper)” in page 23, line 25.

Higher  $N_{INP}$  generally appeared during dust periods and the lower  $N_{INP}$  during marine type periods. High coarse mode particle number concentration is a sign for dust plumes. However, we did not find a good correlation between coarse mode particle number concentration and  $N_{INP}$  and thus did not expand on this topic in the text.

#### Technical corrections

1) p.1 ln.4f SML and ULW might be sources of INPs, but sea and cloud level are compartments of the atmosphere where NINP are measured, not sources. Rephrase.

We replaced “sources” to “compartments”.

2) P.1 ln.7 When mentioning “temperature” be specific in which system the temperature was measured. Here: “trends of EF with temperature.” Temperature of what? Sea water, ambient or in the INP experiment?

It was changed to “with ice nucleation temperature” in page 1, line 7.

3) P.1 ln.8 Same as above. “at any particular temperature” could be understood as if sampling was conducted at different temperatures. The authors should be more specific and say: the temperature to which samples were exposed to in ice nucleation experiment.

We replaced “at any particular temperature” with “at any particular ice nucleation temperature”.

4) P.2 ln.10 Freezing is not the same as ice nucleation. Immersion freezing refers to an ice nucleation mechanism rather than the freezing process. Rephrase.

Following Vali et al. (2015), the term “immersion freezing” can be used in this context: “Immersion freezing refers to ice nucleation initiated by an INP, or equivalent, located within the body of liquid.” In the terminology by Vali et al. (2015), which is followed by many in the community, the one heterogeneous ice nucleation process that needs to be called “ice nucleation” is the deposition ice nucleation, as during that process no liquid water is required.

5) P.2 ln.15 Replace “more effective” with “more active” instead.

Done.

6) P.2 ln.22 Do you mean North African desert?

Yes. We changed “dust” to “desert”.

7) P.2 ln.27 Replace “ice nucleating properties” by “NINP”

Done.

8) P.3 ln.1 Replace “INPs” with “the ice nucleation activity”.

Done.

9) P.3. ln.22 Add: assuming that most INPs activate as CCN.

Done.

10) P.3 ln.23 Specify: “in rain samples”

This is cloud samples, not rain samples. We changed to “in cloud samples”.

11) P.3 ln.31 Replace “for INPs analysis” with “to measure NINP“

We prefer to keep the formulation as it is, as we were not just measuring NINP. We also characterized the INP contributions from the sub- and super-micron range separately and tried to link INP between sea- and cloud-water and in ambient air.

12) P.5 ln.4-6. Repetition of “specially designed”. Delete in line 4-5.

Done.

13) P.5 ln.12 Is there something special about the Digitel filter sampler from the reseller Walter Riemer Messtechnik? If not the manufacturer should be referenced instead.

As far as we understood “Riemer Messtechnik” is the manufacturer (in the sense that the people there make the samplers we use), which is why it was mentioned here. The people from Riemer are the ones who come to us to introduce us to “how to use the instrument”, and whom we contact for problems and repair issues, so Riemer is not a simple reseller.

14) P.5 ln.13 Move (Munktell, MK 360) to after “filters”.

Done.

15) P.8 ln.12 Please add units to variables.

We apologize but it is not clear to us what you want, in this case. We only give a formula, here, with parameters, which are typically given without units (particularly as units might change, as e.g., the number concentration could be given in “per liter” or “per cubic meter” etc.).

16) P.8 ln15 Mention that this sentence refers to individual samples and starting from ln.17 variation between the 9 samples is discussed.

We added, at the end of the first sentence in this paragraph:

“... for both SML and ULW. Note that for each sample a separate INP spectrum is shown.

17) P.8 ln.26 Instead of “This” start the sentence with “The low biological activity in the SML around Cabo Verde”

Done.

18) P.9 Fig.1 Use the same y-axis scale for SML and ULW and include gridlines to facilitate comparing SML to ULW. Consider plotting the data on top of each other.

We changed the y-axis to the same scale. But plotting the data on top of each other is too crowded.

19) P.9 ln.7 Specify if you refer to sampling, or INP experiment technique.

We changed the sentence. Please see page 10, lines 5-10.

20) P.9 ln.10 Delete “the”

Done.

21) P.10 ln.7 “contribute” instead of “contributes”

We deleted Fig. 4. This sentence should also be removed.

22) P.10 ln.7 Replace “few” with “two”

Maybe you mean page 11, line 7. It was changed.

23) P.13 Fig.5 Check unit of y-axis. Should not be %. Add to the figure caption what range is represented by the box and whisker of the boxplot. Due to the limited number of samples it would

be better to just provide the range instead of a boxplot (which requires the assumption of an underlying distribution).

We changed the y-axis label.

The boxes represent the interquartile range. Whiskers represent 10th to 90th percentile. We added this information in the figure caption.

24) P.13 ln.12, 14, 17 Avoid vague qualifiers “more or less”, “only little”, “quite similar”, “mostly” and quantify instead.

Done.

25) P.13 ln.19 Add: “...obvious from Fig.6 that...”

Done.

26) P.14 Fig.6 Add (a) and (b) to the subfigures and add gridlines for easier readability. In the caption put the (a),(b) before describing the subfigure: “... MV PM10 filters during (a) less (cloud time fraction <10%) cloud effected periods and (b) highly...”

Done.

27) P.16 ln.25-28 Give the equation for this calculation.

Done.

28) P.17 Fig.8 First sentence in figure caption is incomplete. Replace “shown by” with “shown as”.

Done.

29) P.18 Fig.9 Caption: “error bars showing” instead “error bars show”

The caption was changed to:

“Atmospheric  $N_{INP}$  are shown as a function of temperature from  $PM_{10}$  filters (black triangles), together with error bars showing the 95% confidence interval.”

30) P.19 ln.26-28 Revise structure of sentence.

It was reformulated to:

“On the other hand, mineral dust is associated with a factor of 1000 higher ice surface site density (a measure to describe the ice activity per particle surface area), compared to SSA (Niemand et al., 2012; DeMott et al., 2016; McCluskey et al., 2018a).”

31) P.19 ln.31 Add: “... ice activity of super-micron mineral dust...”

This would not be correct, as also smaller dust particles can be ice active. Nothing changed.

32) P.20 ln.5 Add: “... associated with biological particles, but has also been observed for supermicron dust samples (Hoose and Möhler, 2012).”

Samples CVAO 1596, CVAO 1641 and CVAO 1643 were heated to 95 °C for 1 hour and a great reduction of  $N_{INP}$  was observed. We revised this whole paragraph, and the sentence you refer to here was deleted, so please refer to the new version of manuscript.

33) P.21 ln.4 You could add: “... do not originate from sea spray, but are dominated by supermicron dust.”

We changed to: “do not originate from sea spray, but are dominated by super-micron dust and/or biological particles.”

34) P.21 ln.9 Instead of “thorough analysis” specify what kind of analysis is shown in the companion paper.

As this is the summary of the present work and not the companion paper, this would make the summary unnecessarily longish. It is mentioned in more detail in the text above what was done in the companion paper, which should suffice, and we would therefore like to leave it as is.

35) P.21 ln.13f Freezing experiments with the devices used for this study should give reliable data up to 0°C and not “roughly” from below -5°C.

In this study, we got  $N_{INP}$  from roughly -5 to -25 °C. So technically you are correct, but in fact it is only this reduced range for the present study, which we talk about in this sentence.

36) P.21 ln.15f Revise after correcting Sec. 3.1.

Done.

37) P.21 ln.21ff Revise after correcting Sec. 3.2.1.

We added the results of the heat treatment to the summary.

38) P.21 ln.25 “quite similar” should be put into perspective based on the limited number of investigated samples.

Changed to: “As MV was in clouds most of the time, only two filters could be collected on MV that were affected by cloud for less than 10% of the sampling time. For these,  $N_{INP}$  were similar at CVAO and MV.”

39) P.21 ln.30f Revise after correcting Sec. 3.3.2

Sec. 3.3.2 did not need any changes that would cause a revision here.

## Reference

Agogué, H., Casamayor, E. O., Joux, F., Obernosterer, I., Dupuy, C., Lantoine, F., Catala, P., Weinbauer, M. G., Reinthaler, T., Herndl, G. J., and Lebaron, P.: Comparison of samplers for the biological characterization of the sea surface microlayer, *Limnology and Oceanography: Methods*, 2, 213-225, 10.4319/lom.2004.2.213, 2004.

Aller, J. Y., Radway, J. C., Kilthau, W. P., Bothe, D. W., Wilson, T. W., Vaillancourt, R. D., Quinn, P. K., Coffman, D. J., Murray, B. J., and Knopf, D. A.: Size-resolved characterization of the polysaccharidic and proteinaceous components of sea spray aerosol, *Atmospheric Environment*, 154, 331-347, <https://doi.org/10.1016/j.atmosenv.2017.01.053>, 2017.

Augustin, S., Wex, H., Niedermeier, D., Pummer, B., Grothe, H., Hartmann, S., Tomsche, L., Clauss, T., Voigtländer, J., Ignatius, K., and Stratmann, F.: Immersion freezing of birch pollen washing water, *Atmos. Chem. Phys.*, 13, 10989-11003, 10.5194/acp-13-10989-2013, 2013.

Chandrakar, K. K., Cantrell, W., Chang, K., Ciochetto, D., Niedermeier, D., Ovchinnikov, M., Shaw, R. A., and Yang, F.: Aerosol indirect effect from turbulence-induced broadening of cloud-droplet size distributions, *Proceedings of the National Academy of Sciences*, 113, 14243-14248, 10.1073/pnas.1612686113, 2016.

DeMott, P. J., Prenni, A. J., Liu, X., Kreidenweis, S. M., Petters, M. D., Twohy, C. H., Richardson, M. S., Eidhammer, T., and Rogers, D. C.: Predicting global atmospheric ice nuclei distributions and their impacts on climate, *Proceedings of the National Academy of Sciences*, 107, 11217-11222, 10.1073/pnas.0910818107, 2010.

DeMott, P. J., Prenni, A. J., McMeeking, G. R., Sullivan, R. C., Petters, M. D., Tobo, Y., Niemand, M., Möhler, O., Snider, J. R., Wang, Z., and Kreidenweis, S. M.: Integrating laboratory and field data to quantify the immersion freezing ice nucleation activity of mineral dust particles, *Atmos. Chem. Phys.*, 15, 393-409, 10.5194/acp-15-393-2015, 2015.

DeMott, P. J., Hill, T. C. J., McCluskey, C. S., Prather, K. A., Collins, D. B., Sullivan, R. C., Ruppel, M. J., Mason, R. H., Irish, V. E., Lee, T., Hwang, C. Y., Rhee, T. S., Snider, J. R., McMeeking, G. R., Dhaniyala, S., Lewis, E. R., Wentzell, J. J. B., Abbatt, J., Lee, C., Sultana, C. M., Ault, A. P., Axson, J. L., Diaz Martinez, M., Venero, I., Santos-Figueroa, G., Stokes, M. D., Deane, G. B., Mayol-Bracero, O. L., Grassian, V. H., Bertram, T. H., Bertram, A. K., Moffett, B.

F., and Franc, G. D.: Sea spray aerosol as a unique source of ice nucleating particles, *Proceedings of the National Academy of Sciences*, 113, 5797-5803, 10.1073/pnas.1514034112, 2016.

Demoz, B. B., Collett, J. L., and Daube, B. C.: On the Caltech Active Strand Cloudwater Collectors, *Atmospheric Research*, 41, 47-62, [https://doi.org/10.1016/0169-8095\(95\)00044-5](https://doi.org/10.1016/0169-8095(95)00044-5), 1996.

Gioda, A., Mayol-Bracero, O. L., Morales-García, F., Collett, J., Decesari, S., Emblico, L., Facchini, M. C., Morales-De Jesús, R. J., Mertes, S., Borrmann, S., Walter, S., and Schneider, J.: Chemical Composition of Cloud Water in the Puerto Rican Tropical Trade Wind Cumuli, *Water, Air, and Soil Pollution*, 200, 3-14, 10.1007/s11270-008-9888-4, 2009.

Gong, X., Wex, H., Müller, T., Wiedensohler, A., Höhler, K., Kandler, K., Ma, N., Dietel, B., Schiebel, T., Möhler, O., and Stratmann, F.: Characterization of aerosol properties at Cyprus, focusing on cloud condensation nuclei and ice-nucleating particles, *Atmos. Chem. Phys.*, 19, 10883-10900, 10.5194/acp-19-10883-2019, 2019.

Haight, F. A.: *Handbook of the Poisson distribution*, 1967.

Igel, A. L., and Heever, S. C. v. d.: The Importance of the Shape of Cloud Droplet Size Distributions in Shallow Cumulus Clouds. Part II: Bulk Microphysics Simulations, *Journal of the Atmospheric Sciences*, 74, 259-273, 10.1175/jas-d-15-0383.1, 2017.

McCluskey, C. S., Hill, T. C. J., Humphries, R. S., Rauker, A. M., Moreau, S., Strutton, P. G., Chambers, S. D., Williams, A. G., McRobert, I., Ward, J., Keywood, M. D., Harnwell, J., Ponsonby, W., Loh, Z. M., Krumbel, P. B., Protat, A., Kreidenweis, S. M., and DeMott, P. J.: Observations of Ice Nucleating Particles Over Southern Ocean Waters, *Geophysical Research Letters*, 45, 11,989-911,997, 10.1029/2018GL079981, 2018a.

McCluskey, C. S., Ovadnevaite, J., Rinaldi, M., Atkinson, J., Belosi, F., Ceburnis, D., Marullo, S., Hill, T. C. J., Lohmann, U., Kanji, Z. A., O'Dowd, C., Kreidenweis, S. M., and DeMott, P. J.: Marine and Terrestrial Organic Ice-Nucleating Particles in Pristine Marine to Continentally Influenced Northeast Atlantic Air Masses, *Journal of Geophysical Research: Atmospheres*, 123, 6196-6212, doi:10.1029/2017JD028033, 2018b.

Miles, N. L., Verlinde, J., and Clothiaux, E. E.: Cloud Droplet Size Distributions in Low-Level Stratiform Clouds, *Journal of the Atmospheric Sciences*, 57, 295-311, 10.1175/1520-0469(2000)057<0295:cdsdl>2.0.co;2, 2000.

O'Sullivan, D., Adams, M. P., Tarn, M. D., Harrison, A. D., Vergara-Temprado, J., Porter, G. C. E., Holden, M. A., Sanchez-Marroquin, A., Carotenuto, F., Whale, T. F., McQuaid, J. B., Walshaw, R., Hedges, D. H. P., Burke, I. T., Cui, Z., and Murray, B. J.: Contributions of biogenic material to the atmospheric ice-nucleating particle population in North Western Europe, *Scientific Reports*, 8, 13821, 10.1038/s41598-018-31981-7, 2018.

Siebert, H., and Shaw, R. A.: Supersaturation Fluctuations during the Early Stage of Cumulus Formation, *Journal of the Atmospheric Sciences*, 74, 975-988, 10.1175/jas-d-16-0115.1, 2017.

Squires, P.: The Microstructure and Colloidal Stability of Warm Clouds, *Tellus*, 10, 256-261, 10.1111/j.2153-3490.1958.tb02011.x, 1958.

Tobo, Y., Prenni, A. J., DeMott, P. J., Huffman, J. A., McCluskey, C. S., Tian, G., Pöhlker, C., Pöschl, U., and Kreidenweis, S. M.: Biological aerosol particles as a key determinant of ice nuclei populations in a forest ecosystem, *Journal of Geophysical Research: Atmospheres*, 118, 10,100-110,110, 10.1002/jgrd.50801, 2013.

Vali, G., DeMott, P. J., Möhler, O., and Whale, T. F.: Technical Note: A proposal for ice nucleation terminology, *Atmos. Chem. Phys.*, 15, 10263-10270, 10.5194/acp-15-10263-2015, 2015.

Welti, A., Müller, K., Fleming, Z. L., and Stratmann, F.: Concentration and variability of ice nuclei in the subtropical maritime boundary layer, *Atmospheric Chemistry and Physics*, 18, 5307-5320, 2018.

Wex, H., Huang, L., Zhang, W., Hung, H., Traversi, R., Becagli, S., Sheesley, R. J., Moffett, C. E., Barrett, T. E., Bossi, R., Skov, H., Hünerbein, A., Lubitz, J., Löffler, M., Linke, O., Hartmann, M., Herenz, P., and Stratmann, F.: Annual variability of ice-nucleating particle concentrations at different Arctic locations, *Atmos. Chem. Phys.*, 19, 5293-5311, 10.5194/acp-19-5293-2019, 2019.

Wilson, T. W., Ladino, L. A., Alpert, P. A., Breckels, M. N., Brooks, I. M., Browse, J., Burrows, S. M., Carslaw, K. S., Huffman, J. A., Judd, C., Kilthau, W. P., Mason, R. H., McFiggans, G., Miller, L. A., Najera, J. J., Polishchuk, E., Rae, S., Schiller, C. L., Si, M., Temprado, J. V., Whale, T. F., Wong, J. P. S., Wurl, O., Yakobi-Hancock, J. D., Abbatt, J. P. D., Aller, J. Y., Bertram, A. K., Knopf, D. A., and Murray, B. J.: A marine biogenic source of atmospheric ice-nucleating particles, *Nature*, 525, 234-238, 10.1038/nature14986, 2015.





# Characterization of aerosol particles at Cape Verde close to sea and cloud level heights - Part 2: ice nucleating particles in air, cloud and seawater

Xianda Gong<sup>1</sup>, Heike Wex<sup>1</sup>, Manuela van Pinxteren<sup>1</sup>, Nadja Triesch<sup>1</sup>, Khamneh Wadinga Fomba<sup>1</sup>, Jasmin Lubitz<sup>1</sup>, Christian Stolle<sup>2,3</sup>, Tiera-Brandy Robinson<sup>3</sup>, Thomas Müller<sup>1</sup>, Hartmut Herrmann<sup>1</sup>, and Frank Stratmann<sup>1</sup>

<sup>1</sup>Leibniz Institute for Tropospheric Research, Leipzig, Germany

<sup>2</sup>Leibniz-Institute for Baltic Sea Research Warnemünde (IOW), Rostock, Germany

<sup>3</sup>Institute for Chemistry and Biology of the Marine Environment, University of Oldenburg, Wilhelmshaven, Germany

**Correspondence:** Xianda Gong (gong@tropos.de)

**Abstract.** Ice nucleating particles (INPs) in the troposphere can form ice in clouds via heterogeneous ice nucleation. Yet, atmospheric number concentrations of INPs ( $N_{INP}$ ) are not well characterized and although there is some understanding of their sources, it is still unclear to what extend different sources contribute, nor if all sources are known. In this work, we examined properties of INPs at Cape Verde from different sourcescompartments, the oceanic sea surface microlayer (SML) and underlying water (ULW), the atmosphere close to both sea and cloud level as well as cloud water.

Both enrichment and depletion of  $N_{INP}$  in SML compared to ULW were observed. The enrichment factor (EF) varied from roughly 0.4 to 11, and there was no clear trend in EF with ice nucleation temperature.

$N_{INP}$  in  $PM_{10}$  sampled at Cape Verde Atmospheric Observatory (CVAO) at any particular ice nucleation temperature spanned around 1 order of magnitude below  $-15^{\circ}C$ , and about 2 orders of magnitude at warmer temperatures ( $>-12^{\circ}C$ ).  $N_{INP}$  in  $PM_1$  were generally lower than those in  $PM_{10}$  at CVAO. About  $83\pm22\%$ ,  $67\pm18\%$  and  $77\pm14\%$  (median $\pm$ standard deviation) of INPs had a diameter  $>1\ \mu m$  at ice activationnucleation temperatures of  $-12$ ,  $-15$ , and  $-18\ ^{\circ}C$ , respectively. Among the 17  $PM_{10}$  samples at CVAO, three  $PM_{10}$  filters showed elevated  $N_{INP}$  at warm temperatures, e.g., above  $0.01\ \text{std L}^{-1}$  at  $-10\ ^{\circ}C$ . After heating samples at  $95\ ^{\circ}C$  for 1 hour, the elevated  $N_{INP}$  at the warm temperatures disappeared, indicating that these highly ice active INPs were most likely biological particles. However, for  $N_{INP}$  in  $PM_1$  at CVAO, this is not the case.  $PM_1$  at CVAO did not show such elevated  $N_{INP}$  at warm temperatures. At these higher temperatures, often biological particles have been found to be ice active. Consequently, the difference in  $N_{INP}$  between  $PM_1$  and  $PM_{10}$  at CVAO suggests that biological ice active particles were present in the super-micron size range.

$N_{INP}$  in  $PM_{10}$  at CVAO was found to be similar to that on Monte Verde (MV, at 744 m a.s.l) during non-cloud events. During cloud events, most INPs on MV were activated to cloud droplets. When highly ice active particles were present in  $PM_{10}$  filters at CVAO, they were not observed in  $PM_{10}$  filters on MV, but in cloud water samples, instead. This is direct evidence that these INPs which are likely biological are activated to cloud droplets during cloud events.

In general, Cape Verde was often affected by dust from the Saharan desert during our measurement. For the observed air masses, atmospheric  $N_{INP}$  in air fit well to the concentrations observed in cloud water. When comparing concentrations of both sea salt and INPs in both seawater and  $PM_{10}$  filters, it can be concluded that sea spray aerosol (SSA) only contributed a minor fraction to the atmospheric  $N_{INP}$ . Therefore it can be said that, unless there would be a significant enrichment of  $N_{INP}$  during the formation of SSA particles,  $N_{INP}$  was mainly dominated by mineral dust at cold temperatures with few contributions from possible biological particles at warmer temperatures. This latter conclusion still holds when accounting for an enrichment of organic carbon in super-micron particles during sea spray generation as reported in literature.

## 1 Introduction

Ice particle formation in tropospheric clouds can affect cloud properties such as cloud lifetime, their radiative effects on the atmosphere, and the formation of precipitation (Hoose and Möhler, 2012; Murray et al., 2012). Ice crystals in the atmosphere can be formed either via homogeneous nucleation below  $-38^{\circ}\text{C}$  or heterogeneous nucleation aided by aerosol particles known as ice nucleating particles (INPs) at warmer temperatures ( $>-38^{\circ}\text{C}$ ) via heterogeneous nucleation aided by aerosol particles known as ice nucleating particles (INPs) at any temperature below  $0^{\circ}\text{C}$ . Immersion freezing refers to the process when an INP becomes immersed in an aqueous solution e.g., through the process of cloud droplet activation (Vali et al., 2015). Immersion freezing is suggested to be the most important freezing process for mixed phase clouds (Ansmann et al., 2008; Westbrook and Illingworth, 2013), and is the process we will focus on in this study.

Dust particles are recognized as effective INPs below  $-20^{\circ}\text{C}$  (Augustin-Bauditz et al., 2014) or even below  $-15^{\circ}\text{C}$  (Hoose and Möhler, 2012; Murray et al., 2012). Submicron dust particles are recognized as effective INPs below  $-20^{\circ}\text{C}$  (Augustin-Bauditz et al., 2014) and super-micron dust particles were reported to be ice active even up to  $-10^{\circ}\text{C}$  (Hoose and Möhler, 2012; Murray et al., 2012). Laboratory studies on natural mineral dusts from different regions have been conducted to quantify the particle's ability to nucleate ice (Niemand et al., 2012; DeMott et al., 2015). Mineral dust particles from deserts are composed of a variety of minerals, and K-feldspar is supposed to be more effective for ice nucleation than other minerals in the mixed-phase cloud temperature regime (Atkinson et al., 2013; Augustin-Bauditz et al., 2014; Niedermeier et al., 2015). However, overall, desert dust particles from diverse sources show comparable ice nucleating efficiency (Boose et al., 2016). Boose et al. (2016) found that ice activity of desert dust particles at temperatures between  $-35$  and  $-28^{\circ}\text{C}$  can be attributed to the sum of the feldspar and quartz content. A high clay content, in contrast, was associated with lower ice nucleation activity. In contrast to field measurements, in laboratory studies often separate types of mineral dusts are examined. Different parameterizations have been employed to summarize the mineral dust particle's ice nucleating ability (Niemand et al., 2012; Ullrich et al., 2017).

A few field measurements have been carried out to quantify the ice nucleation properties of desert dust. Based on airborne measurements, DeMott et al. (2003) found that ice nucleating aerosol particles in air masses over Florida had sources from the North African dust desert. Chou et al. (2011) observed a good correlation between the number concentration of larger particles and INP number concentration ( $N_{INP}$ ) during a Saharan dust event at the Jungfraujoch in the Swiss Alps. Collecting airborne dust over the Saharan desert, Price et al. (2018) observed two orders of magnitude variability in  $N_{INP}$  at any particular

temperature from  $\sim -13$  to  $\sim -25$   $^{\circ}\text{C}$ , which was related to the variability in atmospheric dust loading. ~~while desert dust's ice-nucleating activity was only weakly dependent on the differences in desert sources. This desert dust's ice nucleating activity was only weakly dependent on differences in desert sources, i.e., on the differences in mineral composition that particles emitted from different locations in the desert may have.~~ Schrod et al. (2017) found that mineral dust or a constituent related to dust was a major contributor to ~~the ice nucleating properties~~  $N_{\text{INP}}$  of the aerosol on Cyprus, and  $N_{\text{INP}}$  in elevated dust plumes was on average a factor of 10 higher than  $N_{\text{INP}}$  at ground level, ~~where the dust loading was lower.~~

Ocean water can be a potential source of INPs (Brier and Kline, 1959) ~~which would originate from the biosphere~~. The source of INPs in ocean water might be associated with phytoplankton blooms (Schnell and Vali, 1976). Recently, Wilson et al. (2015) and Irish et al. (2017) found that organic material, with a diameter  $<0.2$   $\mu\text{m}$ , is the major ice nucleator in the sea surface microlayer (SML). Based on a long-term measurement of INPs in the marine boundary layer in the south of and around Australia, Bigg (1973) suggested that INPs in ambient air ~~were contributed by marine aerosol particles were from a distant land source, or from a stratospheric source, and brought to sea level by convective mixing.~~ Schnell and Vali (1976) suggested a marine source could explain the observations of Bigg (1973). DeMott et al. (2016) found that ~~INPs~~ ~~the ice nucleation activity~~ from laboratory generated sea spray aerosol (SSA) aligned well with measurements from diverse regions over the oceans. ~~Further evidence of~~ ~~Furthermore~~, a connection between marine biological activity and  $N_{\text{INP}}$  was uncovered in their laboratory study (DeMott et al., 2016). In pristine marine conditions, such as the Southern Ocean, SSA was the main source of the INP population, but  $N_{\text{INP}}$  was relatively low in the Southern Ocean as well as in the clean marine Northeast Atlantic (McCluskey et al., 2018a, b). These field measurements are consistent with the model work by Burrows et al. (2013), which emphasizes the importance of SSA contribution to INPs in remote marine regions.

It is currently still uncertain whether the coarse mode particles or smaller particles are the major source of atmospheric INPs. Vali (1966) found that the diameters of INPs were mostly between 0.1 and 1  $\mu\text{m}$ . On the high alpine research station Jungfraujoch, Mertes et al. (2007) found that ice residuals were as small as 300 nm and they were mostly present in the submicron particle size range. ~~Modeling studies also suggest that INP are a temperature dependent fraction of all particles with sizes above 500 nm~~ ~~Simultaneous measurements of  $N_{\text{INP}}$  and particle number size distributions were used to develop parameterizations in which~~  $N_{\text{INP}}$  depends on a temperature dependent fraction of all particles with sizes above 500 nm (DeMott et al., 2010, 2015). Conen et al. (2017) found INPs at  $-8$   $^{\circ}\text{C}$  were equally distributed amongst the particles with sizes up to 2.5  $\mu\text{m}$  and with sizes between 2.5 and 10  $\mu\text{m}$ . Other field measurements reported that coarse mode particles were more efficient INP, e.g., INPs (mainly bacterial aggregates and fungal spores) occurred in the size range of 2 - 6  $\mu\text{m}$  (Huffman et al., 2013). Mason et al. (2016) found for Arctic aerosol that  $91 \pm 9\%$ ,  $79 \pm 17\%$ , and  $63 \pm 21\%$  of INPs had an aerodynamic diameter of  $>1$   $\mu\text{m}$  at ice activation temperatures of  $-15$ ,  $-20$ , and  $-25$   $^{\circ}\text{C}$ , respectively. Creamean et al. (2018) also found that super-micron or coarse mode particles are the most proficient INPs at warmer temperatures in the Arctic ~~boundary layer~~ and they might be biological INPs. Concerning biological INP, it should be mentioned that it is well understood by now that these feature macromolecules of only some ten nanometers in size at the most (Pummer et al., 2015). Some of them are easily separated from their carrier (e.g., from pollen and fungal spores), while others are embedded in the cell membrane (e.g., for bacteria), ~~but based on these above cited literature results, it seems that most of the biological INPs still occur together with their original carrier in the atmosphere~~ ~~but based on the fact~~

that most atmospheric INPs seem to be super-micron in size, as observed in the above cited literature, it seems that most of the biological ice active macromolecules still occur together with their original carrier in the atmosphere.

Direct measurement of  $N_{INP}$  in the cloud water can be used to estimate concentrations of INPs in the air assuming that most INPs activate as CCN. Joly et al. (2014) measured total and biological (i.e., heat-sensitive) INPs between  $-5$  to  $-14$   $^{\circ}\text{C}$  in 5 cloud samples from the summit of Puy de Dôme (1465 m a.s.l., France). Petters and Wright (2015) summarized many INP spectra obtained from rain water, melted sleet, snow and hail samples at different sampling locations and reported a range of  $N_{INP}$  for these precipitation samples. Based on a shipborne measurement of the east coast of Nova Scotia, Canada, Schnell 10 (1977) directly compared  $N_{INP}$  in the seawater to that in the fog water and found that  $N_{INP}$  in fog water and seawater appeared to vary quite independently of each other. As one part of the here presented study, these field measurement values will be compared with values obtained from our measurement campaign in the framework of the MarParCloud (Marine biological production, organic aerosol particles and marine clouds: a Process Chain) project.

During the MarParCloud project, samples collected for INPs analysis include: SML and underlying water (ULW) from the ocean upwind of the island; quartz fiber filter samples of atmospheric aerosol, collected on a tower installed at the island shore (inlet height: 42 m a.s.l) and on a mountaintop (inlet height: 746 m a.s.l); and cloud water collected during cloud events 15 on the mountaintop. In this study, we will first discuss  $N_{INP}$  in the SML and ULW. We will then discuss  $N_{INP}$  in the air, including a comparison of  $N_{INP}$  in  $PM_{10}$  and  $PM_1$  and a comparison of  $N_{INP}$  close to both sea and cloud level. Lastly,  $N_{INP}$  in the cloud water will be discussed. In addition, we will provide a feasible way to link  $N_{INP}$  in ambient air, ocean water and 20 cloud water. This connection can be drawn only during times when there were cloud events on the mountaintop, together with data on number concentrations on cloud condensation nuclei ( $N_{CCN}$ ). Respective information was derived and discussed in an accompanying paper (Gong et al., 2019b). For more information about the campaign itself, we refer to an upcoming overview paper by van Pinxteren et al.

## 2 Experiment and methods

### 2.1 Sampling sites and sample types

#### 2.1.1 Sampling site

25 The measurements were carried out The measurement campaign was carried out on São Vicente island at Cape Verde from 13 September to 13 October, 2017. We set up three measurement stations at Cape Verde, at the Cape Verde Atmospheric Observatory (CVAO), on Monte Verde (MV) and an Ocean Station (OS). CVAO ( $16^{\circ}51'49$  N,  $24^{\circ}52'02$  W) is located in the northwest  
northeastern shore of the island of São Vicente, 70 m from the coastline about 10 m a.s.l. Filter samplers were installed on 30 top of a 32 m tower. MV ( $16^{\circ}52'11$  N,  $24^{\circ}56'02$  W) is located on a mountaintop (744 m a.s.l),  $\sim$ 7 km away to the west of CVAO. Filter samplers were situated on the ground with the inlet 2 m above the bottom, upwind of any installations on the mountaintop. The OS covered an area at  $\sim$  $16^{\circ}53'30$  N,  $\sim$  $24^{\circ}54'00$  W, with a distance of at least 5 km from the island. Details on the measurement site and the meteorological conditions can be found in the accompanying paper (Gong et al., 2019b). In

short, the conditions at Cape Verde were quite stable, with temperature of on average 26.6 °C at CVAO and 21.2 °C at MV and wind speeds between 0.6 and 9.7 m s<sup>-1</sup> with directions from the northeast.

In the following, the different samples collected during the campaign are described in detail. All of these samples were stored at -20 °C right after sampling. After the campaign the long-term storage and transport of the collected samples from 5 Cape Verde to the Leibniz Institute for Tropospheric Research (TROPOS), Germany was carried out in a cooled container at -20 °C. At TROPOS, all samples were again stored frozen at -20 °C until analysis was done. Measurement sites, locations, sample types and additional information are summarized in Tab. 1.

**Table 1.** Measurement sites, locations, sample types and measurement instruments.

Measurement site	Location	Sample type	Instrument
CVAO	16°51'49 N, 24°52'02 W	PM <sub>1</sub> quartz fiber filter	INDA
	inlet height: 42 m a.s.l	PM <sub>10</sub> quartz fiber filter	INDA
MV	16°52'11 N, 24°56'02 W	PM <sub>10</sub> quartz fiber filter	INDA
	inlet height: 746 m a.s.l	Cloud water	LINA, INDA
OS	~16°53'30 N, ~24°54'00 W	SML	LINA, INDA
		ULW	LINA, INDA

Following the description of the sampling, we will briefly introduce the measurement methods related to INPs, including freezing devices,  $N_{INP}$  calculation and measurement uncertainties. Note that all the times presented here are in UTC (corresponding to local time +1). For better comparison, all ambient particle number concentrations in this study are given for 10 standard temperature and pressure (STP, 0 °C and 1013.25 hPa).

### 2.1.2 Seawater sampling

Seawater samples were taken at the OS by using a fishing boat at a distance of at least 5 km from the coast (off-shore samples). The SML samples were collected using a glass plate sampler (Harvey and Burzell, 1972; Irish et al., 2017; van Pinxteren et al., 15 2017). The glass plate had a surface area of 2000 cm<sup>-2</sup> and was immersed vertically into the ocean and then withdrawn at a slow rate (between 5 to 10 cm s<sup>-1</sup>) and allowed to drain for less than 5 s. The surface film adhering to the surface of the glass was scraped off from both sides of the glass plate with a framed Teflon wiper into a 1 liter glass bottle. For each SML sample, several liters were collected and 1 liter was required ~55 dips. Based on the amount of material collected, the number of dips and the area of the plate, the averaged thickness of the layer collected was calculated as ~91.0 µm. ULW samples 20 were collected at the same time and location as the SML samples. ULW was collected from a depth of 1 m by [a specially designed device, which consists of](#) a glass bottle mounted on a telescopic rod in order to monitor sampling depth. The bottle was opened underwater at the intended sampling depth with a specifically designed seal-opener. After collection, the glass bottles

containing both the SML and ULW samples were kept in a freezer at  $-20\text{ }^{\circ}\text{C}$  up to the analysis. During the campaign, 9 SML and 9 ULW samples were collected for INP analysis. Details of SML and ULW samples, including the sampling time, location, salinity and additional information are provided in the supplement, Tab. S1.

### 2.1.3 Aerosol particle sampling

5 Particle sampling was done using high-volume samplers with either a  $\text{PM}_{10}$ -inlet and or a  $\text{PM}_1$ -inlet (Digitel filter sampler DHA-80, Walter Riemer Messtechnik, Germany) operating with an average flow rate of  $\sim 500\text{ L min}^{-1}$  for 24 hours sampling periods. The high-volume samples were collected on 150 mm in diameter quartz fiber filters (Munktell, MK 360) filters with an effective sampling area of 140 mm in diameter. The filters were preheated in our laboratory at  $110\text{ }^{\circ}\text{C}$  for 24 hours to remove the organic carbon background. After sampling, the filters were transported to a freezer where they were kept at  $-20$   
10  $^{\circ}\text{C}$ . For INP analysis, a fractioncircular piece of these filters of 2  $\text{cm}^2$  cm in diameter was used from which then smaller pieces were punched out for the analysis (see section 2.2). From CVAO, there were 17 and 19 filters from  $\text{PM}_{10}$  and  $\text{PM}_1$  collection (CVAO  $\text{PM}_{10}$  and CVAO  $\text{PM}_1$ ), respectively, and at MV, 17 filters were collected for  $\text{PM}_{10}$  (MV  $\text{PM}_{10}$ ). Field blind filters were obtained by inserting clean filters into the Digitel sampler for a period of 24 hours without loading them. Three blind filters were collected during this campaign. Details of filter samples, including sampling time, duration, total volume and additional  
15 information can be found in the supplement, Tab. S2 (CVAO  $\text{PM}_{10}$ ), Tab. S3 (CVAO  $\text{PM}_1$ ) and Tab. S4 (MV  $\text{PM}_{10}$ ).

### 2.1.4 Cloud water sampling

During the campaign, MV was in clouds roughly 58% of the time (a detailed analysis on this can be found in Gong et al. (2019b)). Cloud water was collected with CASCC2 (Caltech Active Strand Cloud Collector Version 2) at MV. All cloud drop sizes were collected in one bulk sample. Drops were collected by inertial impaction on Teflon strands with a diameter of 508  
20  $\mu\text{m}$ . The 50% lower size cut for the CASCC2 was approximately  $3.5\text{ }\mu\text{m}$  diameter. The flow rate through the CASCC2 was approximately  $5.8\text{ m}^3\text{ min}^{-1}$ . The CASCC2 is described in more details in Demoz et al. (1996). Between cloud events, the cloud water sampler was cleaned with a large amount ( $\sim 5\text{ L}$ ) of ultrapure water. Once the collector was cleaned, a blank was taken by spraying about 200 mL of ultrapure water into the collection strands in the collector and subsequent sampling of this water. After collection, the cloud water samples were kept in a freezer at  $-20\text{ }^{\circ}\text{C}$ . During the campaign, 13 cloud samples were  
25 collected for INP analysis. The details of cloud samples, including sampling time, duration, volume and additional information are provided in the supplement, Tab. S5.

## 2.2 Freezing devices

Two droplet freezing devices called LINA (Leipzig Ice Nucleation Array) and INDA (Ice Nucleation Droplet Array) have been set up at TROPOS in Germany. The design of LINA was inspired by Budke and Koop (2015). Briefly, 90 droplets with the  
30 volume of  $1\text{ }\mu\text{L}$  were pipetted from the samples onto a thin hydrophobic glass slide, with each droplet being placed separately into its own compartment. After pipetting, the compartments were sealed at the top with another glass slide, to prevent the

droplets from evaporation and to prevent ice seeding from neighboring droplets. The droplets were cooled on a Peltier element with a cooling rate of  $1 \text{ K min}^{-1}$  down to  $-35 \text{ }^{\circ}\text{C}$ , while the setup was illuminated by a circular light source from above. Once the cooling started, pictures were taken every 6 s by a camera. The number of frozen versus unfrozen droplets was derived automatically by an image identification program in Python. LINA was employed to measure SML, ULW and cloud water samples in this study. More detailed parameters and the temperature calibration of LINA and its application can be found in previous studies (Chen et al., 2018; Gong et al., 2019a).

The design of INDA was inspired by Conen et al. (2012), but deploying PCR-trays instead of separate tubes. For quartz fiber filters, circular pieces with a diameter of 1 mm were punched out. Each of the 96 wells of a PCR-tray were filled with the filter piece together with  $50 \mu\text{L}$  of ultrapure water. For SML, ULW and cloud water samples,  $50 \mu\text{L}$  of the water samples was filled into each PCR-tray. After sealing by a transparent foil, the PCR-tray was placed on a sample holder and immersed into a bath thermostat, where it was illuminated from below with a LED light source. The bath thermostat then decreased the temperature with a cooling rate of approximately  $1 \text{ K min}^{-1}$ . Real-time images of the PCR-tray were recorded every 6 s by a CCD (charge-coupled device) camera. Frozen droplets can be identified based on the brightness change during the freezing process. A program recorded the actual temperature of the cooling bath and related it to the real-time images from the CCD camera. The temperature in the PCR-trays had been calibrated. More detailed parameters and temperature calibration of INDA and its application can be found in previous studies (Chen et al., 2018; Hartmann et al., 2019).

## 2.3 Deriving $N_{\text{INP}}$

### 2.3.1 Basic calculation

Based on Vali (1971), the cumulative concentration of INP ( $N_{\text{INP}}$ ) as a function of temperature per air or water volume can be calculated by:

$$N_{\text{INP}}(\theta) = \frac{-\ln(1 - f_{\text{ice}}(\theta))}{V} \quad (1)$$

with

$$f_{\text{ice}}(\theta) = \frac{N(\theta)}{N_{\text{total}}} \quad (2)$$

where  $N_{\text{total}}$  is the number of droplets and  $N(\theta)$  is the number of frozen droplets at temperature  $\theta$ . Eq. 1 accounts for the possibility of the presence of multiple INPs in one vial by assuming that INPs are Poisson distributed. This way, the cumulative number of INP active at any temperature will be obtained although only the most ice active INP (nucleating ice at the highest temperature) present in each droplet/well will be observed. As for the quartz fiber filters,  $V$  is the volume of air collected onto one circular 1 mm filter piece placed in each well, resulting in airborne  $N_{\text{INP}}$ . The information of the air volume can be found in the supplement, Tab. S2, Tab. S3 and Tab. S4. As for the SML, ULW and cloud water,  $V$  is the volume of droplet/well ( $V_{\text{LINA}}=1 \mu\text{L}$ ,  $V_{\text{INDA}}=50 \mu\text{L}$ ), resulting in  $N_{\text{INP}}$  per volume of water. Compared to the droplets examined in a LINA measurement, INDA measurements have a larger volume of water in each well. The larger volume of water corresponds to a higher probability of

the presence of INPs in each well, therefore INDA can detect INPs at warmer temperatures, where INP are more scarce. In this study, the derived  $N_{\text{INP}}$  from LINA and INDA measurements were combined when both instruments were deployed.

### 2.3.2 Uncertainty and background

Because the number of INPs present in the [washing](#) water is usually small (some single up to a few tens of INPs per examined droplet/well), and the number of droplets/wells considered in our measurements is limited, statistical errors need to be considered in the data evaluation. Therefore, confidence intervals for  $f_{\text{ice}}$  were determined using the method suggested by Agresti and Coull (1998). [These confidence intervals were estimated according to the improved Wald interval which implicitly assumes a normal approximation for binomially distributed measurement errors](#). Previous studies (McCluskey et al., 2018a; Suski et al., 2018; Gong et al., 2019a) used the same method to calculate the freezing devices' measurement uncertainties.

For the quartz fiber filters, a background freezing signal resulting from the field blind filters was determined by doing a regular INDA measurement with these filters. Measured  $N_{\text{INP}}$  from the sampled filters was corrected by subtracting the averaged background concentrations determined for the blind filters. [A detailed explanation of background subtraction can be found in the supplement of, as explained in](#) Wex et al. (2019). All values for airborne  $N_{\text{INP}}$  presented in the following are background-corrected. [A detailed description of the background subtraction method and background values are provided in the supplement. For those samples that were already collected in a liquid state \(ULW, SML and cloud water \), a background correction was not done.](#)

### 2.3.3 Salinity correction of SML and ULW

SML and ULW samples were adjusted to account for the freezing depression caused by dissolved salts in sea water. First, based on Kreidenweis et al. (2005), the water activity can be calculated by:

$$a_w = \frac{n_{\text{water}}}{n_{\text{water}} + i * n_{\text{solute}}} \quad (3)$$

where the  $n_{\text{solute}}$  and  $n_{\text{water}}$  are the number of moles of solute and water in solution, respectively.  $i$  is the van't Hoff factor (Pruppacher and Klett, 2010). We assumed sea salt to be mainly sodium chloride, for which the van't Hoff factor is 2. The freezing depression temperature as a function of  $a_w$  was taken from Koop and Zobrist (2009). In our study, this was roughly a correction by 2.2 °C.

### 2.4 Active surface site density

A thorough analysis of particle number size distributions (PNSDs) has been presented in Gong et al. (2019b), and based on these PNSDs we derived the particle surface area size distributions (PASDs) for use in this study (to be seen in the supplement, Fig. S14). This provides an opportunity to determine the temperature-dependent cumulative active surface site density ( $n_s$ ) for aerosol particles. The  $n_s$  is a measure of how well an aerosol acts as a seed surface for ice nucleation. The  $n_s$  can be calculated as:

$$n_s = \frac{N_{\text{INP}}(\theta)}{A_{\text{total}}} \quad (4)$$

Where  $A_{\text{total}}$  is the concentration of the total particle surface area.

For cases where a single type of aerosol, such as one type of mineral dust, is examined in laboratory studies,  $A_{\text{total}}$  can be the total particle surface area. However, when field experiments are done, using the total particle surface area of the atmospheric aerosol assumes that all particles contribute to INP and have the same  $n_s$ , while the vast majority of these particles will not even be an INP. On the other hand, singling out the contribution of separate INP types in the atmospheric aerosol and relying  $n_s$  only to them by using their contribution to the total surface area is at least demanding if not often impossible. This has to be kept in mind when interpreting heterogeneous ice nucleation in terms of  $n_s$ .

### 3 Results

#### 3.1 INP in SML and ULW

Based on Eq. 1, the derived  $N_{\text{INP}}$  in seawater as a function of temperature is shown in Fig. 1, for both SML and ULW. Note that for each sample a separate INP spectrum is shown. Error bars show the 95% confidence interval. For completeness,  $f_{\text{ice}}$  of all seawater samples is shown in the supplement, Fig. S1 (measured by LINA) and Fig. S2 (measured by INDA). The variation of  $N_{\text{INP}}$  at any particular temperature is within one order of magnitude. Included in Fig. 1 are previous studies of  $N_{\text{INP}}$  measured east of Greenland in the Arctic (shown as red box) and east of America in the North Atlantic Ocean (shown as black box) from Wilson et al. (2015).

The concentration range detected for ULW in Wilson et al. (2015) (both in the Arctic and the North Atlantic Ocean) roughly agrees with our data. In Wilson et al. (2015),  $N_{\text{INP}}$  in the SML in the North Atlantic Ocean is at the lower end of that found in the Arctic. A possible reason for this difference could be the biological activity of the ocean water. Wilson et al. (2015) found that organic material was correlated to  $N_{\text{INP}}$  in SML, and that  $N_{\text{INP}}$  per gram of total organic carbon in the Arctic and the North Atlantic Ocean were comparable. A recent study found that the SML at Cape Verde was oligotrophic, which is supported by the low Chlorophyll-a and transparent exopolymer particles concentrations found during the MarParCloud campaign (Robinson et al., 2019). This The low biological activity in the SML around Cape Verde could be the reason why  $N_{\text{INP}}$  in SML in this study is lower than those reported in Wilson et al. (2015).

To better quantify the enrichment or depletion of  $N_{\text{INP}}$  in SML to ULW, we derived an enrichment factor (EF). An enrichment might be expected as organic material is known to attach to air bubbles rising to the ocean surface. The EF in SML was calculated by dividing  $N_{\text{INP}}$  in SML ( $N_{\text{INP, SML}}$ ) by the respective  $N_{\text{INP}}$  measured in ULW ( $N_{\text{INP, ULW}}$ ), as the below equation shows:

$$\text{EF} = \frac{N_{\text{INP, SML}}}{N_{\text{INP, ULW}}} \quad (5)$$

Enrichment of  $N_{\text{INP}}$  in the SML is indicated when  $\text{EF} > 1$ , while depletion is indicated when  $\text{EF} < 1$ . Fig. 2 shows the EF as a function of the temperature at which  $N_{\text{INP}}$  was determined in the freezing devices. Both enrichment and depletion were observed, but there is no clear trend of the EF with temperature. Most of the variation seen here is likely caused by measurement uncertainties, which are indicated in Fig. S3 in the supplement. EF varied from 0.36 to 11.40 at  $-15^{\circ}\text{C}$  and from 0.36

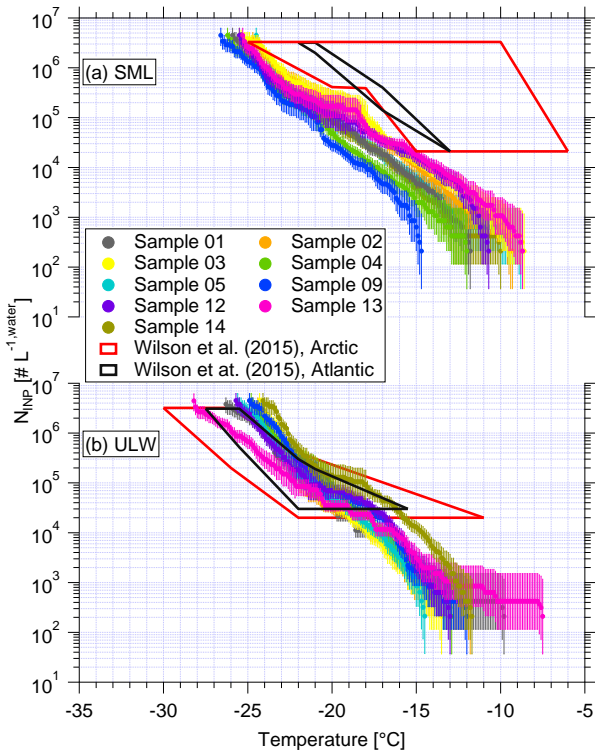


**Figure 1.**  $N_{INP}$  as a function of temperature in SML (a) and ULW (b). Error bars show the 95% confidence interval. Previous field measurements of  $N_{INP}$  in seawater by Wilson et al. (2015) are compared, as shown by red and black boxes.

to 7.11 at  $-20^{\circ}\text{C}$ . By comparing  $T_{10}$  (the temperature at which 10% of droplets had frozen) for the SML and ULW, Wilson et al. (2015) observed higher enrichment of INPs in SML in both the Arctic and the North Atlantic Ocean. However, Irish et al. (2017) observed both enrichment and depletion of INPs in SML in the Arctic, similar to the observation made in the present study.

These differences in EF between studies might partially be due to differences in the techniques deployed and different SML thickness in our and the other studies. SML samples were estimated to be about  $\sim 91.0\text{ }\mu\text{m}$  thick in this study, while for Wilson et al. (2015) those were between 6 to 83  $\mu\text{m}$ . It is interesting to note that we used glass dipping for the samples analyzed in herein, while both glass dipping and a rotating drum sampler were used in Wilson et al. (2015). Previous studies pointed out that rotating drum sampler and the glass dipping method probe different thicknesses of the SML, thus making a direct comparison of both SML thickness as well as enrichment factors generally difficult (Agogué et al., 2004; Aller et al., 2017).

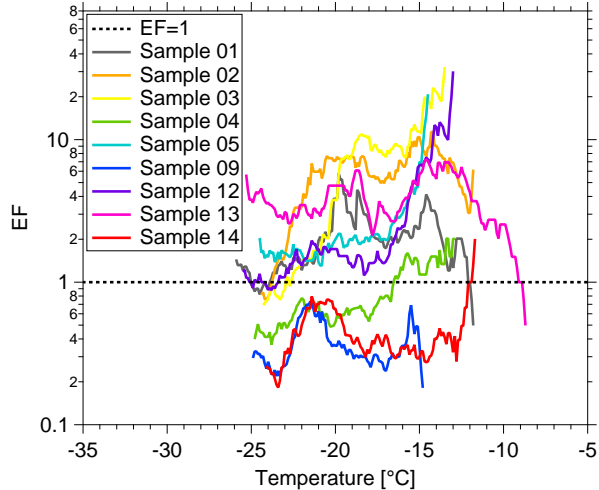


**Figure 2.** EF as function of [ice nucleation](#) temperature. The EF=1 is shown by dashed line.

### 3.2 $N_{\text{INP}}$ in air

Three different sets of filter samples were collected at CVAO and MV, i.e., CVAO PM<sub>10</sub>, CVAO PM<sub>1</sub> and MV PM<sub>10</sub>. In [the](#) this section, we will discuss  $N_{\text{INP}}$  at CVAO for the two different size classes and compare  $N_{\text{INP}}$  from close to the sea level (CVAO) to that at cloud level (MV).

#### 5 3.2.1 $N_{\text{INP}}$ close to sea level

##### CVAO PM<sub>10</sub>

$N_{\text{INP}}$  as a function of temperature from CVAO PM<sub>10</sub> filters and CVAO PM<sub>1</sub> filters are shown in Fig. 3(a) and (b). Error bars show the 95% confidence interval. The respective values of  $f_{\text{ice}}$  are shown in the supplement, Fig. S4 (CVAO PM<sub>10</sub>) and Fig. S8 (CVAO PM<sub>1</sub>), together with the results from the blind filters. The CVAO PM<sub>10</sub> filter samples were all active at  $-11.3^{\circ}\text{C}$  and 10 the highest freezing temperature was found to be  $-5.0^{\circ}\text{C}$ . Filter samples collected in Cape Verde over the period 2009-2013 for INP measurement were reported by Welti et al. (2018), and they are shown as gray background in Fig. 3(a). The measured  $N_{\text{INP}}$  in this study is within the  $N_{\text{INP}}$  range presented by Welti et al. (2018).

15  $N_{\text{INP}}$  at any particular temperature span around 1 order of magnitude below  $-15^{\circ}\text{C}$ , and about 2 orders of magnitude at warmer temperatures. This is consistent with the previous studies from O'Sullivan et al. (2018) and Gong et al. (2019a), who carried out field measurement in northwestern Europe and the eastern Mediterranean, respectively. A few samples (CVAO

1596, CVAO 1641 and CVAO 1643) showed elevated concentrations above 0.01 std L<sup>-1</sup> at -10 °C. Biological particles usually contribute to INPs at this moderate supercooling temperature (Kanji et al., 2017; O'Sullivan et al., 2018).

5 Biological INPs contain specific ice-nucleating proteins. These proteins are disrupted and denatured by heating which causes them to lose their ice-nucleating ability. However, the inorganic ice-nucleating material, such as dust particles, is insensitive to heat (Wilson et al., 2015; O'Sullivan et al., 2018). Therefore, a commonly used heat treatment was deployed to assess the contribution of biological INPs to the total INPs in this study. Samples CVAO 1596, CVAO 1641 and CVAO 1643 were heated to 95 °C for 1 hour and the resulting  $N_{INP}$  are shown in Fig. S6. A clear comparison of before and after heating  $f_{ice}$  is shown in Fig. S7. A large reduction of more than one order of magnitude in  $N_{INP}$  at  $T > -15$  °C was observed in the samples after heating. The reductions in  $N_{INP}$  became smaller at colder temperature and were, for example, less than one order of magnitude 10 at  $T = -20$  °C. This shows that biological aerosol contributed a large fraction of total INPs in PM<sub>10</sub> at  $T > -20$  °C.

The correlation of  $N_{INP}$  at two different temperatures was calculated. The correlation of  $N_{INP}$  at different temperatures within one sample was calculated, by comparing each  $N_{INP}$  at each temperature to that at each other temperature at which a measurement had been made. That was done separately for each of the samples. For temperature steps of 0.1 °C,  $N_{INP}$  at every temperature was correlated to that at every other temperature in the measurement range. With increasing difference in temperatures, the 15 variation in  $N_{INP}$  at two temperatures become less correlated. As long as the examined temperature difference was less than 2 °C,  $N_{INP}$  were correlated. But when looking at this in a broader picture, in the temperature region down to  $\sim -16.8$  °C,  $N_{INP}$  at all temperatures correlated well with that at all other temperatures, with coefficient of determination ( $R^2$ ) > 0.8 and  $p < 0.01$ . The same was true for  $N_{INP}$  in the temperatures region  $< -18.4$  °C. In between these two temperature regimes (between  $> -16.8$  °C and  $< -18.4$  °C), the correlation of  $N_{INP}$  was clearly lower. Therefore, it might be expected that INPs that are active 20 in these two temperature regimes originated from different sources.

### CVAO PM<sub>1</sub> in comparison to CVAO PM<sub>10</sub>

$N_{INP}$  in PM<sub>1</sub> filters are also determined in this study (as shown in Fig. 3(b)). An initial observation of the data shows that the bulk of the data of  $N_{INP}$  for CVAO PM<sub>1</sub> is below that for CVAO PM<sub>10</sub>. Fig. 4 shows the probability density function (PDF) of  $N_{INP}$  in CVAO PM<sub>10</sub> (black) and CVAO PM<sub>1</sub> (red) at -12 °C (a), -15 °C (b) and -18 °C (c). These temperatures were chosen because for each of them the filters 25 contributes data. Comparing  $N_{INP}$  for PM<sub>1</sub> and PM<sub>10</sub>, a few two key features are evident :

1. Larger particles, i.e., super-micron ones, were more efficient INPs, which is independent of temperature in the examined range.
2. Smaller particles, i.e., submicron ones, exhibited an equal spread of about 1 order of magnitude in  $N_{INP}$  for the whole temperature range (see Fig. 3(b)). The elevated  $N_{INP}$  at warm temperatures which are seen for CVAO PM<sub>10</sub> are not observed 30 for CVAO PM<sub>1</sub>.

As for the first feature, we calculated the ratio of  $N_{INP}$  in super-micron size range to  $N_{INP}$  in PM<sub>10</sub> during the same time period and found that 83±22%, 67±18% and 77±14% (median±standard deviation) of INPs had a diameter of >1  $\mu$ m at ice activation temperatures of -12, -15, and -18 °C, respectively. On average, over all temperatures, this INP number fraction for super-micron particles is roughly 70% (shown for a higher temperature resolution in Fig. 4), almost independent of temperature.

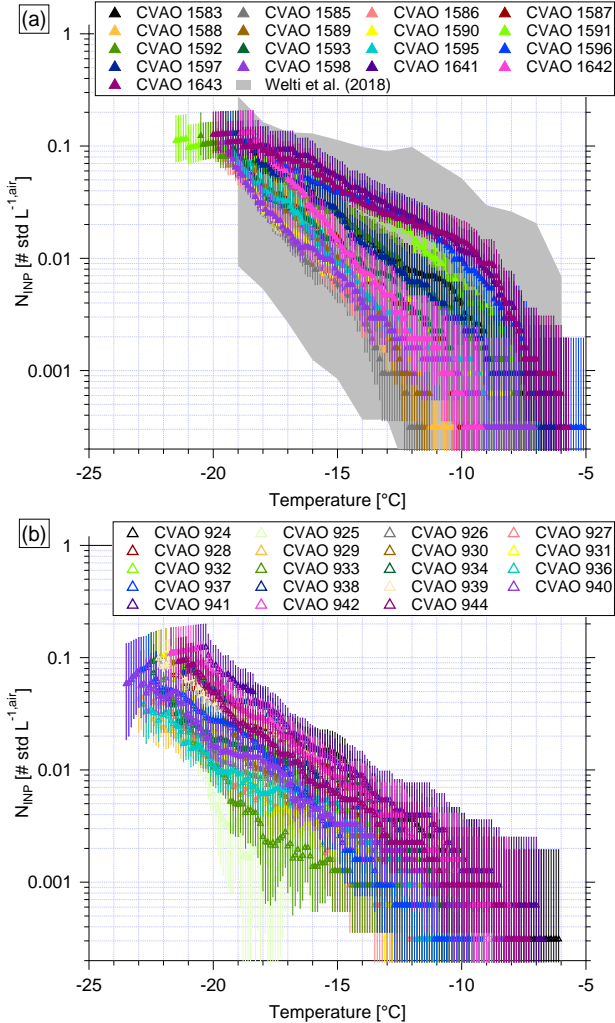


**Figure 3.**  $N_{INP}$  as a function of temperature from CVAO PM<sub>10</sub> filters (a) and CVAO PM<sub>1</sub> filters (b). The field measurement of  $N_{INP}$  in PM<sub>10</sub> by Welti et al. (2018) is shown by gray shadow in Fig. (a). Error bars show the 95% confidence interval.

Mason et al. (2016) and Creamean et al. (2018) also found that the majority of INPs is in the super-micron size range. However, they see even increasing fractions towards higher temperatures. For the present study, as said above, only three of the examined 17 filters showed clearly elevated  $N_{INP}$  at high temperatures, so overall such an increase was not observed.

As for the second feature, looking at Fig. 3(b), we found that  $N_{INP}$  spread about 1 order of magnitude at any temperature from  $-12$  to  $-20$  °C. As outlined above, a few PM<sub>10</sub> samples showed elevated concentrations at warm temperatures, showing up as a “bump” in the freezing curves at higher temperatures. This bump at warm temperatures was not observed for the CVAO PM<sub>1</sub> filters.  $N_{INP}$  of CVAO 932, CVAO 942 and CVAO 944 (sampled at the same time as CVAO 1596, CVAO 1641 and CVAO 1643) are all below  $0.001 \text{ std L}^{-1}$  at  $-10$  °C. As mentioned above, INP active at comparably high temperatures [are generally](#)

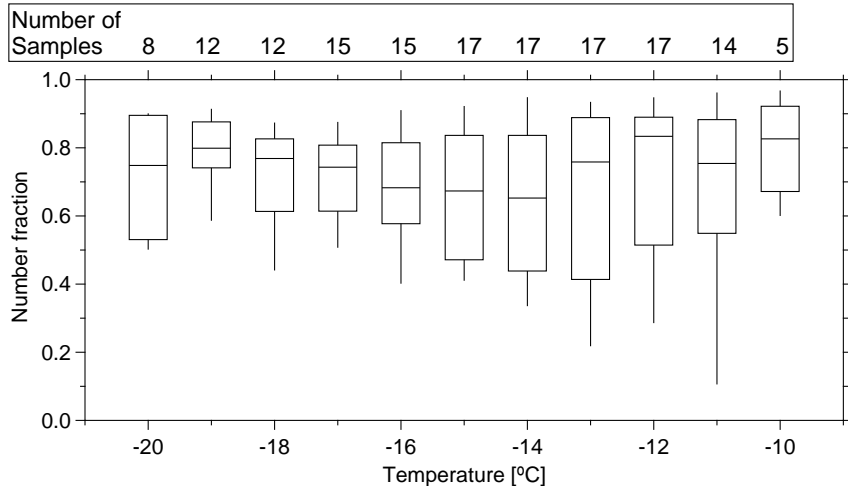


**Figure 4.** Boxplot of number fraction of INPs in the size range of  $>1 \mu\text{m}$  as a function of temperature. The boxes represent the interquartile range. Whiskers represent 10th to 90th percentile. The number of samples indicated on top of the figure shows how many different samples contributed at the different temperatures.

assumed were found to be biological in origin (e.g., Kanji et al., 2017; O’Sullivan et al., 2018) in this study, and our findings suggest the comparison between  $\text{PM}_{10}$  and  $\text{PM}_1$  samples show that there are biological INPs in the CVAO  $\text{PM}_{10}$  samples that are absent in the CVAO  $\text{PM}_1$  samples, i.e., that these likely the detected biological INPs are super-micron in size. This suggests that these biological INPs might originate from long-range transport, as marine biological INPs were usually reported to be submicron in size (Wilson et al., 2015; Irish et al., 2017). The contribution of SSA to INPs will be discussed further in section 3.4.

5

### 3.2.2 $N_{\text{INP}}$ at cloud level

In the companion paper (Gong et al., 2019b), we discussed PNSD and CCN number concentration ( $N_{\text{CCN}}$ ) at CVAO and MV. We found that particles are mainly well mixed in the marine boundary layer and derived the periods with cloud events, with a time resolution of  $\sim 30$  minutes, at MV. In the present study,  $N_{\text{INP}}$  in  $\text{PM}_{10}$  at CVAO and MV are compared. The fraction of 10 time during which there was a cloud event to the total sampling time (cloud time fraction) for each filter is summarized in the supplement, Tab. S4. All of the filters were more or less affected by cloud events with a cloud time fraction from 4.17 to 100%, with two filters being affected only little (cloud time fraction  $< 10\%$ ), i.e., MV 1602 and MV 1603. When comparing results from these two filters to those from filters sampled at the same time at CVAO (see Fig. 5(a)), we found that  $N_{\text{INP}}$  are quite similar close to sea level (CVAO) and cloud level (MV). This is in line with what was discussed in the companion paper (Gong 15 et al., 2019b), i.e., the marine boundary is often well mixed at Cape Verde.

Fig. 5(b) compares  $N_{\text{INP}}$  at CVAO and MV when MV filters were mostly collected during cloud events with cloud time fractions  $> 90\%$ . During the cloud events, the filters did not collect droplets larger than  $10 \mu\text{m}$  because of the inlet cutoff. It is obvious from Fig. 5 that for these cases,  $N_{\text{INP}}$  at MV is much lower than that at CVAO, implying that particularly INPs that

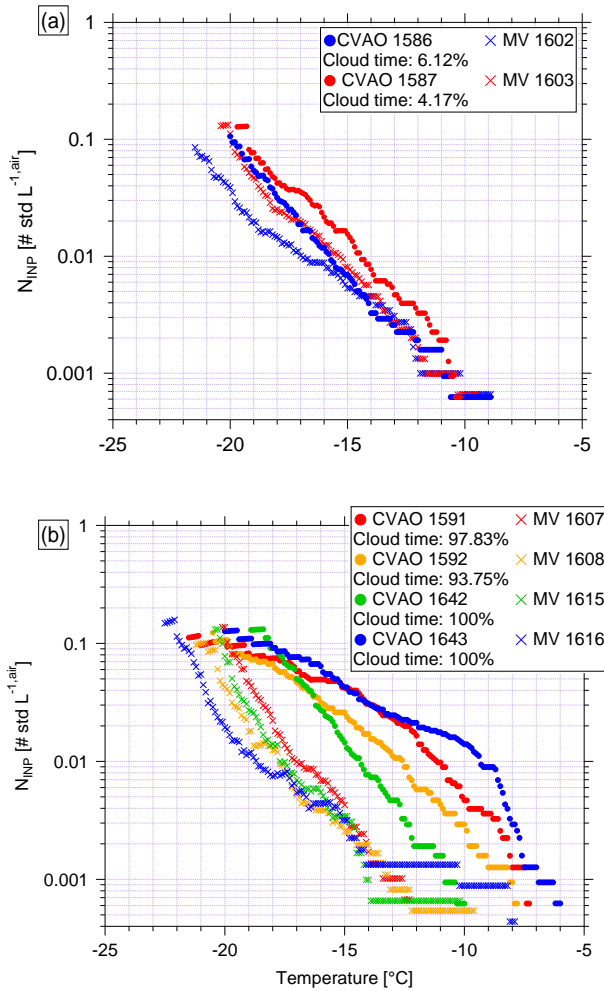


**Figure 5.**  $N_{INP}$  as a function of temperature from CVAO PM<sub>10</sub> filters and MV PM<sub>10</sub> filters during (a) less (cloud time fraction <10%) cloud effected periods (a) and (b) highly (cloud time fraction >90%) cloud effected periods (b).

were ice active above  $\sim -17^\circ \text{C}$  were activated to cloud droplets to a large degree. But note that even when filters have a cloud time fraction of 100% (MV 1615 and MV 1616), the respective filters still had clearly more INPs on them than the field blind filters (see supplement, Fig S9). This might indicate that either not all INPs are activated to cloud droplets, or, on the other hand, that some INPs were only recently activated to a cloud droplet and the droplet size was smaller than  $10 \mu\text{m}$ . [These observations are consistent with results by Siebert and Shaw \(2017\) who observed broad cloud droplet size distributions in a size range from  \$\sim 5\$  to  \$25 \mu\text{m}\$  in shallow cumulus clouds, with the maximum of the distribution still being below  \$10 \mu\text{m}\$ .](#)

Concerning the super-micron particles of likely biological origin that activated ice already at  $-10^\circ \text{C}$  and above (Fig. 4), it is observed that the related corresponding bump is not seen in the corresponding data from MV (MV 1610, MV 1614 and MV

1616 - to be seen in the supplement, Fig. S10). This indicates that these INPs were all activated to cloud droplets during the cloud events, and we will come back to this below.

### 3.3 INP in cloud water

#### 3.3.1 Main characteristics and $N_{\text{INP}}$ in cloud water

5 Thirteen cloud water samples were collected during cloud events in this study. Sampling durations varied from 2.5 to 13 hours and volumes varied from 78 to 544 mL. The most abundant inorganic species were  $\text{Na}^+$  and  $\text{Cl}^-$ , followed by  $\text{SO}_4^{2-}$ ,  $\text{NO}_3^-$  and  $\text{Mg}^{2+}$ . For example, the mass concentration of  $\text{Na}^+$  and  $\text{Cl}^-$  varied from 5.00 to 46.11 and 9.27 to 70.30  $\text{mg L}^{-1}$ , with a mean value of 17.31 and 28.86  $\text{mg L}^{-1}$ , respectively. [Somehow different values which are still roughly in the same range were reported by Gioda et al. \(2009\)](#), [who found in Puerto Rico the  \$\text{Na}^+\$  and  \$\text{Cl}^-\$  concentration in the cloud water varied from 3.79 to 15.53 and 5.90 to 23.20  \$\text{mg L}^{-1}\$ , with a mean of 10.74 and 15.67  \$\text{mg L}^{-1}\$ , respectively, which are comparable to this study.](#)

10 All of the above mentioned parameters are summarized in the supplement, Tab. S5.

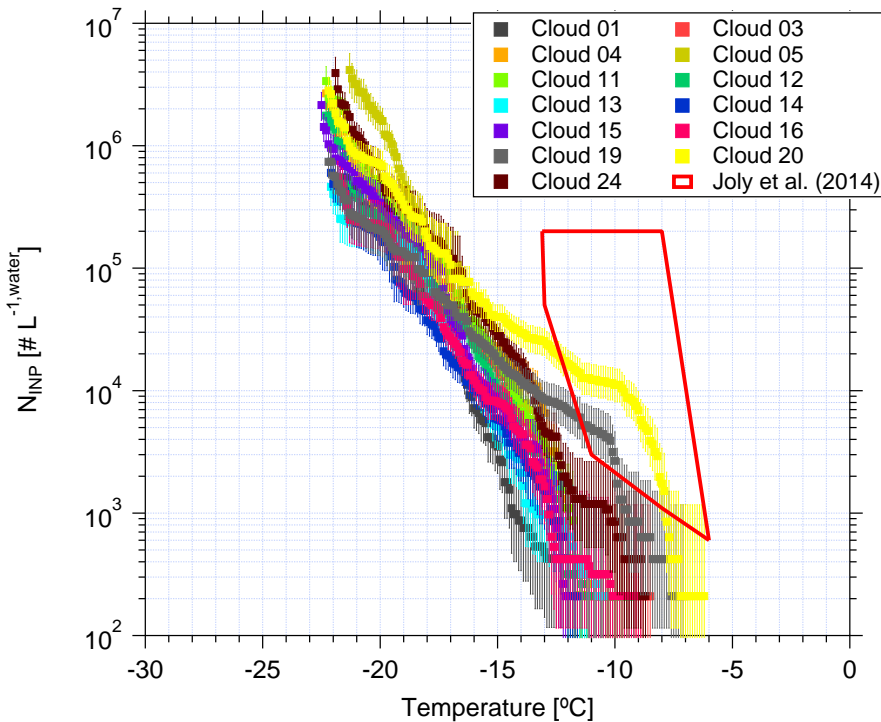


**Figure 6.**  $N_{\text{INP}}$  as a function of temperature in cloud water. Error bars show the 95% confidence interval. Previous field measurements of  $N_{\text{INP}}$  in cloud water by Joly et al. (2014) are compared, as shown by the red box.

Based on Eq. 1, the derived  $N_{\text{INP}}$  as a function of temperature is shown in Fig. 6. Error bars represent the 95% confidence interval. For completeness,  $f_{\text{ice}}$  for cloud water is shown in the supplement, Fig. S12 (measured by LINA) and Fig. S13

(measured by INDA).  $N_{\text{INP}}$  at any particular temperature span less than 1 order of magnitude below  $-15^{\circ}\text{C}$ , while they span 2 orders of magnitude at warmer temperatures. We observed elevated  $N_{\text{INP}}$  in the cloud water at warm temperatures (above  $1000 \text{ L}^{-1}$  at  $-10^{\circ}\text{C}$ ) particularly for the Cloud 19, Cloud 20 and Cloud 24 samples. Joly et al. (2014) measured the total and biological (i.e., heat-sensitive) INPs between  $-5$  to  $-14^{\circ}\text{C}$  from the summit of Puy de Dôme (1465 m a.s.l., France), as shown 5 in the red box in Fig. 6. Joly et al. (2014) observed very high concentrations of both biological particles and  $N_{\text{INP}}$ . Agreement of  $N_{\text{INP}}$  in cloud water all over the world was not expected, since the sources of INPs are different in different locations.

When highly ice active particles were present for CVAO  $\text{PM}_{10}$  filters (CVAO 1596, CVAO 1641 and CVAO 1643), they were not observed for MV  $\text{PM}_{10}$  (MV 1610, MV1614 and MV 1616, which had cloud time fractions of 52, 87 and 100%, respectively), but instead were found in cloud water samples (Cloud 19, Cloud 20 and Cloud 24). This is in line with what 10 was outlined in section 3.2.2 that these highly ice active particles were activated to cloud droplets during cloud events. Periods during which clouds were present at MV, together with the sampling periods of all cloud water samples and selected CVAO  $\text{PM}_{10}$  filters (those that had higher  $N_{\text{INP}}$  at warm temperatures, CVAO 1596, CVAO 1641 and CVAO 1643) can be checked in the supplement, Fig. S11.

### 3.3.2 Connecting INPs in the cloud water with these in the air

15 In the following,  $N_{\text{INP}}$  in the cloud water will be compared to that in the air. To be able to do this, we used measured values of  $N_{\text{CCN}}$  to calculate cloud droplet number concentrations. These, together with an assumption on cloud droplet size ( $d_{\text{drop}}$ ) yields the volume of cloud water per volume of air, given as  $F_{\text{cloud\_air}}$  in Eq. 6:

$$F_{\text{cloud\_air}} = N_{\text{CCN}} * \pi / 6 * d_{\text{drop}}^3 \quad (6)$$

For the calculation, we used  $N_{\text{CCN}}$  measured at CVAO at a supersaturation of 0.30% (Gong et al., 2019b).  $N_{\text{CCN}}$  was 20 averaged for the different periods when each cloud water sample was collected. The chosen supersaturation corresponds to a critical diameter of roughly 80 nm, which is at the Hoppel minimum of the respective particle number size distributions (Gong et al., 2019b), indicating that this is indeed the relevant supersaturation occurring in the prevailing clouds. Based on previous studies (Miles et al., 2000; Bréon et al., 2002; Igel and Heever, 2017; Siebert and Shaw, 2017), we assumed that  $d_{\text{drop}}$  varies between 7 and 20  $\mu\text{m}$  and did separate estimates for these two values and additionally for 15  $\mu\text{m}$ . The calculation based on this 25 size range of cloud droplets should cover all that can be expected to occur.

Following this approach,  $F_{\text{cloud\_air}}$  varied from  $4.2 * 10^{-7}$  to  $1.1 * 10^{-6}$ , with a median of  $8.5 * 10^{-7}$ . To see how reliable these values are, we also examined the following: assuming all sodium chloride particles were activated to cloud droplets,  $F_{\text{cloud\_air}}$  can be also estimated from the ratio of sodium chloride mass concentration in air to that in cloud water. This ratio varied from  $1.1 * 10^{-7}$  to  $4.2 * 10^{-7}$ , which is at the lower end but still comparable to  $F_{\text{cloud\_air}}$  as we derived it above. Previous studies 30 used the liquid water content (LWC), which is a measure of the mass of the water in a cloud in a specified amount of dry air. Typical ranges for LWC in thicker clouds are between 0.2 and 0.8  $\text{g m}^{-3}$  (Rangno and Hobbs, 2005; Petters and Wright, 2015), corresponding to  $F_{\text{cloud\_air}}$  between  $2 * 10^{-7}$  to  $8 * 10^{-7}$ , which again agreed well with the above given values derived for this study.

With this  $F_{\text{cloud\_air}}$ ,  $N_{\text{INP}}$  in the respective volume of air can be compared to  $N_{\text{INP}}$  in this volume of cloud water when assuming that all INPs are CCN, which, based on the super-micron size of most of the INPs alone, is likely. To do so,  $N_{\text{INP}}$  obtained for cloud water was multiplied by  $F_{\text{cloud\_air}}$  (for the three different assumptions on  $d_{\text{drop}}$ ) to yield  $N_{\text{INP}}$  in the air ( $N_{\text{INP,air}}$ ), given in Eq. 7:

$$5 \quad N_{\text{INP,air}} = F_{\text{cloud\_air}} * N_{\text{INP,cloud}} \quad (7)$$

Fig. 7 shows the measured  $N_{\text{INP}}$  in the air as a function of temperature by squares. Derived  $N_{\text{INP,air}}$  from cloud water (calculated with a  $d_{\text{drop}}$  of  $15\mu\text{m}$ ) are shown by triangles. The samples with comparatively high numbers of INPs active at warm temperatures, are shown in different colors. CVAO 1596, CVAO 1641 and CVAO 1643 are shown by green squares (the rest shown by blue squares) and derived  $N_{\text{INP,air}}$  from samples collected for Cloud 19, Cloud 20 and Cloud 24 are shown by brown triangles (the rest shown by red triangles). The range of values indicated for  $N_{\text{INP,air}}$  was obtained from using 7 and  $20\mu\text{m}$  cloud droplet size, with  $7\mu\text{m}$  droplets yielding the lower boundary and  $20\mu\text{m}$  the upper one.

There is general agreement between measured and derived  $N_{\text{INP}}$  in air, however, with some variation where the values derived from cloud water samples are somewhat lower. This might be connected to a less than optimal sampling efficiency of the cloud water sampler, which has a 50% collection efficiency at  $3.5\mu\text{m}$ . Also the spread in the derived values, originating 15 from the different assumed  $d_{\text{drop}}$ , is rather large. Nevertheless, it is striking that at least within an order of magnitude, based on our comparably simple assumptions, an agreement between concentrations of INP in the air and in cloud water is found.

### 3.4 INPs originating from sea spray

In the following section, it will briefly be discussed whether SSA contributed noticeably to INPs in the air. Assuming sea salt and INPs to be similarly distributed in both, seawater and air (i.e., assuming that INPs would not be enriched during the 20 production of sea spray),  $N_{\text{INP}}$  in the air originating from sea spray ( $N_{\text{INP}}^{\text{sea spray,air}}$ ) can be calculated based on Eq. 8:

$$N_{\text{INP}}^{\text{sea spray,air}} = \frac{\text{NaCl}_{\text{mass,air}}}{\text{NaCl}_{\text{mass,seawater}}} * N_{\text{INP}}^{\text{seawater}} \quad (8)$$

where  $\text{NaCl}_{\text{mass,air}}$  and  $\text{NaCl}_{\text{mass,seawater}}$  are sodium chloride mass concentrations in air and seawater, respectively.  $N_{\text{INP}}^{\text{seawater}}$  is the INP number concentration in the seawater (this calculation can be done similarly for both SML and ULW).

$\text{NaCl}_{\text{mass,air}}$  and  $\text{NaCl}_{\text{mass,seawater}}$  can be found in the supplement, Tab. S1 and Tab. S2.  $\text{NaCl}_{\text{mass,seawater}}$  was very stable, with 25 a median value  $\sim 31\text{ g L}^{-1}$ .  $\text{NaCl}_{\text{mass,air}}$  showed large variability from 3.40 to  $17.76\text{ mg L}^{-1}\mu\text{g m}^{-3}$ , with a median of  $13.08\text{ mg L}^{-1}\mu\text{g m}^{-3}$ . Based on Eq. 8, the resulting  $N_{\text{INP}}^{\text{sea spray,air}}$  are shown in blue (derived from SML) and green (derived from ULW) in Fig. 8. Irish et al. (2019b) used the same method to get  $N_{\text{INP}}^{\text{sea spray,air}}$  in the Arctic (without considering enrichment of INPs in sea salt particles during sea spray generation), as shown by purple (derived from SML) and brown (derived from ULW) boxes in Fig. 8. As discussed in section 3.1,  $N_{\text{INP}}$  from ULW at Cape Verde are comparable to the Arctic, and the NaCl ratios were close to  $10^{-10}$  in both studies, therefore,  $N_{\text{INP}}^{\text{sea spray,air}}$  (derived from ULW) are also comparable. A high enrichment of  $N_{\text{INP}}$  in SML to ULW was observed in the Arctic (Irish et al., 2019b). Therefore,  $N_{\text{INP}}^{\text{sea spray,air}}$  (derived from SML) in the Arctic was also higher than in this study.

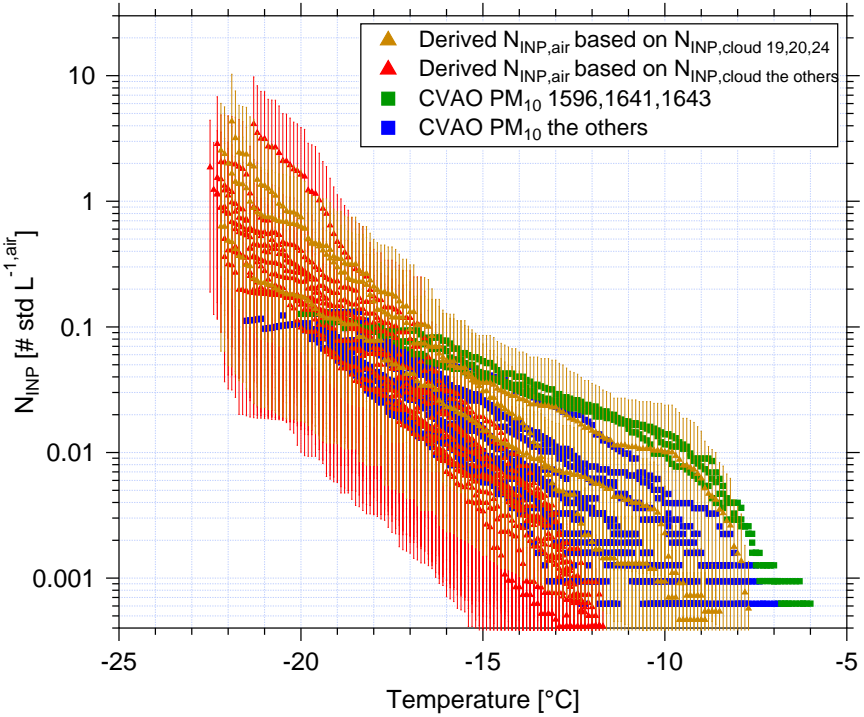


**Figure 7.** The measured atmospheric  $N_{\text{INP}}$  as a function of ice nucleation temperature in the air are shown as squares. The derived  $N_{\text{INP,air}}$  based on INP concentrations measured for cloud water are shown by as triangles. The samples with highly ice active INPs at warm temperatures, are shown in a different color than the others: CVAO 1596, CVAO 1641 and CVAO 1643 are shown by as green squares and derived  $N_{\text{INP,air}}$  based on Cloud 19, Cloud 20 and Cloud 24 are shown by as brown triangles. The uncertainty range indicated for the derived  $N_{\text{INP,air}}$  originate from calculations with 7 and 20  $\mu\text{m}$  cloud droplet size.

Fig. 8 includes  $N_{\text{INP}}$  from  $\text{PM}_{10}$  in this study (shown by black triangles). These values are roughly 4 orders of magnitude above our  $N_{\text{INP}}^{\text{sea spray,air}}$ . But Fig. 8 also shows airborne  $N_{\text{INP}}$  as derived for the Southern Ocean (McCluskey et al., 2018a) and the Northeast Atlantic (only clean sector, McCluskey et al., 2018b), which are all above our  $N_{\text{INP}}^{\text{sea spray,air}}$ . As mentioned above, we did not consider a possible enrichment of INPs in SSA compared to the SML or ULW samples. Previous studies 5 found an enrichment of organic carbon in submicron sea spray particles of about  $10^4$  to  $10^5$  (Keene et al., 2007; van Pinxteren et al., 2017), and this value decreased to  $10^2$  for super-micron particles (Keene et al., 2007; Quinn et al., 2015). It is not clear if INPs are included in the organic carbon for which the enrichment was observed. Also, the INPs we detected in this study were mostly in the super-micron size range. If we increased  $N_{\text{INP}}^{\text{sea spray,air}}$  by about 2 orders of magnitude in agreement 10 to the enrichment observed for super-micron organic carbon, the resulting  $N_{\text{INP}}^{\text{sea spray,air}}$  becomes comparable to sea spray INPs measured in the Southern Ocean (McCluskey et al., 2018a) and the Northeast Atlantic (McCluskey et al., 2018b). But even when considering such an enrichment of INPs, INPs originating from sea spray would only explain a small fraction of all INPs contributing to the measured airborne  $N_{\text{INP}}$  in the air at Cape Verde.

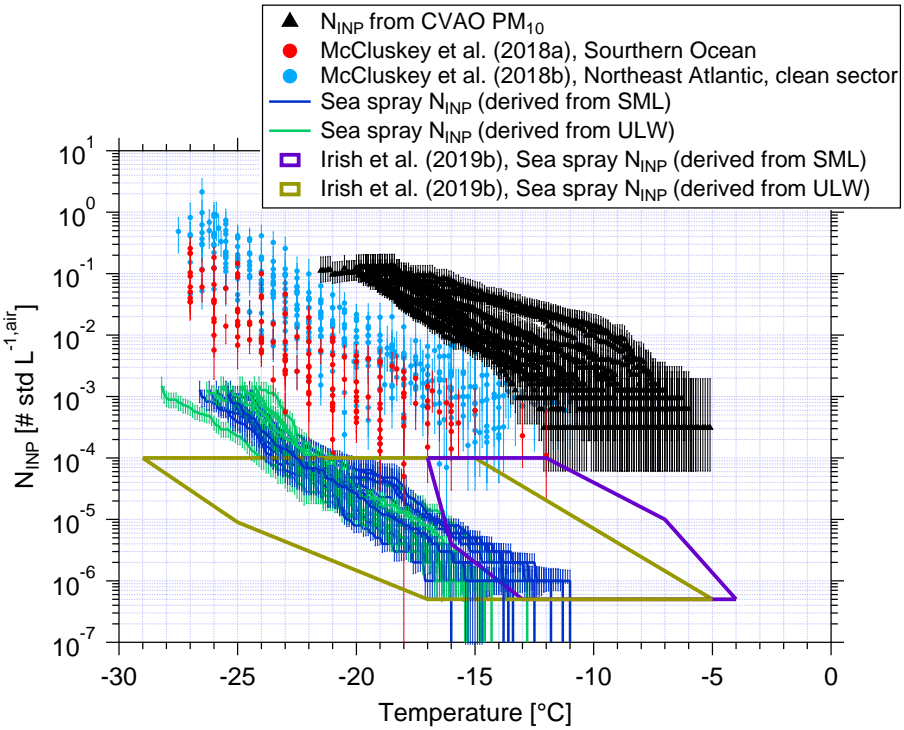


**Figure 8.** Atmospheric  $N_{INP}$  are shown as a function of temperature from  $PM_{10}$  filters (black triangles), and error bars show together with error bars showing the 95% confidence interval.  $N_{INP}$  as a function of temperature from McCluskey et al. (2018a, b) are shown by red and light blue dots, respectively. Error bars show the 95% confidence interval.  $N_{INP}^{sea\ spray,air}$  from this study are shown by blue (derived from SML) and green lines (derived from ULW).  $N_{INP}^{sea\ spray,air}$  from Irish et al. (2019b) are shown by purple (derived from SML) and brown (derived from ULW) boxes.

#### 4 Discussion

$N_{INP}$  close to sea and cloud level height were compared. One major point of interest is to know whether ground-based measurements can be used to infer aerosol properties at the cloud level. In this study, we found that  $N_{INP}$  are quite similar close to sea level (CVAO) and cloud level (MV) during non-cloud events. But it should still be noted that we only have a small number 5 of filter samples representing non-cloud events in this study. During the observed cloud events, most INPs at MV are activated to cloud droplets. The above findings are in line with what was discussed in the companion paper (Gong et al., 2019b), i.e., (1) the marine boundary is often well mixed at Cape Verde and PNSDs and  $N_{CCN}$  are similar close to both sea and cloud level; (2) during cloud events, larger particles are activated to cloud droplets.

Most INPs are in the super-micron size range at Cape Verde. We found that about 70% of INPs had a diameter of  $>1\ \mu m$  10 at ice activation temperatures between  $-10$  and  $-20\ ^\circ C$ . Mason et al. (2016) and Creamean et al. (2018) also found that the majority of INPs is in the super-micron size range in the Arctic, in agreement with the results we obtained here.

Above we derived that  $N_{\text{INP}}$  contributed from SSA only accounted for a minor fraction of total  $N_{\text{INP}}$  in the air, as well as in the cloud water at Cape Verde. This still holds even when considering a possible enrichment of INPs in SSA up to  $10^2$ , which is an enrichment as given in literature for super-micron organic particles (Keene et al., 2007; Quinn et al., 2015). ~~It can similarly be seen when considering that it has been described in literature that mineral dust is associated with a factor of 1000 higher ice surface site density (a measure to describe the ice activity per particle surface area), compared to SSA at temperatures from  $-12$  to  $-35$  °C~~ ~~On the other hand, mineral dust is associated with a factor of 1000 higher ice surface site density (a measure to describe the ice activity per particle surface area), compared to SSA~~ (Niemand et al., 2012; DeMott et al., 2016; McCluskey et al., 2018a). In our study, the super-micron particles that make up a large fraction of the INPs we observed were mainly mineral dust, as described in the accompanying study (Gong et al., 2019b). The comparably high ice activity of super-micron mineral dust and the presence of mainly dust particles in the super-micron size range in our study again supports that indeed most INPs observed in this study were not from sea spray. This is in line with results from Si et al. (2018) and Irish et al. (2019a), both done in the Arctic, where it was also concluded that SSA only contributed little to the INP population. The commonality of these two studies from the Arctic and the present study is that land was still close enough so that terrestrial sources can have contributed to the observed INPs.

While the above arguments suggest that INPs in our study were mostly mineral dust particles, there were also some measurements with comparably high INP concentrations at temperatures of  $-10$  °C and above. Although it cannot be ruled out that desert dust particles might be ice active at such high temperatures, by examining the reaction of some highly ice active samples to heating, described in Sec. 3.2.1, we found that the most highly ice active INPs on these samples were biological particles. It is an open question where these highly ice active biological INPs originated. Such high ice activity is typically associated with biological particles. The times during which these highly ice active INPs were observed were times when air masses came from Southern Europe, traveling along the African coast and meanwhile crossing over the region of the Canary Islands. Therefore, for these specific samples, a contribution of INPs from these land sources might be assumed.

Finally, in the following, we will compare  $n_s$  derived from our data with that from literature. In Fig. 9, we show the surface site density derived for our data  $N_{\text{INP}}$  from CVAO PM<sub>10</sub> filters (as shown by black boxes) following Niemand et al. (2012) (details on the surface area are given in the supplement, Fig. S14), together with parameterizations for  $n_s$  given by Niemand et al. (2012), Ullrich et al. (2017) and McCluskey et al. (2018b), and the measured  $n_s$  given by DeMott et al. (2016) and Price et al. (2018). Niemand et al. (2012) derived  $n_s$  from a laboratory study, based on aerosol consisting purely of desert dust particles. It is therefore reasonable that these mineral dust related  $n_s$  values are the largest values shown in Fig. 9, as they are purely related to the mineral dust surface area of an aerosol. All other values shown in Fig. 9 were derived for atmospheric measurements, and the surface area used to derive  $n_s$  was always based on measured particle number concentrations. Price et al. (2018) carried out airborne measurements in dust laden air over the tropical Atlantic. Parameterizations from McCluskey et al. (2018b) were done for pristine SSA over the Northeast Atlantic and both laboratory and atmospheric measurements of SSA were the base for the  $n_s$  parameterization given in DeMott et al. (2016). These available  $n_s$  parameterizations from previous literature may not be representative for Cape Verde, but we will still compare with them here.  $n_s$  derived for our study coincides with the upper range of parameterizations that are otherwise reported for SSA but are clearly lower than values reported for atmospheric desert dust aerosol. This is striking since, as discussed above, INPs observed in this study most likely do not originate from

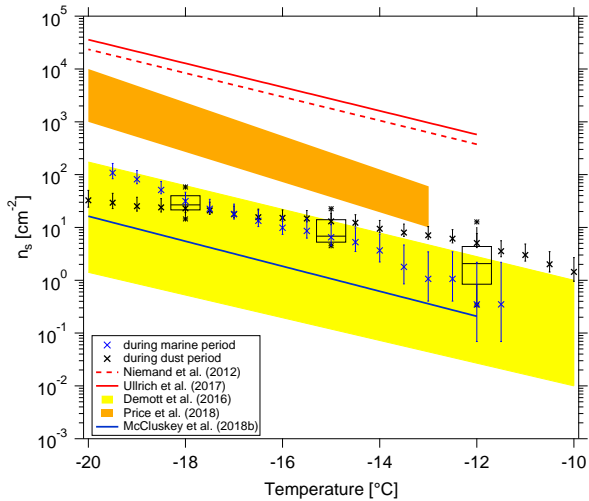


**Figure 9.**  $n_s$  as a function of temperature in this study is shown by black boxes. The boxes represent the interquartile range. Whiskers represent 10th to 90th percentile. Data not included between the whiskers are plotted as an outlier with a star. Two  $n_s$  parameterizations (Niemand et al., 2012; Ullrich et al., 2017) for pure desert dust are shown in dashed and solid red lines, respectively.  $n_s$  parameterizations from McCluskey et al. (2018b) for pristine SSA over the Northeast Atlantic are shown as a solid blue line. We also compare to recent data from airborne measurement in a dust layer by Price et al. (2018) in brown shadow and from nascent laboratory generated and ambient SSA by DeMott et al. (2016) in yellow shadow, respectively.  $n_s$  during the most clean marine (CVAO 1585) and most dusty (CVAO 1591) periods are shown as blue and black crosses, respectively.

sea spray, but are dominated by super-micron dust and/or biological particles. This raises the question if and how  $n_s$  should be used to parameterize atmospheric INP measurements, which, however, is a question far too prominent to be answered in this study.

CVAO is a place where marine and dust particles strongly intersect, and both particle types contribute to the surface area. In the companion paper, we have classified the aerosol at CVAO into four different types. Here, in addition to looking at 5 average values as presented above, we selected the most clean marine (CVAO 1585) and most dusty (CVAO 1591) samples for a separate calculation of  $n_s$  and added the results to Fig. 9. The  $n_s$  is clearly higher for the sample collected during the dusty period than during the marine period at higher temperatures (roughly  $>-16$  °C). However, at temperatures below  $-18$  °C it is the other way around. In general, results for these vastly different cases are both still close to the upper limit of the parameterizations reported for SSA.

10 These comparisons to literature raise the question if and how  $n_s$  should be used to parameterize atmospheric INP measurements, which, however, is a question far too prominent to be answered in this study. In general, it is still an open issue to which extent  $N_{INP}$  can be parameterized, based on one or a few parameters, to reliably describe  $N_{INP}$  for different locations around the globe. It might prove necessary to develop separate parameterizations for different locations or air masses, as it was already started for parameterizations based on particle number concentrations (see e.g., DeMott et al. (2010); Tobo et al. (2013); DeMott et al. (2018)).

## 5 Summary and conclusions

The MarParCloud campaign took place in September and October 2018 on the island of Cape Verde to investigate aerosols prevailing in the Atlantic Ocean. In addition to a thorough analysis of the atmospheric aerosol particles and CCN in a companion paper (Gong et al., 2019b), samples collected for INPs analysis in this study include: sea surface microlayer (SML) and 5 underlying water (ULW) from the ocean upwind of the island; quartz fiber filter samples of atmospheric aerosol, collected on a tower installed at the island shore and on a 744 m high mountaintop, as well as cloud water collected during cloud events on the mountaintop.  $N_{INP}$  were measured offline with two types of freezing devices, yielding results in the temperature range from roughly  $-5$  to  $-25$   $^{\circ}C$ .

Both enrichment and depletion of  $N_{INP}$  in SML to ULW were observed. The enrichment factors (EF) varied from 0.36 to 10 11.40 and from 0.36 to 7.11 at  $-15$  and  $-20$   $^{\circ}C$ , respectively, and were generally independent of the freezing temperature [at which  \$N\_{INP}\$  was determined in the freezing devices..](#)

The measured  $N_{INP}$  in this study is consistent with the previous study of Welti et al. (2018), who characterized INPs sampled at CVAO over a time period of 4 years. A few CVAO PM<sub>10</sub> filter samples (CVAO 1596, CVAO 1641 and CVAO 1643) showed elevated  $N_{INP}$  at high temperatures, e.g., above 0.01 std L<sup>-1</sup> at  $-10$   $^{\circ}C$ . [These elevated values disappeared after heating the samples at 95  \$^{\circ}C\$  for 1 hour. Therefore, biological particles appear to contribute to INPs at these moderate supercooling temperatures. Biological particles usually contributed the INPs at this moderate supercooling temperatures \(Kanji et al., 2017; O'Sullivan et al., 2018\).](#)

About  $83 \pm 22\%$ ,  $67 \pm 18\%$  and  $77 \pm 14\%$  (median  $\pm$  standard deviation) of INPs had a diameter  $>1$   $\mu m$  at ice activation temperatures of  $-12$ ,  $-15$ , and  $-18$   $^{\circ}C$ , respectively, and over the whole examined temperature range, on average roughly 70% of all INPs were super-micron, independent of the temperature. The highly ice active INPs were not found on the CVAO PM<sub>1</sub> filters, which suggests that most of these likely biological INPs are in the super-micron size range.

[\$N\_{INP}\$  were quite similar at CVAO and MV during non-cloud events. As MV was in clouds most of the time, only two filters could be collected on MV that were affected by cloud for less than 10% of the sampling time. For these,  \$N\_{INP}\$  were similar at CVAO and MV. During cloud events, most INPs at MV were activated into cloud droplets. These findings aligned very well with the companion paper, i.e., during non-cloud events, PNSDs and  \$N\_{CCN}\$  are similar at CVAO and MV, while during cloud events, larger particles at MV are activated to clouds \(see Fig. 8 in the companion paper\). When highly ice active particles were present on CVAO PM<sub>10</sub> filters, they were not observed on MV PM<sub>10</sub> filters, but were instead observed in the respective cloud water samples. This shows that these INPs are activated into cloud droplets during cloud events.](#)

By comparing  $N_{INP}$  derived for the different examined samples, it was found that values in air and in cloud water agreed well. We also compared atmospheric  $N_{INP}$  to those in SML and ULW, based on the ratio of sodium chloride concentrations 30 measured for the atmosphere and for SML and ULW. From that we concluded that marine INPs from sea spray can only explain a small fraction of all atmospheric INPs at Cape Verde, unless there would be an enrichment of INPs from SML to the atmosphere by at least a factor of  $10^4$ . Such an enrichment, however, is higher than anything observed for organic compounds in super-micron particles so far. Generally low INP concentrations are found over remote oceanic regions, compared to locations closer to land masses, implying that the ocean is a weak source of INPs, compared to land. Summarizing, it can be assumed

that most atmospheric INPs detected in the present study were mainly contributed by the dust particles at cold temperatures possibly with few contributions from biological particles at warmer temperatures.

*Data availability.* The data are available through the World Data Center PANGAEA (<https://www.pangaea.de/>) in the near future. A link to the data can be found under this paper's assets tab on ACP's journal website.

5 *Author contributions.* X. Gong wrote the manuscript with contributions from H. Wex and M. van Pinxteren. C. Stolle, N. Triesch and B. Robinson collected ocean water samples. X. Gong, M. van Pinxteren and N. Triesch collected filter samples. K. W. Fomba collected cloud water samples. X. Gong and J. Lubitz performed INP measurements. X. Gong preformed data evaluation. X. Gong, H. Wex and F. Stratmann discussed the results and further analysis after the campaign. All co-authors proofread and commented the manuscript.

*Competing interests.* The authors declare that they have no conflict of interests.

10 *Acknowledgements.* The works were carried out in the framework of the MarParCloud project. The authors acknowledge the Leibniz Association SAW funding for the project “Marine biological production, organic aerosol particles and marine clouds: a Process Chain (MarPar-Cloud)“, SAW-2016-TROPOS-2.

## References

Agogué, H., Casamayor, E. O., Joux, F., Obernosterer, I., Dupuy, C., Lantoine, F., Catala, P., Weinbauer, M. G., Reinthaler, T., Herndl, G. J., and Lebaron, P.: Comparison of samplers for the biological characterization of the sea surface microlayer, *Limnology and Oceanography: Methods*, 2, 213–225, <https://doi.org/10.4319/lom.2004.2.213>, <https://aslopubs.onlinelibrary.wiley.com/doi/abs/10.4319/lom.2004.2.213>, 5 2004.

Agresti, A. and Coull, B. A.: Approximate is Better than “Exact” for Interval Estimation of Binomial Proportions, *The American Statistician*, 52, 119–126, <https://doi.org/10.1080/00031305.1998.10480550>, <https://doi.org/10.1080/00031305.1998.10480550>, 1998.

Aller, J. Y., Radway, J. C., Kilthau, W. P., Bothe, D. W., Wilson, T. W., Vaillancourt, R. D., Quinn, P. K., Coffman, D. J., Murray, B. J., and Knopf, D. A.: Size-resolved characterization of the polysaccharidic and proteinaceous components of sea spray aerosol, *Atmospheric Environment*, 10 154, 331–347, <https://doi.org/https://doi.org/10.1016/j.atmosenv.2017.01.053>, <http://www.sciencedirect.com/science/article/pii/S1352231017300699>, 2017.

Ansmann, A., Tesche, M., Althausen, D., Müller, D., Seifert, P., Freudenthaler, V., Heese, B., Wiegner, M., Pisani, G., Knippertz, P., and Dubovik, O.: Influence of Saharan dust on cloud glaciation in southern Morocco during the Saharan Mineral Dust Experiment, *Journal of Geophysical Research: Atmospheres*, 113, <https://doi.org/10.1029/2007jd008785>, <https://agupubs.onlinelibrary.wiley.com/doi/abs/10.1029/2007JD008785>, 2008.

Atkinson, J. D., Murray, B. J., Woodhouse, M. T., Whale, T. F., Baustian, K. J., Carslaw, K. S., Dobbie, S., O’Sullivan, D., and Malkin, T. L.: The importance of feldspar for ice nucleation by mineral dust in mixed-phase clouds, *Nature*, 498, 355, <https://doi.org/10.1038/nature12278> <https://www.nature.com/articles/nature12278#supplementary-information>, <https://doi.org/10.1038/nature12278>, 2013.

20 Augustin-Bauditz, S., Wex, H., Kanter, S., Ebert, M., Niedermeier, D., Stolz, F., Prager, A., and Stratmann, F.: The immersion mode ice nucleation behavior of mineral dusts: A comparison of different pure and surface modified dusts, *Geophysical Research Letters*, 41, 7375–7382, <https://doi.org/10.1002/2014gl061317>, <https://agupubs.onlinelibrary.wiley.com/doi/abs/10.1002/2014GL061317>, 2014.

Bigg, E. K.: Ice Nucleus Concentrations in Remote Areas, *Journal of the Atmospheric Sciences*, 30, 1153–1157, [https://doi.org/doi:10.1175/1520-0469\(1973\)030<1153:INCIRA>2.0.CO;2](https://doi.org/doi:10.1175/1520-0469(1973)030<1153:INCIRA>2.0.CO;2), <http://journals.ametsoc.org/doi/abs/10.1175/1520-0469%281973%29030%3C1153%3AINCIRA%3E2.0.CO%3B2>, 1973.

25 Boose, Y., Welti, A., Atkinson, J., Ramelli, F., Danielczok, A., Bingemer, H. G., Plötze, M., Sierau, B., Kanji, Z. A., and Lohmann, U.: Heterogeneous ice nucleation on dust particles sourced from nine deserts worldwide – Part 1: Immersion freezing, *Atmospheric Chemistry and Physics*, 16, 15 075–15 095, <https://doi.org/10.5194/acp-16-15075-2016>, <https://www.atmos-chem-phys.net/16/15075/2016/>, 2016.

Bréon, F.-M., Tanré, D., and Generoso, S.: Aerosol Effect on Cloud Droplet Size Monitored from Satellite, *Science*, 295, 834–838, 30 <https://doi.org/10.1126/science.1066434>, <https://science.sciencemag.org/content/sci/295/5556/834.full.pdf>, 2002.

Brier, G. W. and Kline, D. B.: Ocean Water as a Source of Ice Nuclei, *Science*, 130, 717–718, <https://doi.org/10.1126/science.130.3377.717>, 1959.

Budke, C. and Koop, T.: BINARY: an optical freezing array for assessing temperature and time dependence of heterogeneous ice nucleation, *Atmos. Meas. Tech.*, 8, 689–703, <https://doi.org/10.5194/amt-8-689-2015>, <http://www.atmos-meas-tech.net/8/689/2015/>, 2015.

35 Burrows, S. M., Hoose, C., Pöschl, U., and Lawrence, M. G.: Ice nuclei in marine air: biogenic particles or dust?, *Atmos. Chem. Phys.*, 13, 245–267, <https://doi.org/10.5194/acp-13-245-2013>, <https://www.atmos-chem-phys.net/13/245/2013/>, 2013.

Chen, J., Wu, Z., Augustin-Bauditz, S., Grawe, S., Hartmann, M., Pei, X., Liu, Z., Ji, D., and Wex, H.: Ice-nucleating particle concentrations unaffected by urban air pollution in Beijing, China, *Atmos. Chem. Phys.*, 18, 3523–3539, <https://doi.org/10.5194/acp-18-3523-2018>, <https://www.atmos-chem-phys.net/18/3523/2018/>, 2018.

Chou, C., Stetzer, O., Weingartner, E., Jurányi, Z., Kanji, Z. A., and Lohmann, U.: Ice nuclei properties within a Saharan dust event 5 at the Jungfraujoch in the Swiss Alps, *Atmos. Chem. Phys.*, 11, 4725–4738, <https://doi.org/10.5194/acp-11-4725-2011>, <http://www.atmos-chem-phys.net/11/4725/2011/>, 2011.

Conen, F., Henne, S., Morris, C. E., and Alewell, C.: Atmospheric ice nucleators active  $\geq -12^{\circ}\text{C}$  can be quantified on PM<sub>10</sub> filters, *Atmos. Meas. Tech.*, 5, 321–327, <https://doi.org/10.5194/amt-5-321-2012>, <https://www.atmos-meas-tech.net/5/321/2012/>, 2012.

Conen, F., Eckhardt, S., Gundersen, H., Stohl, A., and Yttri, K. E.: Rainfall drives atmospheric ice-nucleating particles in the coastal climate of 10 southern Norway, *Atmos. Chem. Phys.*, 17, 11 065–11 073, <https://doi.org/10.5194/acp-17-11065-2017>, <https://www.atmos-chem-phys.net/17/11065/2017/>, 2017.

Creamean, J. M., Kirpes, R. M., Pratt, K. A., Spada, N. J., Maahn, M., de Boer, G., Schnell, R. C., and China, S.: Marine and terrestrial influences on ice nucleating particles during continuous springtime measurements in an Arctic oilfield location, *Atmos. Chem. Phys.*, 18, 18 023–18 042, <https://doi.org/10.5194/acp-18-18023-2018>, <https://www.atmos-chem-phys.net/18/18023/2018/>, 2018.

DeMott, P. J., Sassen, K., Poellot, M. R., Baumgardner, D., Rogers, D. C., Brooks, S. D., Prenni, A. J., and Kreidenweis, S. M.: African dust 15 aerosols as atmospheric ice nuclei, *Geophysical Research Letters*, 30, n/a–n/a, <https://doi.org/10.1029/2003GL017410>, <http://dx.doi.org/10.1029/2003GL017410>, 2003.

DeMott, P. J., Prenni, A. J., Liu, X., Kreidenweis, S. M., Petters, M. D., Twohy, C. H., Richardson, M. S., Eidhammer, T., and Rogers, D. C.: Predicting global atmospheric ice nuclei distributions and their impacts on climate, *Proceedings of the National Academy of Sciences*, 20 107, 11 217–11 222, <https://doi.org/10.1073/pnas.0910818107>, <http://www.pnas.org/content/107/25/11217.abstract>, 2010.

DeMott, P. J., Prenni, A. J., McMeeking, G. R., Sullivan, R. C., Petters, M. D., Tobo, Y., Niemand, M., Möhler, O., Snider, J. R., Wang, Z., and Kreidenweis, S. M.: Integrating laboratory and field data to quantify the immersion freezing ice nucleation activity of mineral dust particles, *Atmos. Chem. Phys.*, 15, 393–409, <https://doi.org/10.5194/acp-15-393-2015>, <https://www.atmos-chem-phys.net/15/393/2015/>, 2015.

DeMott, P. J., Hill, T. C. J., McCluskey, C. S., Prather, K. A., Collins, D. B., Sullivan, R. C., Ruppel, M. J., Mason, R. H., Irish, V. E., Lee, T., Hwang, C. Y., Rhee, T. S., Snider, J. R., McMeeking, G. R., Dhaniyala, S., Lewis, E. R., Wentzell, J. J. B., Abbatt, J., Lee, C., Sultana, C. M., Ault, A. P., Axson, J. L., Diaz Martinez, M., Venero, I., Santos-Figueroa, G., Stokes, M. D., Deane, G. B., Mayol-Bracero, O. L., Grassian, V. H., Bertram, T. H., Bertram, A. K., Moffett, B. F., and Franc, G. D.: Sea spray aerosol as a unique source of 25 ice nucleating particles, *Proceedings of the National Academy of Sciences*, 113, 5797–5803, <https://doi.org/10.1073/pnas.1514034112>, <http://www.pnas.org/content/113/21/5797.abstract>, 2016.

Demoz, B. B., Collett, J. L., and Daube, B. C.: On the Caltech Active Strand Cloudwater Collectors, *Atmospheric Research*, 41, 47–62, [https://doi.org/https://doi.org/10.1016/0169-8095\(95\)00044-5](https://doi.org/https://doi.org/10.1016/0169-8095(95)00044-5), <http://www.sciencedirect.com/science/article/pii/0169809595000445>, 1996.

Gioda, A., Mayol-Bracero, O. L., Morales-García, F., Collett, J., Decesari, S., Emblico, L., Facchini, M. C., Morales-De Jesús, R. J., Mertes, 30 S., Borrmann, S., Walter, S., and Schneider, J.: Chemical Composition of Cloud Water in the Puerto Rican Tropical Trade Wind Cumuli, *Water, Air, and Soil Pollution*, 200, 3–14, <https://doi.org/10.1007/s11270-008-9888-4>, <https://doi.org/10.1007/s11270-008-9888-4>, 2009.

Gong, X., Wex, H., Müller, T., Wiedensohler, A., Höhler, K., Kandler, K., Ma, N., Dietel, B., Schiebel, T., Möhler, O., and Stratmann, F.: Characterization of aerosol properties at Cyprus, focusing on cloud condensation nuclei and ice nucleating particles, *Atmos. Chem. Phys. Discuss.*, 2019, 1–34, <https://doi.org/10.5194/acp-2019-198>, <https://www.atmos-chem-phys-discuss.net/acp-2019-198/>, 2019a.

Gong, X., Wex, H., Voigtländer, J., Fomba, K. W., Weinhold, K., van Pinxteren, M., Henning, S., Müller, T., Herrmann, H., and Stratmann, F.: Characterization of aerosol particles at Cape Verde close to sea and cloud level heights – Part 1: particle number size distribution, cloud condensation nuclei and their origins, *Atmos. Chem. Phys. Discuss.*, 2019, 1–31, <https://doi.org/10.5194/acp-2019-585>, <https://www.atmos-chem-phys-discuss.net/acp-2019-585/>, 2019b.

Hartmann, M., Blunier, T., Brügger, S., Schmale, J., Schwikowski, M., Vogel, A., Wex, H., and Stratmann, F.: Variation of Ice Nucleating Particles in the European Arctic Over the Last Centuries, *Geophysical Research Letters*, 0, <https://doi.org/10.1029/2019GL082311>, <https://agupubs.onlinelibrary.wiley.com/doi/abs/10.1029/2019GL082311>, 2019.

Harvey, G. W. and Burzell, L. A.: A simple microlayer method for small samples, *Limnology and Oceanography*, 17, 156–157, <https://doi.org/doi:10.4319/lo.1972.17.1.0156>, <https://aslopubs.onlinelibrary.wiley.com/doi/abs/10.4319/lo.1972.17.1.0156>, 1972.

Hoose, C. and Möhler, O.: Heterogeneous ice nucleation on atmospheric aerosols: a review of results from laboratory experiments, *Atmos. Chem. Phys.*, 12, 9817–9854, <https://doi.org/10.5194/acp-12-9817-2012>, <http://www.atmos-chem-phys.net/12/9817/2012/>, 2012.

Huffman, J. A., Prenni, A. J., DeMott, P. J., Pöhlker, C., Mason, R. H., Robinson, N. H., Fröhlich-Nowoisky, J., Tobe, Y., Després, V. R., Garcia, E., Gochis, D. J., Harris, E., Müller-Germann, I., Ruzene, C., Schmer, B., Sinha, B., Day, D. A., Andreae, M. O., Jimenez, J. L., Gallagher, M., Kreidenweis, S. M., Bertram, A. K., and Pöschl, U.: High concentrations of biological aerosol particles and ice nuclei during and after rain, *Atmos. Chem. Phys.*, 13, 6151–6164, <https://doi.org/10.5194/acp-13-6151-2013>, <https://www.atmos-chem-phys.net/13/6151/2013/>, 2013.

Igel, A. L. and Heever, S. C. v. d.: The Importance of the Shape of Cloud Droplet Size Distributions in Shallow Cumulus Clouds. Part II: Bulk Microphysics Simulations, *Journal of the Atmospheric Sciences*, 74, 259–273, <https://doi.org/10.1175/jas-d-15-0383.1>, <https://journals.ametsoc.org/doi/abs/10.1175/JAS-D-15-0383.1>, 2017.

Irish, V. E., Elizondo, P., Chen, J., Chou, C., Charette, J., Lizotte, M., Ladino, L. A., Wilson, T. W., Gosselin, M., Murray, B. J., Polishchuk, E., Abbott, J. P. D., Miller, L. A., and Bertram, A. K.: Ice-nucleating particles in Canadian Arctic sea-surface microlayer and bulk seawater, *Atmos. Chem. Phys.*, 17, 10 583–10 595, <https://doi.org/10.5194/acp-17-10583-2017>, <https://www.atmos-chem-phys.net/17/10583/2017/>, 2017.

Irish, V. E., Hanna, S. J., Willis, M. D., China, S., Thomas, J. L., Wentzell, J. J. B., Cirisan, A., Si, M., Leaitch, W. R., Murphy, J. G., Abbott, J. P. D., Laskin, A., Girard, E., and Bertram, A. K.: Ice nucleating particles in the marine boundary layer in the Canadian Arctic during summer 2014, *Atmos. Chem. Phys.*, 19, 1027–1039, <https://doi.org/10.5194/acp-19-1027-2019>, <https://www.atmos-chem-phys.net/19/1027/2019/>, 2019a.

Irish, V. E., Hanna, S. J., Xi, Y., Boyer, M., Polishchuk, E., Ahmed, M., Chen, J., Abbott, J. P. D., Gosselin, M., Chang, R., Miller, L. A., and Bertram, A. K.: Revisiting properties and concentrations of ice-nucleating particles in the sea surface microlayer and bulk seawater in the Canadian Arctic during summer, *Atmos. Chem. Phys.*, 19, 7775–7787, <https://doi.org/10.5194/acp-19-7775-2019>, <https://www.atmos-chem-phys.net/19/7775/2019/>, 2019b.

Joly, M., Amato, P., Deguillaume, L., Monier, M., Hoose, C., and Delort, A. M.: Quantification of ice nuclei active at near 0 °C temperatures in low-altitude clouds at the Puy de Dôme atmospheric station, *Atmos. Chem. Phys.*, 14, 8185–8195, <https://doi.org/10.5194/acp-14-8185-2014>, <https://www.atmos-chem-phys.net/14/8185/2014/>, 2014.

Kanji, Z. A., Ladino, L. A., Wex, H., Boose, Y., Burkert-Kohn, M., Cziczo, D. J., and Krämer, M.: Overview of Ice Nucleating Particles, Meteorological Monographs, 58, 1.1–1.33, <https://doi.org/10.1175/amsmonographs-d-16-0006.1>, <https://journals.ametsoc.org/doi/abs/10.1175/AMSMONOGRAPHSD-16-0006.1>, 2017.

Keene, W. C., Maring, H., Maben, J. R., Kieber, D. J., Pszenny, A. A. P., Dahl, E. E., Izaguirre, M. A., Davis, A. J., Long, M. S., Zhou, 5 Smoydzin, L., and Sander, R.: Chemical and physical characteristics of nascent aerosols produced by bursting bubbles at a model air-sea interface, *Journal of Geophysical Research: Atmospheres*, 112, <https://doi.org/10.1029/2007jd008464>, <https://agupubs.onlinelibrary.wiley.com/doi/abs/10.1029/2007JD008464>, 2007.

Koop, T. and Zobrist, B.: Parameterizations for ice nucleation in biological and atmospheric systems, *Physical Chemistry Chemical Physics*, 11, 10 839–10 850, <https://doi.org/10.1039/B914289D>, <http://dx.doi.org/10.1039/B914289D>, 2009.

10 Kreidenweis, S., Koehler, K., DeMott, P., Prenni, A., Carrico, C., and Ervens, B.: Water activity and activation diameters from hygroscopicity data-Part I: Theory and application to inorganic salts, *Atmospheric Chemistry and Physics*, 5, 1357–1370, 2005.

Mason, R. H., Si, M., Chou, C., Irish, V. E., Dickie, R., Elizondo, P., Wong, R., Brintnell, M., Elsasser, M., Lassar, W. M., Pierce, K. M., 15 Leaitch, W. R., MacDonald, A. M., Platt, A., Toom-Sauntry, D., Sarda-Estève, R., Schiller, C. L., Suski, K. J., Hill, T. C. J., Abbatt, J. P. D., Huffman, J. A., DeMott, P. J., and Bertram, A. K.: Size-resolved measurements of ice-nucleating particles at six locations in North America and one in Europe, *Atmos. Chem. Phys.*, 16, 1637–1651, <https://doi.org/10.5194/acp-16-1637-2016>, <https://www.atmos-chem-phys.net/16/1637/2016/>, 2016.

20 McCluskey, C. S., Hill, T. C. J., Humphries, R. S., Rauker, A. M., Moreau, S., Strutton, P. G., Chambers, S. D., Williams, A. G., McRobert, I., Ward, J., Keywood, M. D., Harnwell, J., Ponsonby, W., Loh, Z. M., Krummel, P. B., Protat, A., Kreidenweis, S. M., and DeMott, P. J.: Observations of Ice Nucleating Particles Over Southern Ocean Waters, *Geophysical Research Letters*, 45, 11,989–11,997, <https://doi.org/10.1029/2018GL079981>, <https://doi.org/10.1029/2018GL079981>, 2018a.

McCluskey, C. S., Ovadnevaite, J., Rinaldi, M., Atkinson, J., Belosi, F., Ceburnis, D., Marullo, S., Hill, T. C. J., Lohmann, U., Kanji, Z. A., O'Dowd, C., Kreidenweis, S. M., and DeMott, P. J.: Marine and Terrestrial Organic Ice-Nucleating Particles in Pristine Marine to Continentally Influenced Northeast Atlantic Air Masses, *Journal of Geophysical Research: Atmospheres*, 123, 6196–6212, <https://doi.org/10.1029/2017JD028033>, <https://agupubs.onlinelibrary.wiley.com/doi/abs/10.1029/2017JD028033>, 2018b.

25 Mertes, S., Verheggen, B., Walter, S., Connolly, P., Ebert, M., Schneider, J., Bower, K. N., Cozic, J., Weinbruch, S., Baltensperger, U., and Weingartner, E.: Counterflow Virtual Impactor Based Collection of Small Ice Particles in Mixed-Phase Clouds for the Physico-Chemical Characterization of Tropospheric Ice Nuclei: Sampler Description and First Case Study, *Aerosol Science and Technology*, 41, 848–864, <https://doi.org/10.1080/02786820701501881>, <https://doi.org/10.1080/02786820701501881>, 2007.

Miles, N. L., Verlinde, J., and Clothiaux, E. E.: Cloud Droplet Size Distributions in Low-Level Stratiform Clouds, *Journal of the Atmospheric Sciences*, 57, 295–311, [https://doi.org/10.1175/1520-0469\(2000\)057<0295:cdsdl>2.0.co;2](https://doi.org/10.1175/1520-0469(2000)057<0295:cdsdl>2.0.co;2), <https://journals.ametsoc.org/doi/abs/10.1175/1520-0469%282000%29057%3C0295%3ACDSDIL%3E2.0.CO%3B2>, 2000.

Murray, B. J., O'Sullivan, D., Atkinson, J. D., and Webb, M. E.: Ice nucleation by particles immersed in supercooled cloud droplets, *Chemical Society Reviews*, 41, 6519–6554, <https://doi.org/10.1039/C2CS35200A>, <http://dx.doi.org/10.1039/C2CS35200A>, 2012.

Niedermeier, D., Augustin-Bauditz, S., Hartmann, S., Wex, H., Ignatius, K., and Stratmann, F.: Can we define an asymptotic value for 30 the ice active surface site density for heterogeneous ice nucleation?, *Journal of Geophysical Research: Atmospheres*, 120, 5036–5046, <https://doi.org/10.1002/2014JD022814>, <https://agupubs.onlinelibrary.wiley.com/doi/abs/10.1002/2014JD022814>, 2015.

Niemand, M., Möhler, O., Vogel, B., Vogel, H., Hoose, C., Connolly, P., Klein, H., Bingemer, H., DeMott, P., Skrotzki, J., and Leisner, T.: A Particle-Surface-Area-Based Parameterization of Immersion Freezing on Desert Dust Particles, *Journal of the Atmospheric Sciences*, 69, 3077–3092, <https://doi.org/10.1175/jas-d-11-0249.1>, <http://journals.ametsoc.org/doi/abs/10.1175/JAS-D-11-0249.1>, 2012.

O'Sullivan, D., Adams, M. P., Tarn, M. D., Harrison, A. D., Vergara-Temprado, J., Porter, G. C. E., Holden, M. A., Sanchez-Marroquin, 5 A., Carotenuto, F., Whale, T. F., McQuaid, J. B., Walshaw, R., Hedges, D. H. P., Burke, I. T., Cui, Z., and Murray, B. J.: Contributions of biogenic material to the atmospheric ice-nucleating particle population in North Western Europe, *Scientific Reports*, 8, 13 821, <https://doi.org/10.1038/s41598-018-31981-7>, <https://doi.org/10.1038/s41598-018-31981-7>, 2018.

Petters, M. and Wright, T.: Revisiting ice nucleation from precipitation samples, *Geophysical Research Letters*, 42, 8758–8766, <https://doi.org/10.1002/2015GL065733>, <https://agupubs.onlinelibrary.wiley.com/doi/abs/10.1002/2015GL065733>, 2015.

10 Price, H. C., Baustian, K. J., McQuaid, J. B., Blyth, A., Bower, K. N., Choularton, T., Cotton, R. J., Cui, Z., Field, P. R., Gallagher, M., Hawker, R., Merrington, A., Miltenberger, A., Neely III, R. R., Parker, S. T., Rosenberg, P. D., Taylor, J. W., Trembath, J., Vergara-Temprado, J., Whale, T. F., Wilson, T. W., Young, G., and Murray, B. J.: Atmospheric Ice-Nucleating Particles in the Dusty Tropical Atlantic, *Journal of Geophysical Research: Atmospheres*, 123, 2175–2193, <https://doi.org/10.1002/2017JD027560>, <https://agupubs.onlinelibrary.wiley.com/doi/abs/10.1002/2017JD027560>, 2018.

15 Pruppacher, H. and Klett, J.: *Microphysics of Clouds and Precipitation*, vol. 18, Springer Science & Business Media, 2010.

Pummer, B. G., Budke, C., Augustin-Bauditz, S., Niedermeier, D., Felgitsch, L., Kampf, C. J., Huber, R. G., Liedl, K. R., Loerting, T., Moschen, T., Schauperl, M., Tollinger, M., Morris, C. E., Wex, H., Grothe, H., Pöschl, U., Koop, T., and Fröhlich-Nowoisky, J.: Ice nucleation by water-soluble macromolecules, *Atmos. Chem. Phys.*, 15, 4077–4091, <https://doi.org/10.5194/acp-15-4077-2015>, <https://www.atmos-chem-phys.net/15/4077/2015/>, 2015.

20 Quinn, P. K., Collins, D. B., Grassian, V. H., Prather, K. A., and Bates, T. S.: Chemistry and Related Properties of Freshly Emitted Sea Spray Aerosol, *Chemical Reviews*, 115, 4383–4399, <https://doi.org/10.1021/cr500713g>, <http://dx.doi.org/10.1021/cr500713g>, 2015.

Rangno, A. L. and Hobbs, P. V.: Microstructures and precipitation development in cumulus and small cumulonimbus clouds over the warm pool of the tropical Pacific Ocean, *Quarterly Journal of the Royal Meteorological Society*, 131, 639–673, <https://doi.org/10.1256/qj.04.13>, <https://rmets.onlinelibrary.wiley.com/doi/abs/10.1256/qj.04.13>, 2005.

25 Robinson, T. B., Stolle, C., and Wurl, O.: Depth is Relative: The Importance of Depth on TEP in the Near Surface Environment, *Ocean Sci. Discuss.*, 2019, 1–20, <https://doi.org/10.5194/os-2019-79>, <https://www.ocean-sci-discuss.net/os-2019-79/>, 2019.

Schnell, R. C.: Ice Nuclei in Seawater, Fog Water and Marine Air off the Coast of Nova Scotia: Summer 1975, *Journal of the Atmospheric Sciences*, 34, 1299–1305, [https://doi.org/doi:10.1175/1520-0469\(1977\)034<1299:INISFW>2.0.CO;2](https://doi.org/doi:10.1175/1520-0469(1977)034<1299:INISFW>2.0.CO;2), <http://journals.ametsoc.org/doi/abs/10.1175/1520-0469%281977%29034%3C1299%3AINISFW%3E2.0.CO%3B2>, 1977.

30 Schnell, R. C. and Vali, G.: Biogenic Ice Nuclei: Part I. Terrestrial and Marine Sources, *Journal of the Atmospheric Sciences*, 33, 1554–1564, [https://doi.org/doi:10.1175/1520-0469\(1976\)033<1554:BINPIT>2.0.CO;2](https://doi.org/doi:10.1175/1520-0469(1976)033<1554:BINPIT>2.0.CO;2), <http://journals.ametsoc.org/doi/abs/10.1175/1520-0469%281976%29033%3C1554%3ABINPIT%3E2.0.CO%3B2>, 1976.

Schrod, J., Weber, D., Drücke, J., Keleshis, C., Pikridas, M., Ebert, M., Cvetković, B., Nickovic, S., Marinou, E., Baars, H., Ansmann, A., Vrekoussis, M., Mihalopoulos, N., Sciare, J., Curtius, J., and Bingemer, H. G.: Ice nucleating particles over the Eastern Mediterranean measured by unmanned aircraft systems, *Atmos. Chem. Phys.*, 17, 4817–4835, <https://doi.org/10.5194/acp-17-4817-2017>, <https://www.atmos-chem-phys.net/17/4817/2017/>, 2017.

35 Si, M., Irish, V. E., Mason, R. H., Vergara-Temprado, J., Hanna, S. J., Ladino, L. A., Yakobi-Hancock, J. D., Schiller, C. L., Wentzell, J. J. B., Abbatt, J. P. D., Carslaw, K. S., Murray, B. J., and Bertram, A. K.: Ice-nucleating ability of aerosol particles and possible sources at three

coastal marine sites, *Atmos. Chem. Phys.*, 18, 15 669–15 685, <https://doi.org/10.5194/acp-18-15669-2018>, <https://www.atmos-chem-phys.net/18/15669/2018/>, 2018.

Siebert, H. and Shaw, R. A.: Supersaturation Fluctuations during the Early Stage of Cumulus Formation, *Journal of the Atmospheric Sciences*, 74, 975–988, <https://doi.org/10.1175/jas-d-16-0115.1>, <https://journals.ametsoc.org/doi/abs/10.1175/JAS-D-16-0115.1>, 2017.

5 Suski, K. J., Hill, T. C. J., Levin, E. J. T., Miller, A., DeMott, P. J., and Kreidenweis, S. M.: Agricultural harvesting emissions of ice-nucleating particles, *Atmos. Chem. Phys.*, 18, 13 755–13 771, <https://doi.org/10.5194/acp-18-13755-2018>, <https://www.atmos-chem-phys.net/18/13755/2018/>, 2018.

Tobo, Y., Prenni, A. J., DeMott, P. J., Huffman, J. A., McCluskey, C. S., Tian, G., Pöhlker, C., Pöschl, U., and Kreidenweis, S. M.: Biological aerosol particles as a key determinant of ice nuclei populations in a forest ecosystem, *Journal of Geophysical Research: Atmospheres*, 10 118, 10,100–10,110, <https://doi.org/10.1002/jgrd.50801>, <http://dx.doi.org/10.1002/jgrd.50801>, 2013.

Ullrich, R., Hoose, C., Möhler, O., Niemand, M., Wagner, R., Höhler, K., Hiranuma, N., Saathoff, H., and Leisner, T.: A New Ice Nucleation Active Site Parameterization for Desert Dust and Soot, *Journal of the Atmospheric Sciences*, 74, 699–717, <https://doi.org/10.1175/JAS-D-16-0074.1>, <https://doi.org/10.1175/JAS-D-16-0074.1>, 2017.

Vali, G.: Sizes of Atmospheric Ice Nuclei, *Nature*, 212, 384–385, <https://doi.org/10.1038/212384a0>, <https://doi.org/10.1038/212384a0>, 1966.

15 Vali, G.: Quantitative Evaluation of Experimental Results an the Heterogeneous Freezing Nucleation of Supercooled Liquids, *Journal of the Atmospheric Sciences*, 28, 402–409, [https://doi.org/10.1175/1520-0469\(1971\)028<0402:qeoera>2.0.co;2](https://doi.org/10.1175/1520-0469(1971)028<0402:qeoera>2.0.co;2), <http://journals.ametsoc.org/doi/abs/10.1175/1520-0469%281971%29028%3C0402%3AQEOERA%3E2.0.CO%3B2>, 1971.

Vali, G., DeMott, P. J., Möhler, O., and Whale, T. F.: Technical Note: A proposal for ice nucleation terminology, *Atmos. Chem. Phys.*, 15, 10 263–10 270, <https://doi.org/10.5194/acp-15-10263-2015>, <https://www.atmos-chem-phys.net/15/10263/2015/>, 2015.

20 van Pinxteren, M., Barthel, S., Fomba, K. W., Müller, K., Von Tümpeling, W., and Herrmann, H.: The influence of environmental drivers on the enrichment of organic carbon in the sea surface microlayer and in submicron aerosol particles—measurements from the Atlantic Ocean, *Elementa: Science of the Anthropocene*, 5, 35, 2017.

Welti, A., Müller, K., Fleming, Z. L., and Stratmann, F.: Concentration and variability of ice nuclei in the subtropical maritime boundary layer, *Atmospheric Chemistry and Physics*, 18, 5307–5320, 2018.

25 Westbrook, C. D. and Illingworth, A. J.: The formation of ice in a long-lived supercooled layer cloud, *Quarterly Journal of the Royal Meteorological Society*, 139, 2209–2221, <https://doi.org/10.1002/qj.2096>, <https://rmets.onlinelibrary.wiley.com/doi/abs/10.1002/qj.2096>, 2013.

Wex, H., Huang, L., Zhang, W., Hung, H., Traversi, R., Becagli, S., Sheesley, R. J., Moffett, C. E., Barrett, T. E., Bossi, R., Skov, H., Hünerbein, A., Lubitz, J., Löffler, M., Linke, O., Hartmann, M., Herenz, P., and Stratmann, F.: Annual variability of ice-nucleating particle concentrations at different Arctic locations, *Atmos. Chem. Phys.*, 19, 5293–5311, <https://doi.org/10.5194/acp-19-5293-2019>, <https://www.atmos-chem-phys.net/19/5293/2019/>, 2019.

30 Wilson, T. W., Ladino, L. A., Alpert, P. A., Breckels, M. N., Brooks, I. M., Browse, J., Burrows, S. M., Carslaw, K. S., Huffman, J. A., Judd, C., Kilthau, W. P., Mason, R. H., McFiggans, G., Miller, L. A., Najera, J. J., Polishchuk, E., Rae, S., Schiller, C. L., Si, M., Temprado, J. V., Whale, T. F., Wong, J. P. S., Wurl, O., Yakobi-Hancock, J. D., Abbatt, J. P. D., Aller, J. Y., Bertram, A. K., Knopf, D. A., and Murray, B. J.: A marine biogenic source of atmospheric ice-nucleating particles, *Nature*, 525, 234–238, <https://doi.org/10.1038/nature14986>, <http://dx.doi.org/10.1038/nature14986>, 2015.

# **Characterization of aerosol particles at Cape Verde close to sea and cloud level heights - Part 2: ice nucleating particles in air, cloud and seawater**

Xianda Gong<sup>1</sup>, Heike Wex<sup>1</sup>, Manuela van Pinxteren<sup>1</sup>, Nadja Triesch<sup>1</sup>, Khamneh Wadinga Fomba<sup>1</sup>, Jasmin Lubitz<sup>1</sup>, Christian Stolle<sup>2,3</sup>, Tiera-Brandy Robinson<sup>3</sup>, Thomas Müller<sup>1</sup>, Hartmut Herrmann<sup>1</sup>, and Frank Stratmann<sup>1</sup>

<sup>1</sup>Leibniz Institute for Tropospheric Research, Leipzig, Germany

<sup>2</sup>Leibniz-Institute for Baltic Sea Research Warnemünde (IOW), Rostock, Germany

<sup>3</sup>Institute for Chemistry and Biology of the Marine Environment, University of Oldenburg, Wilhelmshaven, Germany

**Correspondence:** Xianda Gong (gong@tropos.de)

## S1 Seawater samples

**Table S1.** The information of seawater samples at OS, including sample number, start time, end time, location, salinity, sodium chloride (NaCl) mass concentration, PH value and water temperature.

Sample Number	Start Time yyyy/mm/dd hh:mm:ss	End Time yyyy/mm/dd hh:mm:ss	Location	Salinity [g L <sup>-1</sup> ]	NaCl [g L <sup>-1</sup> ]	PH value	Temperature [°C]
SML01	2017/09/18 12:35:00	2017/09/18 13:00:00	-	-	-	-	-
ULW01	2017/09/18 12:35:00	2017/09/18 13:00:00	-	34.1	29.23	8.14	25.0
SML02	2017/09/20 09:32:00	2017/09/20 10:54:00	16°53'20 N, 24°54'22 W	36.2	31.03	8.11	26.7
ULW02	2017/09/20 09:32:00	2017/09/20 10:54:00	16°53'20 N, 24°54'22 W	36.3	31.11	8.12	26.7
SML03	2017/09/25 10:45:00	2017/09/25 11:48:00	16°53'46 N, 24°54'19 W	36.4	31.20	8.14	25.5
ULW03	2017/09/25 10:45:00	2017/09/25 11:48:00	16°53'46 N, 24°54'19 W	36.4	31.20	8.15	26.0
SML04	2017/09/26 11:05:00	2017/09/26 11:51:00	16°53'50 N, 24°54'27 W	36.1	30.94	8.12	26.4
ULW04	2017/09/26 11:05:00	2017/09/26 11:51:00	16°53'50 N, 24°54'27 W	36.3	31.11	8.15	25.1
SML05	2017/09/27 09:50:00	2017/09/27 11:00:00	16°53'38 N, 24°54'16 W	36.3	31.11	8.15	23.7
ULW05	2017/09/27 09:50:00	2017/09/27 11:00:00	16°53'38 N, 24°54'16 W	36.4	31.20	8.14	24.0
SML09	2017/10/04 09:15:00	2017/10/04 10:00:00	-	-	-	-	-
ULW09	2017/10/04 09:15:00	2017/10/04 10:00:00	-	36.2	31.03	8.23	23.7
SML12	2017/10/07 10:22:00	2017/10/07 11:35:00	16°53'25 N, 24°54'18 W	36.7	31.46	8.22	21.2
ULW12	2017/10/07 10:22:00	2017/10/07 11:35:00	16°53'25 N, 24°54'18 W	36.4	31.20	8.22	21.8
SML13	2017/10/09 09:30:00	2017/10/09 10:17:00	16°53'42 N, 24°54'08 W	36.6	31.37	8.19	21.5
ULW13	2017/10/09 09:30:00	2017/10/09 10:17:00	16°53'42 N, 24°54'08 W	36.4	31.20	8.13	23.6
SML14	2017/10/10 09:30:00	2017/10/10 10:30:00	16°53'43 N, 24°54'13 W	36.4	31.20	8.19	21.7
ULW14	2017/10/10 09:30:00	2017/10/10 10:30:00	16°53'43 N, 24°54'13 W	36.3	31.11	8.18	22.4

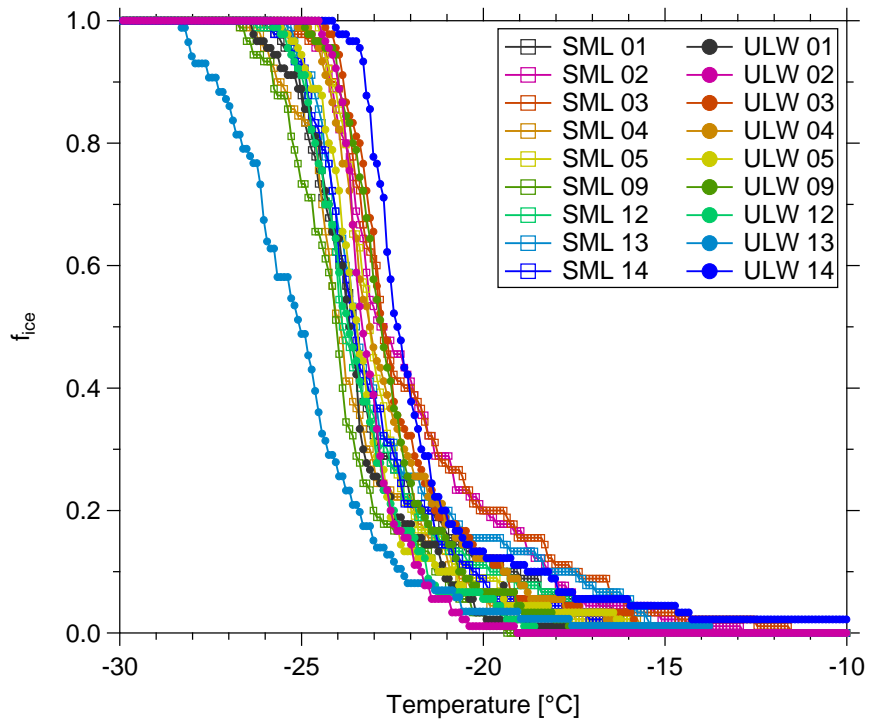


**Figure S1.** Frozen fraction ( $f_{\text{ice}}$ ) measured by LINA as a function of temperature in SML and ULW. All temperatures have been corrected for freezing point depression.

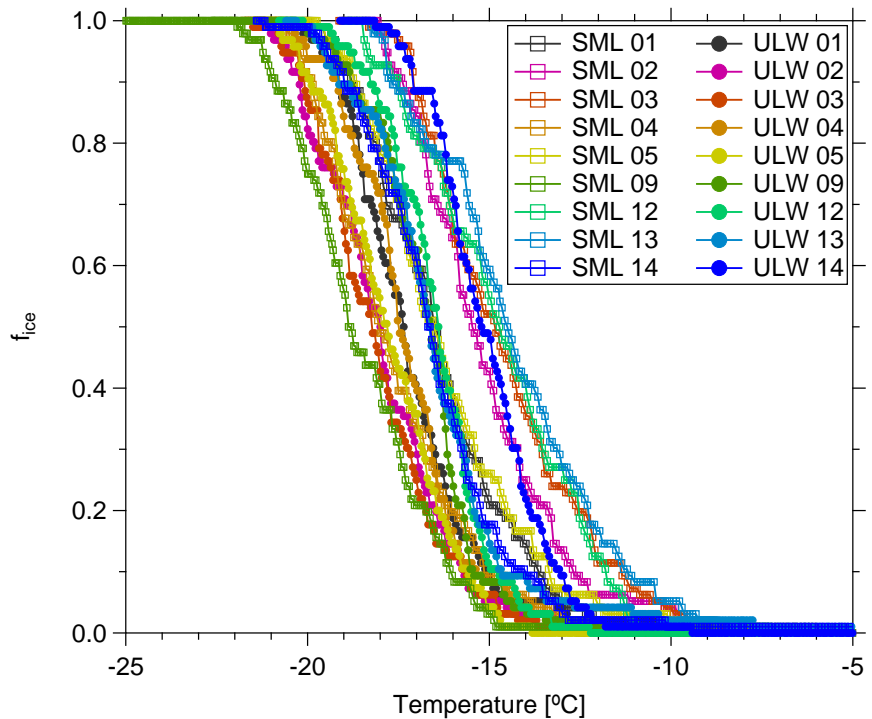


**Figure S2.**  $f_{\text{ice}}$  measured by INDA as a function of temperature in SML and ULW. All temperatures have been corrected for freezing point depression.

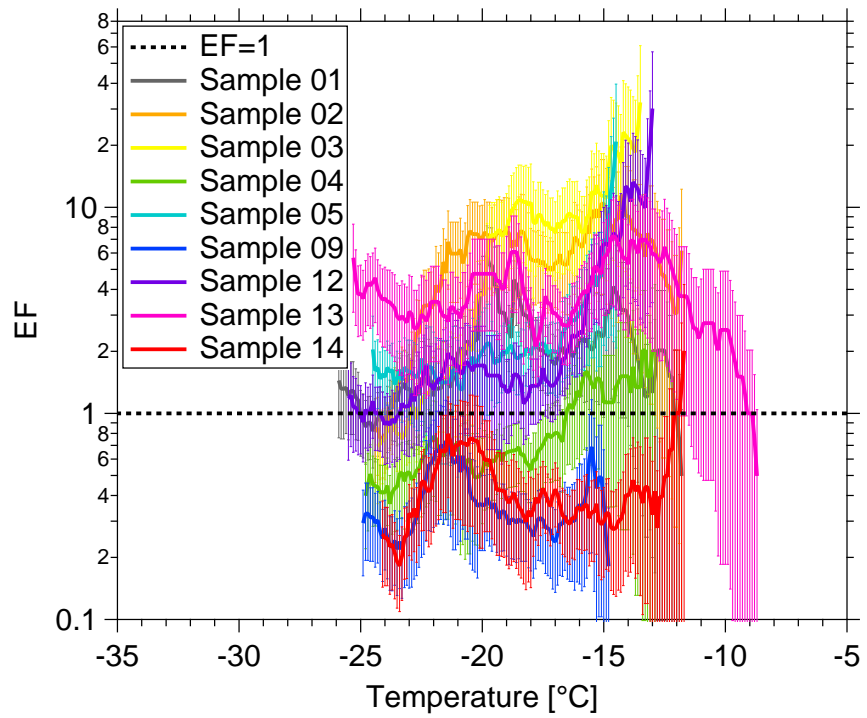


**Figure S3.** EF as function of ice nucleation temperature. The EF=1 is shown by dashed line. Error bars show the measurement uncertainty.

## S2 Filter samples

### S2.1 Background subtraction

$N_{\text{INP}}$  from the field blanks was then subtracted from that of the filter samples, and the result was converted to background corrected atmospheric INP number concentrations, as the below equation shows:

$$5 \quad N_{\text{INP}} = (-\ln(1 - f_{\text{ice,s}}) + \ln(1 - f_{\text{ice,b}}))/V \quad (\text{S1})$$

The corrected atmospheric INP number concentration is  $N_{\text{INP}}$ , the frozen fractions measured for the filter samples and the field blanks are  $f_{\text{ice,s}}$  and  $f_{\text{ice,b}}$ , respectively, and  $V$  is the volume of air sampled in each well.

### S2.2 CVAO PM<sub>10</sub>

**Table S2.** The information of PM<sub>10</sub> filter samples at CVAO, including sample number, start time, end time, duration, total sampling volume, sampling volume per well, sodium (Na<sup>+</sup>) and chloride (Cl<sup>-</sup>) mass concentration, total particle surface area concentration ( $A_{\text{total}}$ ) and sample type.

Sample Number	Start Time yyyy/mm/dd hh:mm:ss	End Time yyyy/mm/dd hh:mm:ss	Duration [ <u>hour</u> <u>minute</u> ]	Total Volume [std <u>L<sup>-1</sup></u> <u>m<sup>3</sup></u> ]	Volume Per Well [std L <sup>-1</sup> ]	Na <sup>+</sup> μg m <sup>-3</sup>	Cl <sup>-</sup> μg m <sup>-3</sup>	$A_{\text{total}}$ μm <sup>2</sup> cm <sup>-3</sup>	Type
CVAO1583	2017/09/19 21:00:00	2017/09/20 21:00:00	1439.34	660.289	33.6882	4.40	6.19	370	PM <sub>10</sub>
CVAO1585	2017/09/22 16:00:00	2017/09/23 16:00:00	1439.34	660.289	33.6882	3.09	4.97	89	PM <sub>10</sub>
CVAO1586	2017/09/23 16:00:00	2017/09/24 16:00:00	1439.34	660.289	33.6882	2.36	3.36	78	PM <sub>10</sub>
CVAO1587	2017/09/24 16:00:00	2017/09/25 16:00:00	1439.34	660.289	33.6882	2.83	3.54	158	PM <sub>10</sub>
CVAO1588	2017/09/25 16:00:00	2017/09/26 16:00:00	1438.90	660.792	33.7139	3.32	4.98	277	PM <sub>10</sub>
CVAO1589	2017/09/26 16:00:00	2017/09/27 16:00:00	1439.61	661.462	33.7481	1.41	1.99	159	PM <sub>10</sub>
CVAO1590	2017/09/27 16:00:00	2017/09/28 16:00:00	1439.71	661.644	33.7573	1.77	2.70	198	PM <sub>10</sub>
CVAO1591	2017/09/28 16:00:00	2017/09/29 16:00:00	1439.73	661.420	33.7459	5.04	8.41	325	PM <sub>10</sub>
CVAO1592	2017/09/29 16:00:00	2017/09/30 16:00:00	1439.73	660.289	33.6882	6.49	11.26	297	PM <sub>10</sub>
CVAO1593	2017/09/30 16:00:00	2017/10/01 16:00:00	1439.73	660.821	33.7153	5.32	8.99	238	PM <sub>10</sub>
CVAO1594	2017/09/29 16:00:00	2017/09/30 16:00:00							Blind filter
CVAO1595	2017/10/01 16:00:00	2017/10/02 16:00:00	1439.36	659.330	33.6393	4.52	6.67	172	PM <sub>10</sub>
CVAO1596	2017/10/02 16:00:00	2017/10/03 16:00:00	1439.71	660.629	33.7056	3.71	6.49	171	PM <sub>10</sub>
CVAO1597	2017/10/03 16:00:00	2017/10/04 16:00:00	1439.71	660.629	33.7056	-	-	169	PM <sub>10</sub>
CVAO1598	2017/10/05 16:00:00	2017/10/06 16:00:00	1439.55	659.264	33.6359	2.58	3.33	162	PM <sub>10</sub>
CVAO1641	2017/10/06 16:00:00	2017/10/07 16:00:00	1439.73	658.670	33.6056	4.67	6.91	244	PM <sub>10</sub>
CVAO1642	2017/10/07 16:00:00	2017/10/08 16:00:00	1439.71	661.187	33.7341	5.46	8.54	271	PM <sub>10</sub>
CVAO1643	2017/10/08 16:00:00	2017/10/09 16:00:00	1439.71	659.785	33.6625	5.22	7.98	230	PM <sub>10</sub>
CVAO1644	2017/10/07 17:00:00	2017/10/08 17:00:00							Blind filter

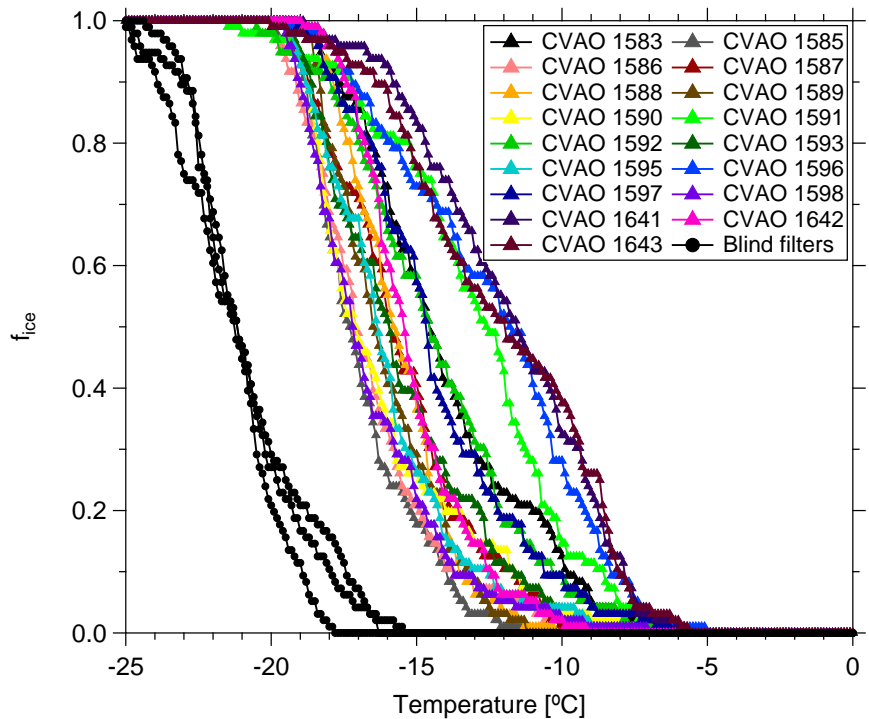


**Figure S4.**  $f_{ice}$  measured by INDA (without background subtraction) as a function of temperature in CVAO PM<sub>10</sub> filters.  $f_{ice}$  of blind filters are shown by black dots.

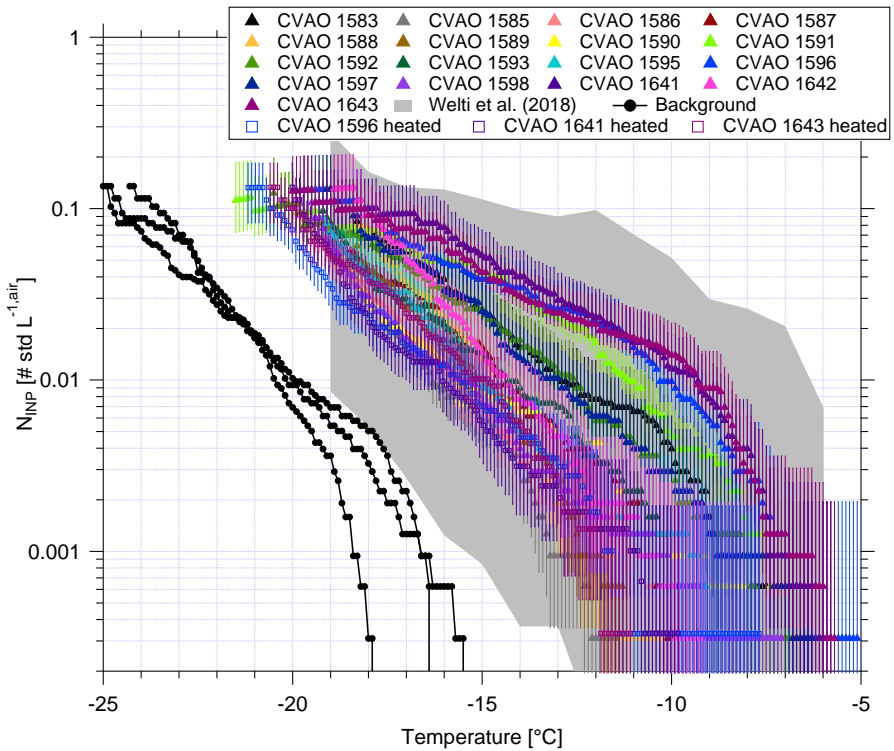


**Figure S5.**  $N_{INP}$  as a function of temperature from CVAO PM<sub>10</sub> filters. The field measurement of  $N_{INP}$  in PM<sub>10</sub> by Welti et al. (2018) is shown by gray shadow. Error bars show the 95% confidence interval. Black dots show the measurement background.

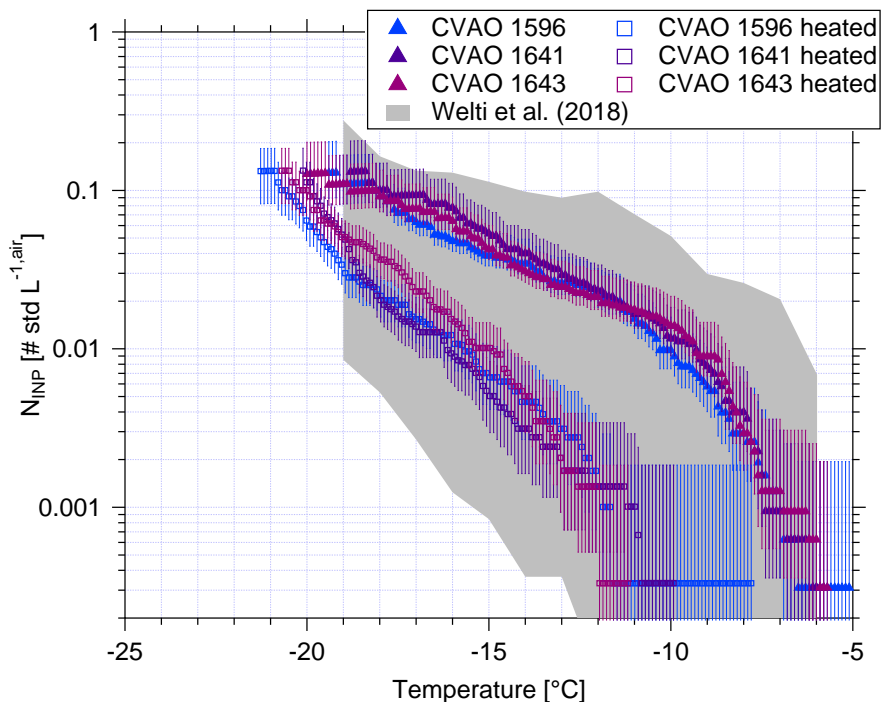


**Figure S6.** Comparison of  $N_{INP}$  as a function of temperature from CVAO 1596, CVAO 1641 and CVAO 1643 before and after heating (CVAO  $PM_{10}$  filters). The field measurement of  $N_{INP}$  in  $PM_{10}$  by Welti et al. (2018) is shown by gray shadow. Error bars show the 95% confidence interval. Background correction is included for all filter samples.

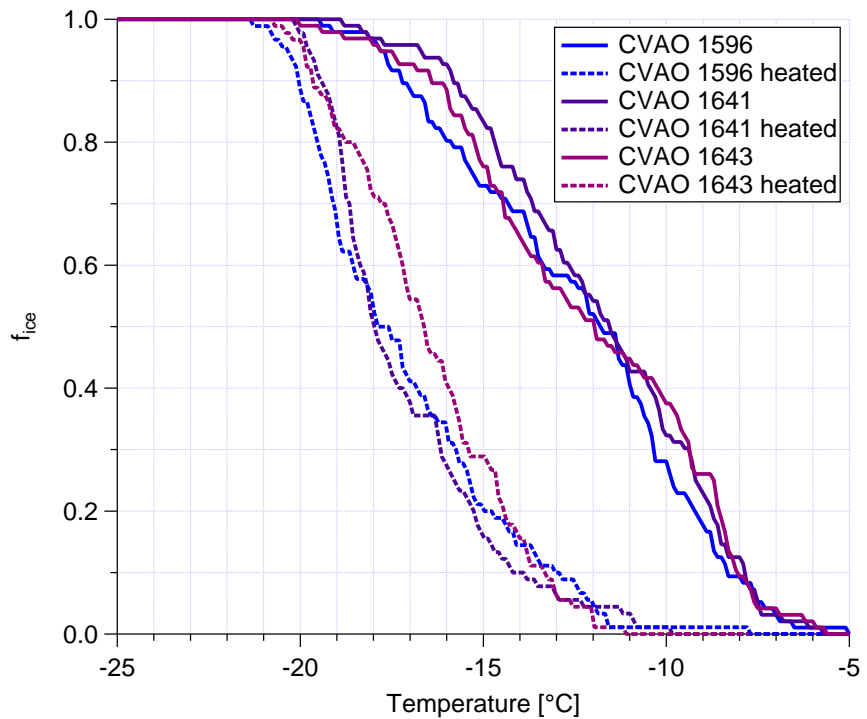


**Figure S7.** Comparison of  $f_{ice}$  measured by INDA (without background subtraction) as a function of temperature from CVAO 1596, CVAO 1641 and CVAO 1643 before and after heating (CVAO PM<sub>10</sub> filters).

## S2.3 CVAO PM<sub>1</sub>

**Table S3.** The information of PM<sub>1</sub> filter samples at CVAO, including sample number, start time, end time, duration, total sampling volume, sampling volume per well and sample type.

Sample Number	Start Time yyyy/mm/dd hh:mm:ss	End Time yyyy/mm/dd hh:mm:ss	Duration [hminute]	Total Volume [std L <sup>-1</sup> m <sup>3</sup> ]	Volume Per Well [std L <sup>-1</sup> ]	Type
CVAO924	2017/09/19 21:00:00	2017/09/20 21:00:00	1439.36	661.200	33.7347	PM <sub>1</sub>
CVAO925	2017/09/21 21:00:00	2017/09/22 21:00:00	1439.36	661.200	33.7347	PM <sub>1</sub>
CVAO926	2017/09/22 16:00:00	2017/09/23 16:00:00	1439.36	661.200	33.7347	PM <sub>1</sub>
CVAO927	2017/09/23 16:00:00	2017/09/24 16:00:00	1439.36	661.200	33.7347	PM <sub>1</sub>
CVAO928	2017/09/24 16:00:00	2017/09/25 16:00:00	1439.36	661.200	33.7347	PM <sub>1</sub>
CVAO929	2017/09/25 16:00:00	2017/09/26 16:00:00	1439.21	664.115	33.8834	PM <sub>1</sub>
CVAO930	2017/09/26 16:00:00	2017/09/27 16:00:00	1439.36	661.200	33.7347	PM <sub>1</sub>
CVAO931	2017/09/27 16:00:00	2017/09/28 16:00:00	1439.36	661.200	33.7347	PM <sub>1</sub>
CVAO932	2017/09/28 16:00:00	2017/09/29 16:00:00	1439.36	661.200	33.7347	PM <sub>1</sub>
CVAO933	2017/09/29 16:00:00	2017/09/30 16:00:00	1439.36	661.200	33.7347	PM <sub>1</sub>
CVAO934	2017/09/30 16:00:00	2017/10/01 16:00:00	1439.36	661.200	33.7347	PM <sub>1</sub>
CVAO935	2017/09/29 16:00:00	2017/09/30 16:00:00				Blind filter
CVAO936	2017/10/01 16:00:00	2017/10/02 16:00:00	1438.53	659.798	33.6632	PM <sub>1</sub>
CVAO937	2017/10/02 16:00:00	2017/10/03 16:00:00	1439.55	660.255	33.6865	PM <sub>1</sub>
CVAO938	2017/10/03 16:00:00	2017/10/04 16:00:00	1439.36	661.200	33.7347	PM <sub>1</sub>
CVAO939	2017/10/04 16:00:00	2017/10/05 16:00:00	1439.36	661.200	33.7347	PM <sub>1</sub>
CVAO940	2017/10/05 16:00:00	2017/10/06 16:00:00	1439.18	661.071	33.7281	PM <sub>1</sub>
CVAO941	2017/10/06 16:00:00	2017/10/07 16:00:00	1439.58	662.336	33.7927	PM <sub>1</sub>
CVAO942	2017/10/07 16:00:00	2017/10/08 16:00:00	1439.58	662.122	33.7817	PM <sub>1</sub>
CVAO944	2017/10/08 16:00:00	2017/10/09 16:00:00	1439.55	660.377	33.6927	PM <sub>1</sub>

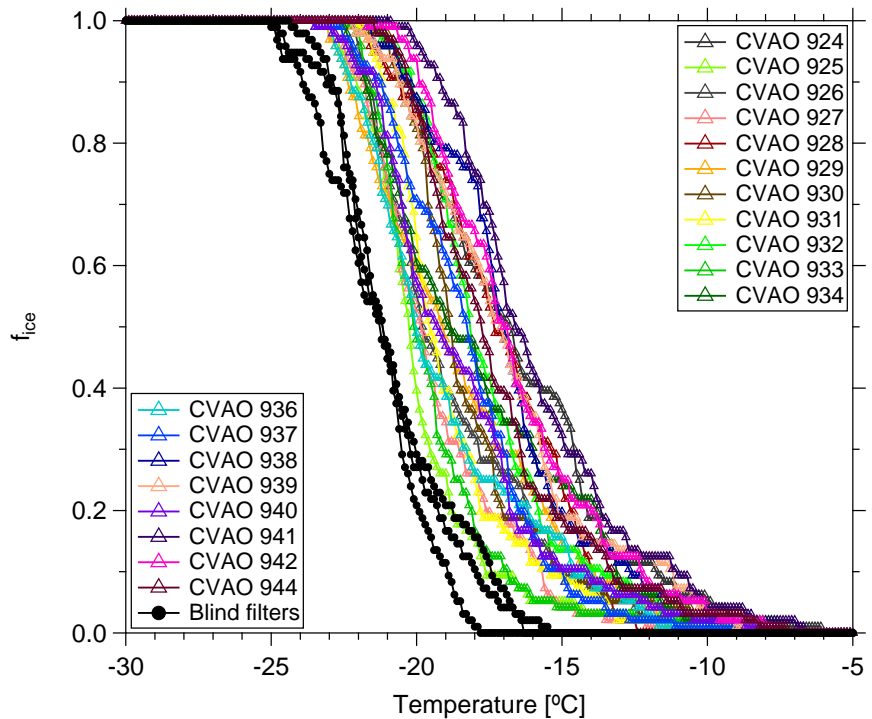


**Figure S8.**  $f_{ice}$  measured by INDA (without background subtraction) as a function of temperature in CVAO PM<sub>1</sub> filters.  $f_{ice}$  of blind filters are shown by black dots.

## S2.4 MV PM<sub>10</sub>

**Table S4.** The information of PM<sub>10</sub> filter samples at MV, including sample number, start time, end time, duration, total sampling volume, sampling volume per well, cloud time (percent of the time MV was in cloud during the filter was sampled) and sample type.

Sample Number	Start Time yyyy/mm/dd hh:mm:ss	End Time yyyy/mm/dd hh:mm:ss	Duration [hminute]	Total Volume [std L <sup>-1</sup> m <sup>3</sup> ]	Volume Per Well [std L <sup>-1</sup> ]	Cloud time [%]	Type
MV1600	2017/09/21 16:39:00	2017/09/22 16:23:00	1382.86	601.870	30.7077	67.44%	PM <sub>10</sub>
MV1601	2017/09/22 16:23:00	2017/09/23 15:59:00	1418.31	615.998	31.4285	17.39%	PM <sub>10</sub>
MV1602	2017/09/23 15:59:00	2017/09/24 16:01:00	1440.60	625.035	31.8896	6.12%	PM <sub>10</sub>
MV1603	2017/09/24 16:01:00	2017/09/25 16:11:00	1449.61	629.660	32.1255	4.17%	PM <sub>10</sub>
MV1604	2017/09/25 16:13:00	2017/09/26 16:19:00	1444.90	627.655	32.0232	61.70%	PM <sub>10</sub>
MV1605	2017/09/26 16:20:00	2017/09/27 16:23:00	1440.58	627.381	32.0092	65.96%	PM <sub>10</sub>
MV1606	2017/09/27 16:23:00	2017/09/28 16:59:00	1464.99	637.541	32.5276	79.59%	PM <sub>10</sub>
MV1607	2017/09/28 17:01:00	2017/09/29 16:28:00	1406.21	611.922	31.2205	97.83%	PM <sub>10</sub>
MV1608	2017/09/29 16:30:00	2017/09/30 16:28:00	1676.36	760.265	38.7890	93.75%	PM <sub>10</sub>
MV1609	2017/10/01 19:02:00	2017/10/02 17:09:00	1326.63	576.405	29.4084	47.73%	PM <sub>10</sub>
MV1610	2017/10/02 17:09:00	2017/10/03 17:09:00	1439.36	624.715	31.8732	52.08%	PM <sub>10</sub>
MV1611	2017/10/03 17:10:00	2017/10/04 16:27:00	1396.11	606.390	30.9383	50.00%	PM <sub>10</sub>
MV1612	2017/10/04 16:27:00	2017/10/05 16:00:00	1408.61	613.421	31.2970	69.05%	PM <sub>10</sub>
MV1613	2017/10/05 16:00:00	2017/10/06 16:01:00	1441.46	627.486	32.0146	79.59%	PM <sub>10</sub>
MV1614	2017/10/06 16:03:00	2017/10/07 16:02:00	1439.46	625.832	31.9302	87.23%	PM <sub>10</sub>
MV1615	2017/10/07 16:02:00	2017/10/08 18:12:00	1439.36	627.485	32.0145	100.00%	PM <sub>10</sub>
MV1616	2017/10/08 18:13:00	2017/10/09 12:04:00	1071.60	467.526	23.8534	100.00%	PM <sub>10</sub>

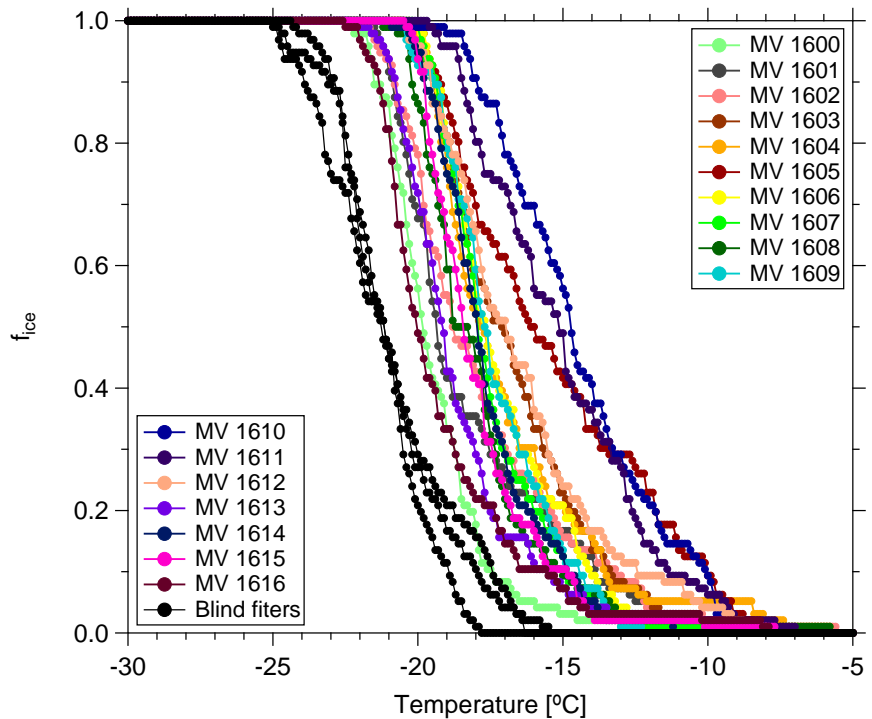


**Figure S9.**  $f_{ice}$  measured by INDA (without background subtraction) as a function of temperature in MV PM<sub>10</sub> filters.  $f_{ice}$  of blind filters are shown by black dots.

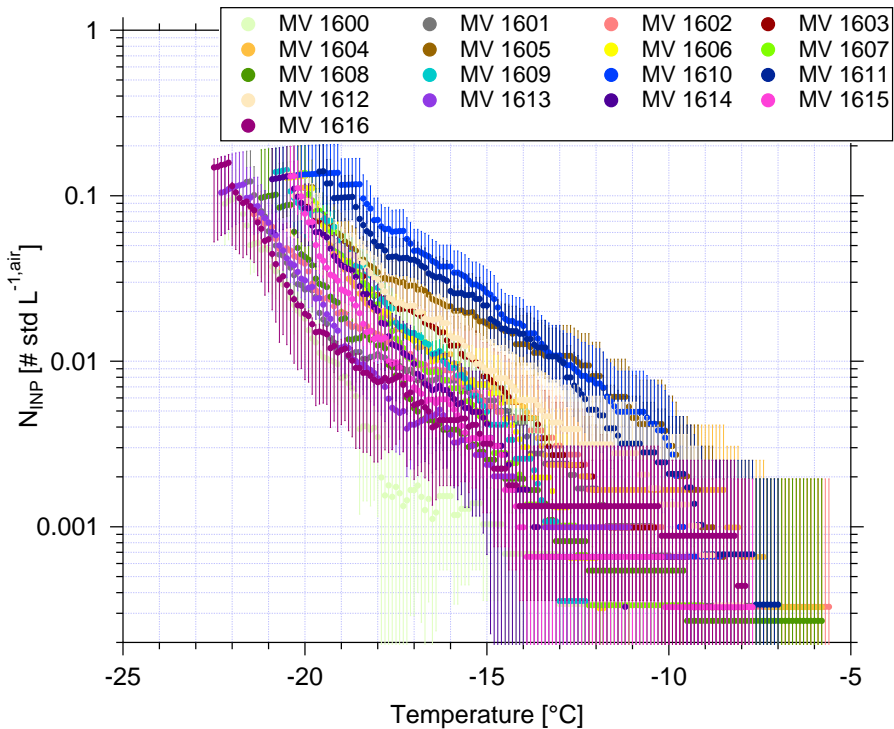


**Figure S10.**  $N_{INP}$  as function of temperature in MV PM<sub>10</sub> filters.  $N_{INP}$  are background-corrected. Error bars show the 95% confidence interval.

### S3 Cloud samples

**Table S5.** The information of cloud water samples, including sample number, start time, end time, duration, volume, sodium ( $\text{Na}^+$ ) and chloride ( $\text{Cl}^-$ ) mass concentration and  $N_{\text{CCN},0.30\%}$ .

Sample Number	Start Time yyyy/mm/dd hh:mm:ss	End Time yyyy/mm/dd hh:mm:ss	Duration (h) [h]	Volume [mL]	$\text{Na}^+$ $\text{mg L}^{-1}$	$\text{Cl}^-$ $\text{mg L}^{-1}$	$N_{\text{CCN},0.30\%}$ $\text{cm}^{-3}$
Cloud01	2017/09/20 13:25:00	2017/09/20 18:20:00	4.92	185	8.44	15.51	551
Cloud03	2017/09/26 19:00:00	2017/09/27 08:00:00	13.00	435	8.32	14.15	387
Cloud04	2017/09/27 19:00:00	2017/09/28 07:30:00	12.50	544	5.00	9.27	239
Cloud05	2017/09/28 19:00:00	2017/09/29 07:30:00	12.50	537	14.18	24.57	560
Cloud11	2017/10/04 19:00:00	2017/10/05 07:30:00	12.50	150	46.11	70.30	481
Cloud12	2017/10/05 07:45:00	2017/10/05 17:38:00	9.88	78	22.75	36.99	494
Cloud13	2017/10/05 17:40:00	2017/10/05 20:10:00	2.50	133	16.97	25.23	442
Cloud14	2017/10/05 20:10:00	2017/10/05 23:30:00	3.33	131	17.31	24.36	473
Cloud15	2017/10/05 23:30:00	2017/10/06 04:00:00	4.50	120	21.85	31.95	491
Cloud16	2017/10/06 04:05:00	2017/10/06 08:00:00	3.92	120	16.87	19.77	445
Cloud19	2017/10/06 18:00:00	2017/10/07 06:30:00	12.50	537	18.34	29.10	482
Cloud20	2017/10/07 06:48:00	2017/10/07 10:48:00	4.00	88	28.19	41.54	510
Cloud24	2017/10/08 19:00:00	2017/10/09 07:00:00	12.00	537	24.54	32.46	625

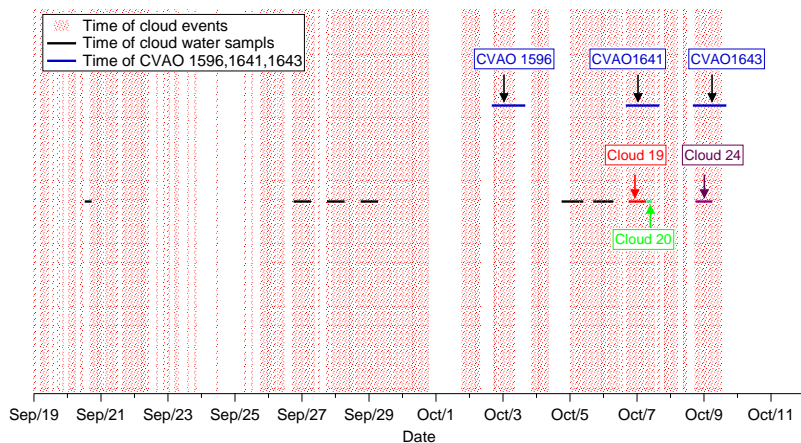


**Figure S11.** Times during which MV was in clouds (in red shadows) and the sampling time of all cloud water and that of some selected CVAO  $\text{PM}_{10}$  filters.

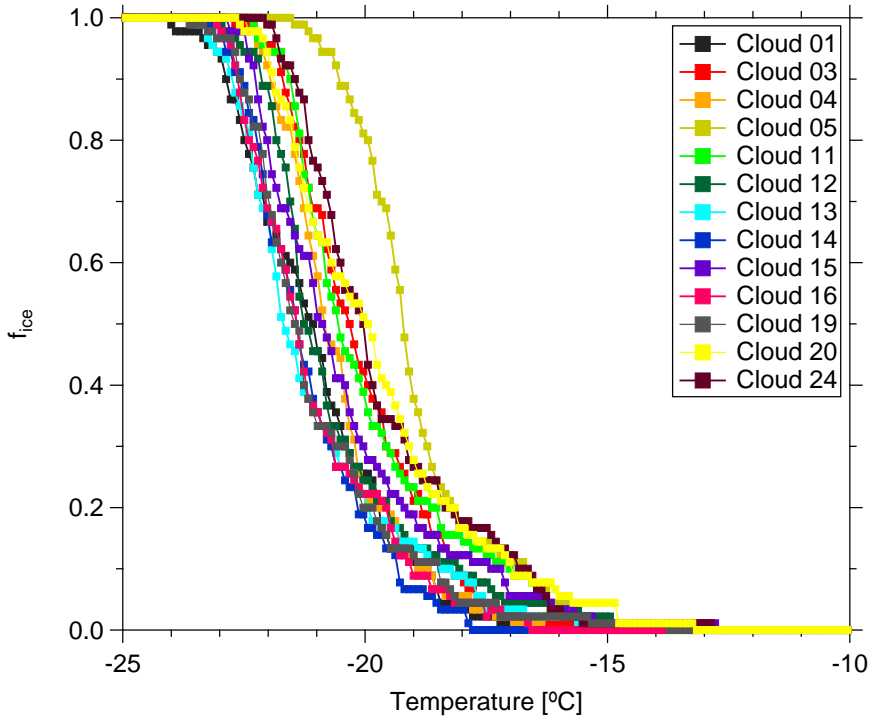


**Figure S12.**  $f_{\text{ice}}$  measured by LINA as a function of temperature in cloud water.

#### S4 Particle surface area size distribution

A thorough aerosol characterization has been done during the measurement campaign, and is described in detail in Gong et al. (2019). Fig. S14 shows the median particle surface area size distribution (PASD) for the whole campaign. Error bars show the 75th and 25th percentiles. Two different modes were observed, i.e., a small mode (30-500 nm) and a larger mode (500 nm-10  $\mu\text{m}$ ). The larger mode particle surface area is about 3 times higher than the small mode. Based on the PASD, the concentrations for the total surface area of the particles were calculated. The total particle surface area concentration ( $A_{\text{total}}$ ) varied from 35 to 824  $\mu\text{m}^2 \text{ cm}^{-3}$ , with a median of 116  $\mu\text{m}^2 \text{ cm}^{-3}$ . The averaged  $A_{\text{total}}$  during each CVAO PM<sub>10</sub> sampling period varied from 78 to 370  $\mu\text{m}^2 \text{ cm}^{-3}$  (summarized in Tab. S2). Based on airborne measurements in the Saharan dust layer, Price et al. (2018) found  $A_{\text{total}}$  mainly above 100 with a maximum of 688  $\mu\text{m}^2 \text{ cm}^{-3}$ , which is higher than values found for this study, likely due to the fact that Cape Verde is at some distance to the Sahara and also that less strong dust events were sampled.

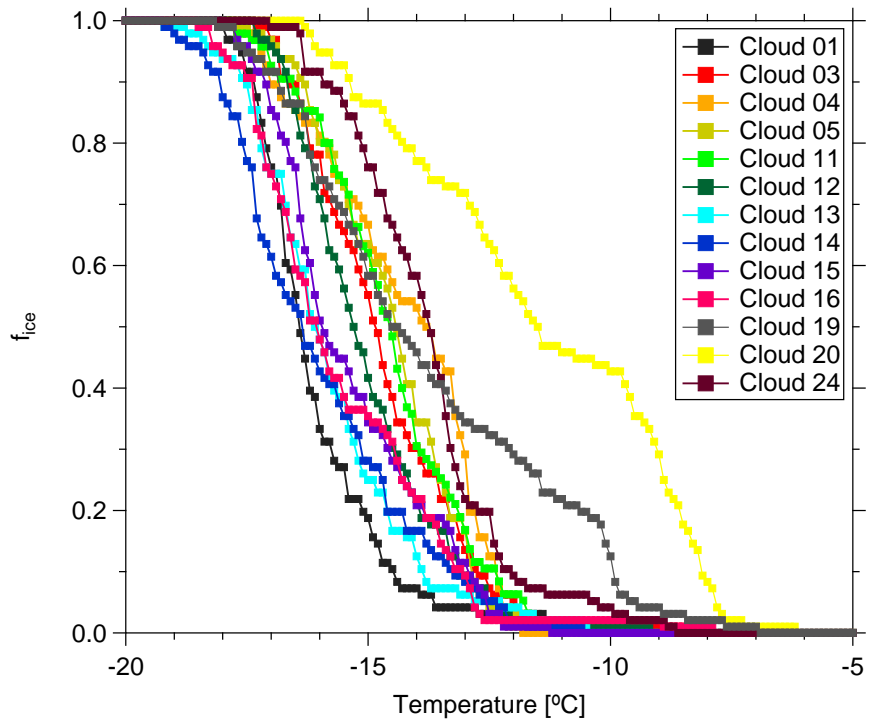


**Figure S13.**  $f_{ice}$  measured by INDA as a function of temperature in cloud water.

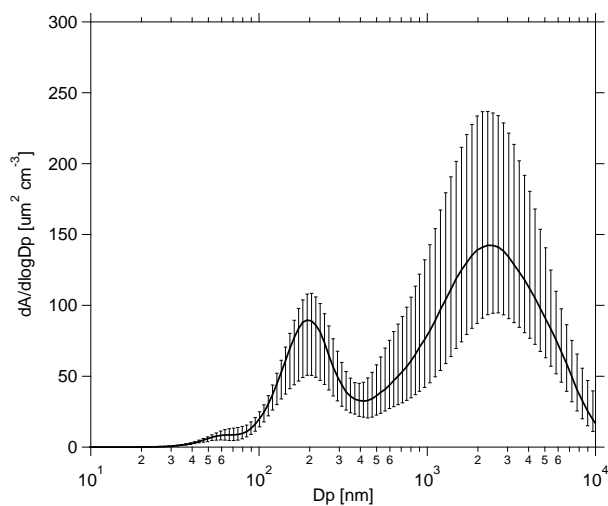


**Figure S14.** The median PASD during the whole campaign. The error bar indicates the range between the 75th and 25th percentiles.

## References

Gong, X., Wex, H., Voigtländer, J., Fomba, K. W., Weinhold, K., van Pinxteren, M., Henning, S., Müller, T., Herrmann, H., and Stratmann, F.: Characterization of aerosol particles at Cape Verde close to sea and cloud level heights – Part 1: particle number size distribution, cloud condensation nuclei and their origins, *Atmos. Chem. Phys. Discuss.*, 2019, 1–31, <https://doi.org/10.5194/acp-2019-585>, <https://www.atmos-chem-phys-discuss.net/acp-2019-585/>, 2019.

5 Price, H. C., Baustian, K. J., McQuaid, J. B., Blyth, A., Bower, K. N., Choularton, T., Cotton, R. J., Cui, Z., Field, P. R., Gallagher, M., Hawker, R., Merrington, A., Miltenberger, A., Neely III, R. R., Parker, S. T., Rosenberg, P. D., Taylor, J. W., Trembath, J., Vergara-Temprado, J., Whale, T. F., Wilson, T. W., Young, G., and Murray, B. J.: Atmospheric Ice-Nucleating Particles in the Dusty Tropical Atlantic, *Journal of Geophysical Research: Atmospheres*, 123, 2175–2193, <https://doi.org/doi:10.1002/2017JD027560>, <https://agupubs.onlinelibrary.wiley.com/doi/abs/10.1002/2017JD027560>, 2018.

10 Welti, A., Müller, K., Fleming, Z. L., and Stratmann, F.: Concentration and variability of ice nuclei in the subtropical maritime boundary layer, *Atmospheric Chemistry and Physics*, 18, 5307–5320, 2018.